TECHNISCHE UNIVERSITÄT MÜNCHEN

Lehrstuhl für Humanbiologie

Plasticity of glial cells in the enteric nervous system during intestinal inflammation

Sebastian Hoff

Vollständiger Abdruck der von der Fakultät Wissenschaftszentrum Weihenstephan für Ernährung, Landnutzung und Umwelt der Technischen Universität München zur Erlangung des akademischen Grades eines

Doktors der Naturwissenschaften

genehmigten Dissertation.

Vorsitzende: Univ.-Prof. Dr. H. Daniel
Prüfer der Dissertation:
1. Univ.-Prof. Dr. M. Schemann
2. Univ.-Prof. Dr. R. M. Schmid

Die Dissertation wurde am 28.07.2008 bei der Technischen Universität München eingereicht und durch die Fakultät Wissenschaftszentrum Weihenstephan für Ernährung, Landnutzung und Umwelt am 21.11.2008 angenommen.

Table of Contents

Abbreviations

AA	Antibiotic-antimycotic
Ab	Antibody
ACTB	Actin beta
AJC	Apical junctional complex
Ala-Lys-AMCA	β-Ala-Lys-Nϵ-7-amino-4-methyl-coumarin-3-acetic acid
AMCA	Aminomethyl-coumarin-acetat
ANOVA	Analysis of variance
AraC	Cytosine β-D-arabinofuranoside
BPE	Brain pituary extract
CD	Crohn's disease
cDNA	Complementary DNA
Cy2	Carbocyanin
Cy3	Indocarbocyanin
Cy5	Indodicarbocyanin
DEPC	Diethyl pyrocarbonate
DMEM	Dulbecco's modified Eagle's medium
DMEM/F12	Dulbecco's modified Eagle's medium nutrient mixture F-12 Ham
DMSO	Dimethyl sulfoxide
DNA	Deoxyribonucleic acid
EDTA	Ethylenediaminetetraacetic acid
EGC	Enteric glial cells
ENS	Enteric nervous system
FBS	Fetal bovine serum
FD	Fluorescein dextran
FGF2	Fibroblast growth factor 2
FSA	Fluorescein sulfonic acid
GDNF	Glial cell line-derived neurotrophic factor
GFAP	Glial fibrillary acidic protein
GFRA1	GDNF family receptor alpha 1
GFRA2	GDNF family receptor alpha 2
HA	Hemagglutinin
HBSS	Hank's balanced salt solution

Abbreviations (*continued*)

HIST3H3	Histone 3, H3
HSVtk	Herpes simplex virus thymidine kinase
IBD	Inflammatory bowel disease
IEC	Intestinal epithelial cells
IFNGR1	Interferon gamma receptor 1
IL10	Interleukin 10
IL13RA1	Interleukin 13 receptor, alpha 1
IL1R1	Interleukin 1 receptor, type I
IL1R2	Interleukin 1 receptor, type II
IL1RAP	Interleukin 1 receptor accessory protein
MHC	Major histocompatibility complex
MP	Myenteric plexus
mRNA	Messenger RNA
NES	Nestin
NGF	Nerve growth factor
NGFR	NGF receptor or p75NGFR
NT-3	Neurotrophin 3
NTRK1	Neurotrophic tyrosine kinase, receptor, type 1 or TrkA
NTRK2	Neurotrophic tyrosine kinase, receptor, type 2 or TrkB
NTRK3	Neurotrophic tyrosine kinase, receptor, type 3 or TrkC
p75NGFR	Low affinity nerve growth factor receptor p75 or NGFR
PB	Phosphate buffer
PBS	Phosphate buffered saline
PCR	Polymerase chain reaction
PGP 9.5	Protein gene product 9.5
RET	Ret proto-oncogene
RNA	Ribonucleic acid
RT-PCR	Real-time PCR
SMP	Submucous plexus
Sox8/9/10	Transcription factors Sox 8, 9 and 10
TER	Transepithelial electrical resistance
TNFRSF1A	Tumor necrosis factor receptor superfamily, member 1A

Figures

Tables

1. Introduction

The enteric nervous system (ENS) is an integral part of the autonomic nervous system and forms a large network of differently shaped, interconnected plexus layers in the wall of the gastrointestinal tract (Furness & Costa 1987). It extends from the esophagus to the anus and associated glands (salivary glands, the pancreas (Kirchgessner & Gershon 1990)) and the gallbladder (Hansen 2003). The ENS controls gastrointestinal motility, secretion, absorption, blood flow and immune and inflammatory functions (Goyal & Hirano 1996). There are two major ganglionated plexuses in the ENS, namely the myenteric (or Auerbach) plexus (MP) and the submucous (or Meissner) plexus (SMP) (Figure 1 and Figure 2).
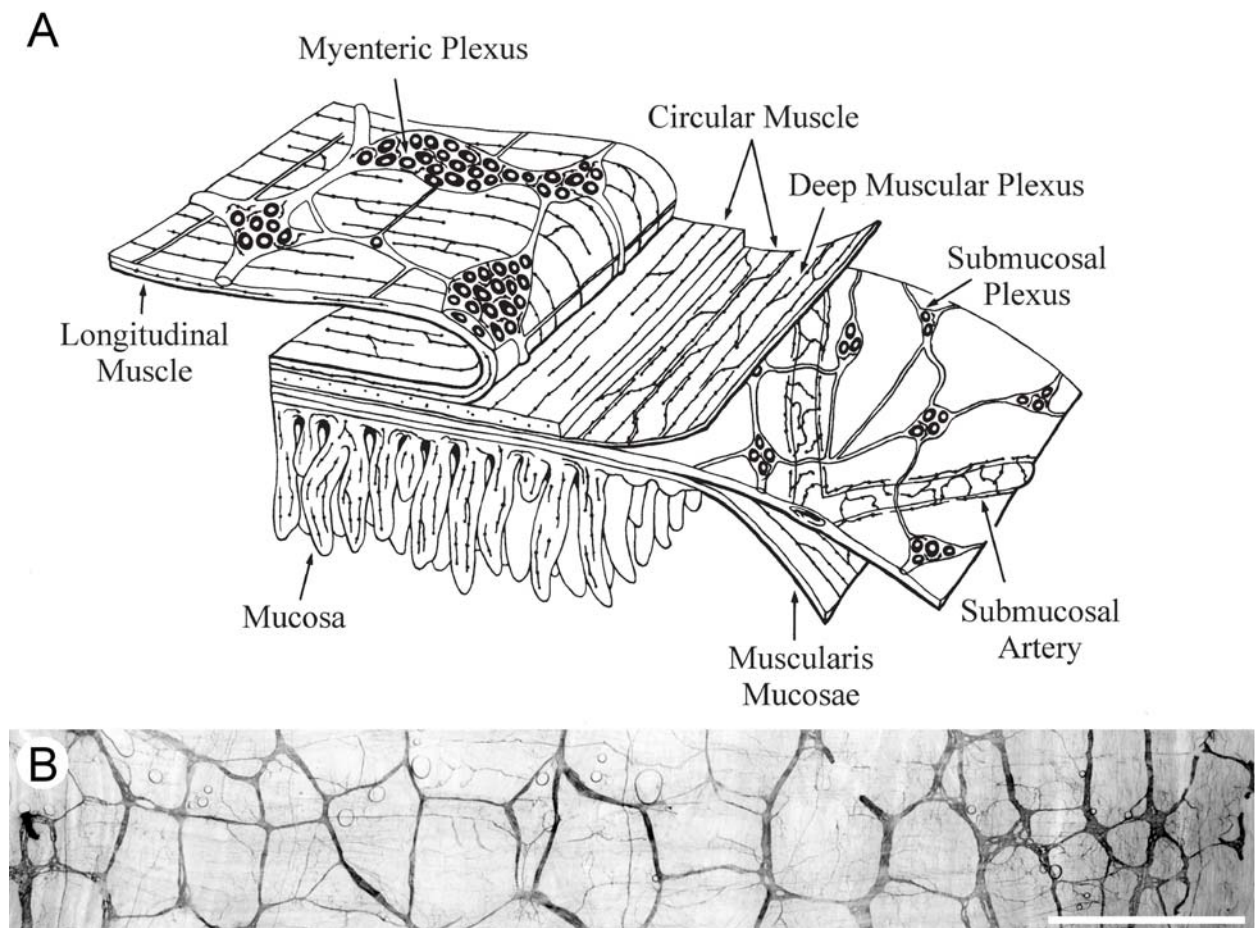
Figure 1. **The enteric nervous system (ENS) consists of two major ganglionated plexus layers**: the myenteric (MP) and the submucous plexus and non-ganglionated plexuses of nerve fibers innervating muscle layers, blood vessels, glands and epithelium. In the human ENS, the submucous plexus can be subdivided into three distinguishable layers. Picture (A) adopted from (Furness & Costa 1980). (B) Whole mount preparation of the MP from human colon stained for the glial marker S100b. Scale bar = 5 mm.

The MP is positioned between the outer longitudinal and inner circular muscle layers throughout the digestive tract, from esophagus to rectum (Hansen 2003). The SMP is located in the submucosa between the circular muscle layer and the muscularis mucosae, being best developed in the small and large intestines (Hansen 2003).

In the human ENS, the SMP is subdivided into three separate plexuses, namely the outer submucous plexus (Schabadasch or Henle plexus) directly adjacent to the circular muscle layer, the inner submucous plexus (Meissner plexus) directly below the muscularis mucosae and an intermediate plexus located between the two (Hoyle & Burnstock 1989, Ibba-Manneschi et al 1995).

Innermost to the luminal side of the gastrointestinal wall lies the mucous plexus right beneath the epithelium. It could be subdivided into a subglandular and a periglandular part, depending on the location of the nerve fiber strands (Wedel et al 1999). Additionally, there are non-ganglionated plexuses of nerve fibers in the ENS innervating the muscle layers, blood vessels, glands and epithelium. In contrast, only 2 ganglionated nerve plexuses can be discerned in the guinea pig ENS (Brookes 2001, Furness & Costa 1980).
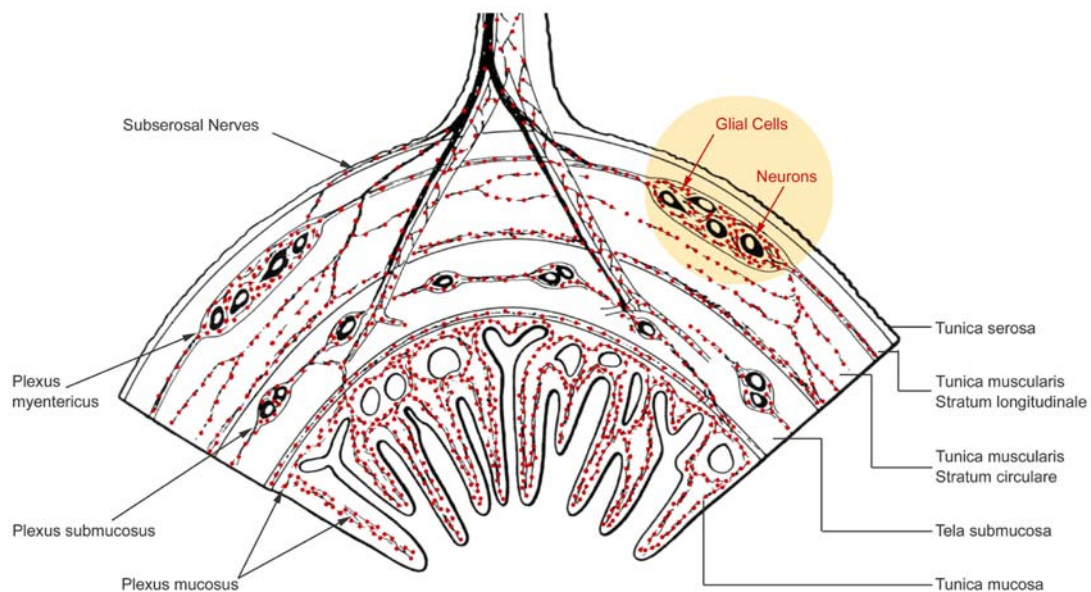
Figure 2.   Enteric glial cells are located at all levels of the gut wall. EGC are symbolized by red dots in this partial cross section of the intestinal tube (Ruhl 2005) after modification from (Furness & Costa 1980).

In both man and guinea pig, enteric plexuses (SMP and MP) are made up from ganglia – consisting of neuronal cell bodies and glial cells with their processes – and interganglionic nerve strands that contain neuronal cell processes accompanied by glial cell bodies and processes. Blood vessels and connective tissue are absent from inside the ganglia or nerve strands (Gabella 1981).

Enteric glial cells (EGC) are star-shaped cells characterized by their relatively small cell body and many processes of variable length and shape (Bjorklund et al 1984, Gabella 1981, Hanani & Reichenbach 1994). Based on morphology two subtypes have been proposed. Within ganglia, EGC are tightly packed and characterized by short (~10-30 nm) and irregularly branched processes; lying in fiber tracts they have long processes (~80 nm) running in parallel to the nerve fibers and being less frequently branched (Gabella 1981, Hanani & Reichenbach 1994). These long laminar processes extend between nerve processes and ensheath multiaxonal bundles, but rarely form a sheath around individual neurites (Cook & Burnstock 1976, Gabella 1981). Ultrastructurally, EGC have several flat endfeet at the lamina surrounding the ganglia or abut on small blood vessels at the border of ganglia or contact the epithelial basement membrane (Gabella 1972, Hanani & Reichenbach 1994). It has also been shown that glial cell bodies lie in close proximity (~1 µm) to epithelial cells (Bush et al 1998, Cornet et al 2001, Neunlist et al 2007, Wedel et al 1999).

EGC are dye-coupled (Hanani et al 1989) and the staining pattern of the intracellularly injected dye Lucifer yellow is comparable to the immunostaining of the gliamarker S100b. They form a dense network at the level of the crypt basis (Figure 3).
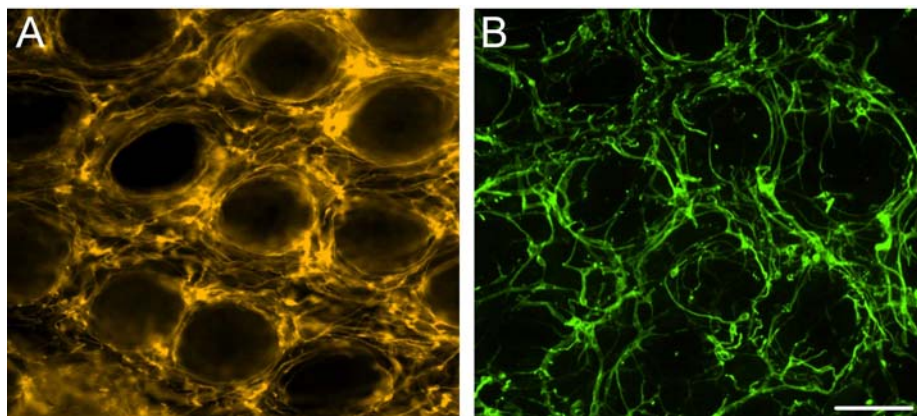
Figure 3. **Enteric glial cells form a dense network at the basis of the crypts.** Whole-mount preparations of the human mucosal plexus from sigmoid colon were stained with the glial and neuronal marker low affinity nerve growth factor receptor p75 (A) and the glial marker S100b (B). Secondary antibodies coupled to Cy3 (A) and Cy2 (B) were used for visualization. Scale bar = 100 µm.

Glial cells of the central nervous system were discovered in 1856 by the pathologist Rudolf Virchow (Virchow 1856). Since their first description in the gastrointestinal tract by Dogiel in 1899 (Dogiel & A.S. 1899), enteric glial cells (EGC) have been assumed to be the most abundant cell type in the ENS (Gabella 1981). However, quantitative data on glial cell numbers in the ENS are limited. A descriptive study of enteric ganglia from different mammals estimated the relative number of neurons and glial cells in the SMP and MP of several gut regions (Gabella & Trigg 1984). In another study, loss of EGC has been described in aged rats where it was accompanied by a proportional decline in neuronal numbers (Phillips et al 2004b). In this model, it is currently unclear if loss of EGC precedes or follows neuronal death. In the human ENS, substantial alterations of glial cells has been described in patients with various functional and/or inflammatory disorders including intractable slow transit constipation and diverticulitis (Bassotti et al 2005, Bassotti et al 2006a, Bassotti et al 2006b, Wedel et al 2002). Changes in EGC numbers were further observed in animal models of inflammatory bowel disease (IBD), as well as in Crohn's disease (CD) patients, potentially reflecting more general functional and structural alterations of the ENS in intestinal inflammation (Collins 1996, Geboes & Collins 1998). While there is evidence for EGC proliferation in a guinea pig model of TNBS ileitis (Bradley, Jr. et al 1997) and in patients with IBD (Collins 1996, Geboes & Collins 1998), a diminished EGC network was unexpectedly reported from a study of intestinal CD tissue sections (Cornet et al 2001). This latter finding, though, was recently challenged by another histomorphological study reporting increased EGC counts in the inflamed human intestine (von Boyen et al 2006a).

The apparent discrepancies in reported glial cell numbers are most likely due to the various approaches currently used to quantify EGC in intestinal tissue samples, some of which reflect the lack of a reliable marker to reproducible identify and quantify EGC in man and laboratory animals (Ruhl 2005). In addition, and even though it is generally agreed that whole-mount preparations allow for the most comprehensive morphometric assessment of the ENS (Wedel et al 1999), many researchers are using un-standardized biopsies, mucosectomy specimens or tissue sections to quantify individual cell types in the gut wall. The findings of such analyses are subsequently extrapolated to estimate overall numbers in the whole gut, which adds to the disparities in the published literature.

To address these issues, the **first aim** of this study was to systematically evaluate the established glial markers in the ENS employing immunohistochemistry in whole-mount preparations from human and guinea pig intestines. Based on these analyses, a

comprehensive set of quantitative data on enteric glia and neurons in all plexus layers of the human ileum and colon is provided, laying the basis for future pathological assessment of glial proliferation or degeneration in the diseased human gut.

Following morphological descriptions of EGC, the next step was to assess glial functions. Historically, glia – a derivation from the Greek word for 'glue' - were considered as packing material of the nervous system. However, nowadays evidence (from mouse models and clinical data) is accruing that EGC have a more vital function in the homeostasis of the gut and that they may play a much more active role in the physiology and pathophysiology of the gastrointestinal tract than traditionally assumed. In two independent transgenic mouse models, the selective ablation of enteric glia was accompanied by irreversible neuronal degeneration (Bush et al 1998) and intestinal disintegration (Bush et al 1998, Cornet et al 2001). Further, glial dysfunction affects the neurochemical coding (Aube et al 2006) and function (Aube et al 2006, Nasser et al 2006) of enteric neurons. Enteric glial cells have been implicated in neuronal transmission, since glutamate synthase, an enzyme possibly involved in breakdown of the neurotransmitter glutamate is only expressed in EGC (Jessen & Mirsky 1983, Kato et al 1990). Evidence for glial involvement in nitrergic neurotransmission comes from the immunohistochemical observation that L-arginine is exclusively located in EGC (Nagahama et al 2001). This amino acid is an essential precursor of the neurotransmitter nitric oxide (NO). Recently, the oligopeptide transporter PEPT2 has been shown to be predominantly expressed by EGC; PEPT2 has the potential to contribute to the clearance of neuropeptide degradation products (Ruhl et al 2005).

Glial cells can also interact with immune cells. EGCs are capable to respond to immune-stimulation with expression of the proinflammatory cytokines IL-1β, IL-6 and tumor necrosis factor-α (TNFα) (Ruhl et al 1994, Ruhl et al 2001c, Ruhl et al 2001a). IL-1β functionally acts through IL-1β receptors and up-regulates IL-6 expression with feedback inhibition of IL-6 (Ruhl et al 2001a). IL-1β can further increase proliferation of EGC *in vitro*, whereas IL-10 has dual effects: in low-dose concentration it suppresses proliferation and at high doses it promotes EGC proliferation (Ruhl et al 2001b). Glial expression of *c-fos*, which is a marker of early cell activation, is also up regulated in isolated EGC cultures and isolated tissues by proinflammatory mediators like IL-1β and TNFα (Ruhl et al 2001c, Tjwa et al 2003). Finally, evidence for the concept that EGC respond to immune stimulation and may act as potent effector cells in tissue inflammation comes from a study demonstrating enhanced secretion of matrix

metalloproteinases in EGC cultures, which then could have the ability to directly act on their microenvironment (Lin et al 2007).

In an *in vitro* model with EGC cultures, the expression of major histocompatibility complex (MHC) class II molecules and ICAM-1 (intercellular adhesion molecule-1), that promote adhesion between T-cells and antigen presenting cells, could be induced by a combination of interferon-γ (IFNγ) and TNFα, giving EGC the ability to process and present antigens efficiently to specific T-cells (Hollenbach et al 2000). More evidence that EGC are immunocompetent cells comes from the observation of upregulated glial expression of MHC class II antigens in ganglia of the SMP and MP and glial processes that ensheathe nerve fibers in IBD (Geboes et al 1992).

In recent years, more attention has been paid to the ENS in inflammatory bowel disease (IBD). There are several studies showing functional and structural alterations of the ENS (Collins 1996, Geboes & Collins 1998, Lomax et al 2005) and, consequently, it has been suggested to be involved in the pathogenesis of IBD.

Inflammatory bowel disease comprises primarily the two disorders Crohn's disease (CD) and ulcerative colitis (UC), which are differentiated based on clinical and histopathology features. While in UC inflammation is typically restricted to the colon, CD can involve all parts of the gastrointestinal tract from mouth to anus, and it is most common in the distal small intestine and colon (Podolsky 2002). Patchy areas of inflammation, which may affect the full thickness of the gut wall from mucosa to serosa and with granulomas found in 15-70% of all CD patients (Chambers & Morson 1979, Okada et al 1991), are hallmark features for CD, whereas in UC the inflamed area is continuous with mucosal involvement only. Diarrhea, abdominal pain and often a concomitant weight loss are symptoms typically seen in CD. Strictures and fistulas are common complications with a need for subsequent surgery (Sands 2002). Clinical features of UC include fever, diarrhea, rectal bleeding and different degrees of abdominal pain. Signs of malnutrition and weight loss are also fairly common (Sands 2002).

Crohn's disease was named after an American gastroenterologist: In 1932, the landmark publication of Crohn, Ginzburg and Oppenheimer described a group of patients with regional inflammation in the terminal ileum (Crohn et al 1932). Over time, there were several terms for this disease, like "terminal ileitis", "regional enteritis" and "granulomatous enterocolitis" but these were all found to be somewhat improper so that

in the end "Crohn's disease" was adopted to encompass the many clinical presentations of this pathological entity (Sands 2002).

Epidemiological studies found geographic and temporal trends of incidence for CD which is most frequently diagnosed among persons 15-30 years of age (Sands 2002). Prevalence of IBD increased in Europe and North America with a sharp rise in incidence in the second half of the last century and is becoming more common in the rest of the world as different countries adopt a Western lifestyle (Loftus 2004). In Germany, about 300,000 people are affected by IBD (Rogler 2007).

This led to the suggestion of an environmental contribution to the manifestation of the disease. Environmental factors that have been proposed to be involved in CD pathogenesis are smoking, which is protective in UC, but detrimental in CD, breast-feeding to be protective for IBD, diet, nonsteroidal anti-inflammatory drugs (NSAIDs), oral contraceptives, antibiotics, stress and inflammation (Sands 2002, Sartor 2006). The etiologies of these (CD and UC) chronic, recurrent, immunologically mediated disorders are still uncertain, but there is compelling evidence for an interplay of genetic, environmental, microbial and immune factors for disease pathogenesis (Sartor 2006).

Genetic factors play an important role in the pathogenesis of inflammatory bowel disease (IBD). Evidence came from epidemiological studies showing different incidence rates for different races and ethnic groups, familial aggregation and high concordance for IBD type in monozygotic vs. dizygotic twins (Annese et al 2003). So far, 4 genes have been associated with CD, with CARD15 (caspase recruitment domain family member 15, formerly known as NOD2) being the first disease gene identified (Hugot et al 2001, Ogura et al 2001). All CD genes are involved in the regulation of innate immunity, mucosal barrier function and bacterial killing (Sartor 2006).

Inflammation in IBD is triggered by stimulation of the mucosal immune system by antigens believed to be of bacterial origin. Bacterial antigens may activate the adaptive immune system by direct interaction of bacterial products that have penetrated the intestinal barrier with immune cells, or they may stimulate the epithelium by contact with receptors of the innate immune system. The epithelium can in turn produce cytokines and chemokines that recruit and activate mucosal immune cells. Classic antigen-presenting cells (e.g. dendritic cells, macrophages) process antigens and present them to CD4+ cells, leading to activation and differentiation of T cells. In patients with CD, the balance of T cells is skewed towards type 1 helper T cells (Th1). Th1 products (e.g. IFNγ) promote a self-sustaining cycle with macrophages that produce key proinflammatory cytokines such as TNFα, IL-1β and IL-6. This cytokine-mediated

response amplification leads to activation of several other cell types, which include fibroblasts, epithelial cells and endothelial cells that recruit immune cells from the vascular circulation to the mucosa, leading to acute tissue injury.

Besides activation of the innate and acquired immune response, there is also loss of tolerance to enteric commensal bacteria in IBD (Sartor 2004). The enteric microflora can act to stimulate immune responses either as adjuvants or antigens. Innate immune responses are activated by adjuvants (e.g. lipopolysaccharide, peptidoglycan, flagellin and nonmethylated DNA) which bind to Toll-like receptors located on innate immune cells, intestinal epithelial cells and mesenchymal cells (Cario 2005). This in turn activates NFκB and mitogen-activated protein kinases, two major signalling pathways in IBD that activate the transcription of proinflammatory and regulatory genes. Acting as antigens, the enteric microflora promotes a cascade with increase in T cells that selectively recognize the antigen through their T cell receptor (Sartor 2006).

Taken together the various ways how EGC are functioning in the gut and the background of the complex etiology of IBD, form the basis for another focus of interest. Therefore, and as a logical consequence derived from the first issue, which was the quantitative evaluation of EGC in healthy tissue, the **second aim** was to assess whether alteration in EGC numbers can be found in tissues of patients with CD or not. Strong evidence from the literature (Geboes & Collins 1998) and a recent publication on myenteric plexitis by an experienced Belgian group in the IBD field (Ferrante et al 2006) corroborates this.

Finally, it has been proposed that a defective mucosal barrier could also contribute to the etiopathogenesis of IBD by allowing for an increased translocation of luminal antigens across the epithelium that overwhelms the net suppressive tone of the mucosal immune system. Under normal conditions, the epithelial lining of the gut wall provides a selective permeability barrier against toxic or noxious luminal agents and microorganisms, while simultaneously controlling and regulating the uptake of nutrients, solutes and water. Mucosal barrier function is regulated by the epithelial apical junctional complex (AJC) consisting of the tight junction and the adherens junction (Ma & Anderson 2006). Major transmembrane proteins in the AJC are occludin, claudins, junctional adhesion molecules (JAMs) and E-cadherin (Laukoetter et al 2006). There are two routes, by which components of the lumen can cross this epithelial barrier, either across cells or across the space between them, referred to as the transcellular and paracellular pathways, respectively (Figure 4).
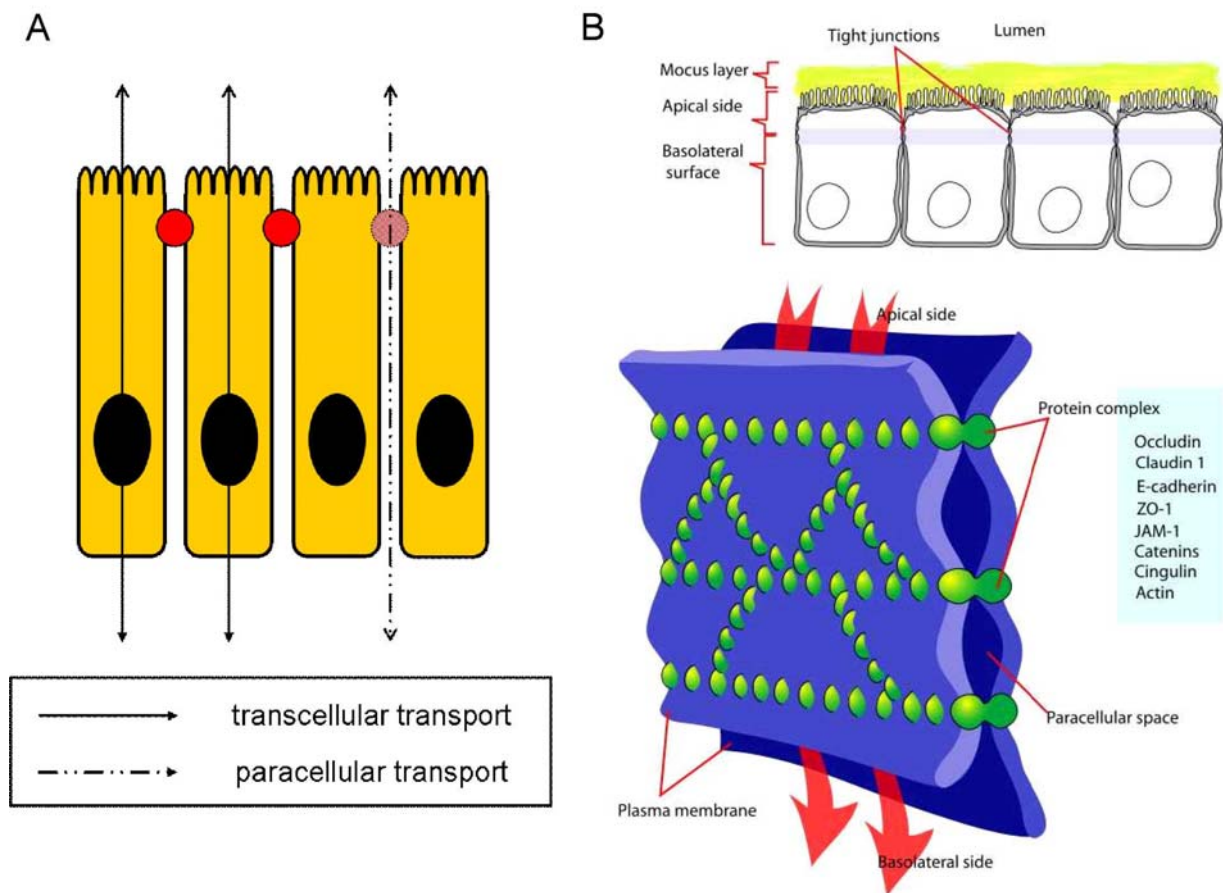
Figure 4. **Schematic of tight junctions located at the apical side of intestinal epithelial cells.** (A) The two main pathways of molecule transport are displayed: the transcellular way through the cell and the paracellular way across tight junctions (symbolized as full red circles). (B) Schematic of tight junctions reduced and enhanced in detail.

The paracellular transport is controlled by tight junctions (TJ). TJs are closely associated areas of two cells whose membranes are joined to form a virtual impermeable barrier to fluid. The TJ barrier is highly regulated and determines the characteristics of the paracellular barrier and its selectivity (Ma & Anderson 2006). Cytokines like IFNγ, TNFα and Interleukin-13 (IL-13) can regulate these TJ (Bruewer et al 2003, Sanders et al 1995). They have the potential to decrease transepithelial resistance (TER), and to increase epithelial permeability, an effect that is reversible and dose-dependent (Bruewer et al 2003, Heller et al 2005, Mullin & Snock 1990, Sanders et al 1995). It has been shown that these cytokine-mediated effects are apoptosis independent (Bruewer et al 2003). Elevated levels of proinflammatory cytokines are a well established occurrence in patients with active Crohn's disease (Raddatz et al 2005, Schreiber et al 1999, Woywodt et al 1999). Therefore, it is most likely that the detection of increased epithelial permeability of the mucosa in CD is cytokine mediated. However, it still has to be determined what the exact source of those cytokines is.

EGC are abundant in the intestinal mucosa and have been shown to be closely juxtaposed to intestinal epithelial cells *in vivo*. As such, they are ideally placed to secrete molecules that can interact with the epithelial basolateral membrane and thus alter mucosal permeability (Figure 3) (Savidge et al 2007). Just recently, new evidence was reported to support glial involvement in the regulation of the intestinal epithelial barrier, and glial-derived S-nitrosoglutathione (GSNO) was identified as a potent inducer of mucosal barrier tightness *in vitro* and *in vivo* (Savidge et al 2007).

The idea, that enteric glia play an important role in intestinal inflammation was powerfully promoted by the development of transgenic mouse models, in which enteric glial cells were selectively ablated. This was achieved either by expression of the herpes simplex virus thymidine kinase gene (HSVtk) (Bush et al 1998) or the influenza virus haemagglutinin (HA) receptor (Cornet et al 2001) under the control of the glial-specific promoter for glial fibrillary acidic protein (GFAP). Administration of the anti-herpetic drug ganciclovir (GCV) to GFAP-HSVtk transgenic animals selectively ablated EGC. Mammalian thymidine kinases cannot phosphorylate GCV, but the viral enzyme (HSVtk) with the triphosphorylated form of GCV inhibiting nucleic polymerases (Bush 2002). In the other model, crossing GFAP-HA transgenic mice with CL4-TCR transgenic mice generates double transgenic animals (GFAP-HA×CL4-TCR) in which most CD8+ T cell target a EGC-specific neoself antigen (Cornet et al 2001). This resulted in mucosal disintegration with consecutive intestinal inflammation and ultimately death of the animals. Loss of peripheral GFAP-expressing EGC in the distal small intestine precedes the intestinal pathology in GFAP-HSVtk transgenic mice treated with the antiviral drug ganciclovir (Bush et al 1998). These observations suggested that mucosal barrier function might be adversely affected by enteric glial cell dysfunction, or, put the other way, that enteric glia supports intestinal epithelial barrier integrity. Thus, interactions between enteric glia and mucosal epithelial cells may have clinical implications in disorders with impaired intestinal permeability such as Crohn's disease (Buhner et al 2006, Fries et al 2005, Suenaert et al 2005), where the enteric glial cell network has been suggested to be significantly disrupted (Cabarrocas et al 2003, Cornet et al 2001).

To shortly sum up, it is proven that EGC play a pivotal role in gut homeostasis and there is also strong evidence for EGC involvement in IBD, but not all results uniformly point into one direction. Therefore, the establishment of a reliable and specific marker to label all EGC opens up a new choice to precisely assess the quantitative alterations of EGC seen in IBD. A comprehensive data set on human EGC numbers and density provides

the basis for this pathological assessment of glial proliferation or degeneration in the diseased human gut. Additionally, it is just a short step from the scope of descriptive measures to question the reasons and principles for the described alterations. Some molecules already have been identified which may be associated with those structural changes seen in IBD.

Neurotrophins are a family of proteins which enhance the growth and induce the survival of neurons and play a role in neuronal differentiation. A number of neurotrophins, such as nerve growth factor (NGF) and neurotrophin-3 (NT-3) as well as the neurotrophic factor glial cell line-derived neurotrophic factor (GDNF) have been implicated in the regulation of intestinal barrier function by EGC. Increased expression of GDNF and NGF was detected in patients with IBD (Di Mola et al 2000, Steinkamp et al 2003). In another approach, immunodepletion of NGF and NT-3 increases the severity of experimental intestinal inflammation (Reinshagen et al 2000). GDNF can downregulate apoptosis rates of intestinal epithelial cells (Steinkamp et al 2003), and the expression of GDNF as well as that of NGF in EGC can be stimulated by these proinflammatory cytokines (von Boyen et al 2006b, von Boyen et al 2006a), which are also found elevated in IBD.

In order to assess the just above listed evidence of EGC involvement in IBD via neurotrophins and neurotrophic factors together with the ability of cytokines to alter the intestinal epithelial permeability in one model, a new approach had to be adopted in which the pivotal role of EGC in the gut can be resembled. Accordingly, the **third aim** of this project addresses those effects EGC exert on epithelial cells and the factors mediating glial-mucosal interactions and their regulation. A unique tissue culture system in which isolated EGC and intestinal epithelial cells are combined was used. This system allows for the evaluation of how the presence or absence of enteric glia changes the functional properties of the epithelial cells and how this is influenced by proinflammatory cytokines. Additionally, the expression of glial factors potentially involved in mucosal regulation (e.g. neurotrophic factors and their receptors) was analyzed.

Overall, this project aimed to expand the understanding of the enteric glial cells as a pivotal part of the ENS. Morphological analyses of healthy (first aim) and inflamed tissues (second aim), as well as functional characterization of glial-epithelial interactions and contributing factors (third aim) were expected to further the understanding of glial-

related mechanisms underlying the multiple stages of gastrointestinal inflammation. The hope for the future is that this understanding will ultimately help to identify a novel avenue for therapeutic approaches to IBD.

2.   Material and Methods

For a complete list of all materials used during this project please see appendix.

2.1.   Morphological analyses (*ex vivo* studies)

2.1.1. Subjects and tissue specimens

Human tissue

Fresh human ileal and colonic tissue samples were obtained from 29 adult patients (14 females, 15 males) with a median age of 65 yrs (range: 43-82 yrs) undergoing surgery in the Department of Surgery at the Medical Clinic in Freising and the Medical Clinic of the Technische Universität Munich (cf. Table S 11). Indications for intestinal resections were: colorectal carcinoma (27), pancreatic carcinoma (1) and multiple colonic polyps (1). Ten specimens of ileum, 10 of ascending colon, and 12 of sigmoid colon were examined, including 3 patients from whom both ileum and ascending colon were available. Informed consent was obtained from all patients, and the study was approved by the Ethics Committee of the Technical University of Munich (project 1071/04). All tissues used for morphometric analyses of controls were macroscopically normal segments from uninvolved resection margins. Resectates from ileum and ascending colon were also used as controls for Crohn's disease tissues. Summarized information about control tissues used for CD comparison is given in Table 1.

Table 1.   Patient characteristics of the subset of control tissues used for comparison with CD tissues.

Patient No.	Age (yrs)	Sex	Diagnosis	Assessed region
1	71	M	Colorectal carcinoma	Ileum
2	77	M	Pancreatic carcinoma	Ileum
3	52	F	Colorectal carcinoma	Ileum
4	65	M	Colorectal carcinoma	Ileum
5	66	F	Colorectal carcinoma	Ileum
6	64	M	Colorectal carcinoma	Ascending colon
7	60	M	Colorectal carcinoma	Ascending colon
8	65	F	Colorectal carcinoma	Ascending colon
9	63	M	Colorectal carcinoma	Ascending colon
10	76	F	Colorectal carcinoma	Ileum, ascending colon
11	68	F	Colorectal carcinoma	Ascending colon
Median age	65	(range: 52-77 yrs)		

Crohn's disease patients and tissue specimens

Crohn's disease (CD) specimens were obtained from 10 patients (5 females, 5 males) with a median age of 44 yrs (range: 17-59 yrs) undergoing surgery in the Department of Gastroenterology in the Hospital Munich-Bogenhausen in Munich. For each patient, one tissue sample was from the acutely inflamed area and another tissue sample was from the uninvolved proximal or distal resection margin, or from both. Eight specimens of unaffected ileum, 5 from the inflamed area (3 ileum, 2 colon) and 7 colonic resectates were assessed. Detailed information on tissue samples from patients with CD is given in Table 2. The Vienna classification was used to categorize the analyzed tissues by clinical phenotypes of CD. The classification comprises the variables age of diagnosis (A1 <40 yrs; A2 ≥40 yrs), disease location (L1 terminal ileum; L2 colon; L3 ileocolon; L4 upper gastrointestinal tract), and disease behavior (B1 non-stricturing non-penetrating; B2 stricturing; B3 penetrating) (Gasche et al 2000). In these patients, CD was proven histologically in resection specimens by experienced pathologists from the Department of Pathology in the Hospital Munich-Bogenhausen in Munich. Informed consent to use the respective tissues for scientific purposes was obtained from all patients, and the study was approved by the local Ethics Committee of the Technical University of Munich.

Table 2.   Characteristics of patients with Crohn's disease.

Patient No.	Age (yrs)	Sex	Reason for resection	CD diagnosed before (yrs)	Vienna classification[1]	Assessed region
1	27	F	Internal fistula	8	A1L1B3	Ileum (prox.; inflamed)
2	37	F	Stenosis	8	A1L1B2	Ileum (prox.), colon (dist.)
3	17	M	Abscess at end of blind fistula	2 month	A1L1B3	Ileum (prox.; inflamed), colon (dist.)
4	59	M	Stenosis	5	A1L3B2	Ileum (prox.), colon (dist.)
5	48	F	-*	-*	A2L3B2	Ileum (prox.), colon (dist.)
6	36	M	Stenosis	17	A1L3B3	Ileum (prox.), colon (dist.)
7	45	M	Conglomerate tumor with loop abscess	5	A2L1B3	Ileum (prox.; inflamed), colon (dist.)
8	46	M	Multiple stenoses	26	A2L3B3	Ileum (prox.)
9	50	F	-*	-*	A2L2B3	Colon (inflamed; dist.)
10	43	F	Enterocutaneous fistula	21	A2L3B3	Colon (inflamed)
Median age	44		(range: 17-59 yrs)			

[1](Gasche et al 2000); *data missing.

2.1.2. Whole-mount preparations

Human specimens

Specimens of resected human tissues were placed in a Sylgard-coated (cf. Table S 9) glass dissection dish (Schott, Mainz) containing ice-cold Krebs' solution that was changed every 10 min. The dissection was performed under a stereo microscope (SZ51; Olympus, Hamburg) equipped with a cold light source (Hightlight 2100; Olympus, Hamburg). Gut segments were split open in longitudinal direction using large scissors (14054-13; Fine Science Tools, Heidelberg) and pinned flat with the mucosal side down.

The SMP layer on the bottom of the dish was slightly stretched with a fine dissection forceps (11252-20; Fine Science Tools, Heidelberg) and insect pins (26002-20; Fine Science Tools, Heidelberg) were placed in the tissue near the edges at a distance of 5-10 mm using another dissection forceps (HTC 091-10; Hammacher, Solingen). The muscle layers with the myenteric plexus (MP) attached were removed from the submucous plexus (SMP) layer using dissection scissors with angled up blades (15013-12; Fine Science Tools, Heidelberg) cutting near the circular muscle layer of the tunica muscularis. The muscle layer coiled up slightly while dissecting and was taken off.

The submucous layer with adherent mucosa was turned around and mounted again in the dish under maximal stretch, which could be exerted without tearing the tissue. Subsequently, the mucosa was removed using a fine dissection forceps (11252-20; Fine Science Tools, Heidelberg). The muscle layer was pinned flat in another dissection dish. Tissues were maximally stretched and fixed in 0.1 M phosphate buffer (PB) containing 4% (w/v) paraformaldehyde and 0.2% (v/v) picric acid at room temperature over night. After three consecutive PB washing steps, fixed tissues were further microdissected: For the MP, longitudinal and circumferential muscle fibers were removed using fine dissection forceps until only the plexus with some adherent muscle fibers was remaining. To obtain the inner, the intermediate and the external SMP, the remaining mucosa and mucous plexus was separated from the submucosa which was subsequently dissected with fine dissection scissors (15396-02; Fine Scinece Tools, Heidelberg) into its three separate layers where the three respective SMP sublayers are situated.

Some tissues, which could not be microdissected immediately after fixation, were stored up to three years in phosphate buffered saline containing 0.1 % (w/v) sodium azide (PBS/NaN$_3$) that was changed every 6-9 month.

Guinea pig samples

Guinea pigs were killed by concussion and exsanguination from their cervical vessels. The entire gastrointestinal tract was quickly removed and placed in Krebs' solution as described above. Specimens of ileum, proximal and distal colon were separated, opened along the mesenteric border, washed, and dissected as described for human tissues except that the SMP was not further separated. Longitudinal muscle myenteric plexus preparations and preparations containing the submucous plexus from ileum, proximal and distal colon of each animal were used for immunohistochemistry.

2.1.3. Antibody characterization

The monoclonal Sox8/9/10 antibody was first described as a Sox10 antiserum (Paratore et al., 2001). Denatured Sox10 holoprotein, which has been produced as bacterial 6xHis fusion protein and purified by Ni-NTA chromatography, was used as antigen to raise an antiserum in mouse (Kuhlbrodt et al 1998). The monoclonal Sox8/9/10 antibody recognizes an epitope within the high-mobility-group DNA-binding domain. Negative controls to assess staining specificity were performed by omitting primary antibodies or using pre-absorbed Sox8/9/10 anti-serum. For pre-absorption, the undiluted Sox8/9/10 anti-serum was incubated with Sox10 protein 1:10 (v/v) at 4°C over night. The Sox10 protein (provided by M. Wegner) was generated as fusion protein from a 25 kD fragment of the Sox10 protein and glutathione-S-transferase (26 kD), and recombinantly produced in bacteria with subsequent purification. Purity of the derived Sox10 protein was 80-90 % at a concentration of 0.1 mg/μl.

The following additional antibodies directed against established glial markers were used:

(1) A polyclonal S100 antibody with a cytoplasmatic staining pattern labeling glial cell bodies and processes. Specificity was established by two-dimensional immunoelectrophoresis displaying only one distinct double peak (S100 A and B) and no reaction with human plasma and cow serum. Using ELISA, the antibody shows no reaction with normal human plasma and cow serum (Dako; on file). As detailed in the results section, the pattern of S100 immunoreactivity obtained with the polyclonal S100 antibody used for the present work is in accordance with previously published results (Krammer et al 1994).

(2) A polyclonal GFAP antibody, which labels glial cell bodies and processes. In two-dimensional immunoelectrophoresis only one distinct precipitate (GFAP) and no reaction with human plasma and cow serum was shown. Using indirect ELISA, the

antibody does not react with normal human plasma and cow serum (Dako; on file). As detailed in the results section, the pattern of GFAP immunoreactivity obtained with the polyclonal GFAP antibody used for the present work is in accordance with previously published results (Ruhl et al 2005).

Both a previously described monoclonal S100 antibody (clone 15E2E2) (Loeffel et al 1985) as well as a previously described monoclonal GFAP antibody (clone 2.2B10) recognizing a 51 kD protein (Lee et al 1984) did not show any discernible immunoreactivity in human ileum and colon (Chemicon and Zytomed, respectively; on file).

(3) A monoclonal p75NGFR antibody (clone NGFR5), which recognizes a 75kD protein (Dianova; on file), showed a cytoplasmatic staining pattern with immunoreactivity in glial cell bodies and processes, but also neuronal fiber-like structures as previously described (Kondyli et al 2005).

Neuronal parts of the ENS were identified with an antibody directed against Neuron-specific Enolase (NSE) which labeled neuronal perikarya and nerve fibers. The polyclonal NSE antibody used for the present work recognizes a 48 kD protein (Marangos et al 1975) and - as detailed in the results section - shows the same pattern of cellular morphology and distribution as previously reported in the ENS (Murphy et al 2007, Parr & Sharkey 1994).

Neuronal protein HuC/HuD (HuC/D) monoclonal (clone 16A11) antibody labeled neuronal cell nuclei and perikarya, recognizing an epitope within the carboxy-terminal domain of HuD (Marusich et al 1994). Staining pattern of cellular morphology and distribution is the same as previously described (Lin et al 2002, Murphy et al 2007). Staining pattern of biotin conjugated HuC/D monoclonal antibody is identical to that of the un-conjugated antibody.

The polyclonal antibody directed against Protein gene product 9.5 (PGP 9.5), *i.e.* an intracellular ubiquitin hydrolase, labeled neuronal perikarya and nerve fibers. As detailed in the results section, the PGP 9.5 antibody used for the present work displayed the same pattern of cellular morphology and distribution as previously published (Parr & Sharkey 1994).

2.1.4. Immunohistochemistry

After dissection, about 1 cm^2 of each whole-mount preparation was processed for immunohistochemistry. After three consecutive rinses with phosphate buffered saline (PBS, pH 7.4) (each for 10 min), specimens were placed in blocking serum (4% horse or goat serum, 0.5% Triton X-100, 0.1% NaN$_3$ in PBS) for 1 hr. Human tissues were incubated with primary antibodies for 40-48 hrs and guinea pig tissues for 12-16 hrs. A list of the primary antibodies used in this study is shown in Table 3. Subsequently, tissues were washed in PBS (3 x 10 min) and incubated with the respective secondary antibodies for 20-24 hrs (human tissues) or 2 hrs (guinea pig tissues). The list of secondary antibodies is provided in Table 4. After incubation with the secondary antibodies, tissues were thoroughly washed (3 x 10 min) and mounted on poly-L-lysine coated glass coverslips (Huang et al 1983) (cf. Table S 9). Whole-mount preparations were assessed under an epifluorescence microscope (BX61 WI, Olympus, Hamburg) fitted with the appropriate filter blocks. The microscope was connected to a SIS Fview II CCD camera and the analySIS 3.1 software (Soft Imaging System GmbH, Münster) for image acquisition and analysis. False-colored pictures were adjusted for contrast and brightness prior to overlay and quantification. All pictures for publication figures were imported into Microsoft PowerPoint 2003 (Microsoft, Unterschleißheim) for alignment and labeling. Graphs were created with SigmaPlot (Systat Software, Erkrath). The finished figures were imported as WMF files into Paint Shop Pro 7 (Corel, Unterschleißheim) without further change and saved as TIF files at 600dpi.

Table 3.   Primary antibodies used in human and guinea pig tissues.

Antibody	Immunogen	Host	Dilution	Source
Neuron-specific enolase (NSE) polyclonal	Gamma-subunit of NSE (or nervous system-specific protein 14-3-2) from rat brain	Rabbit	1:3,000-1:4,000 (human) 1:5,000 (guinea pig)	16625, Polysciences, Eppelheim, Germany
Neuronal protein HuC/HuD (HuC/D) monoclonal (clone 16A11)	12 residue synthetic peptide representing amino acids 240-251 from human HuD recognizing an epitope within the carboxy-terminal domain of HuD	Mouse	1:50	A21271, Molecular Probes, purchased from MoBiTec, Göttingen, Germany
HuC/HuD (HuC/D) (biotin conjugate) monoclonal	12 residue synthetic peptide representing amino acids 240-251 from human HuD recognizing an epitope within the carboxy-terminal domain of HuD	Mouse	1:50	A21272, Molecular Probes, purchased from MoBiTec, Göttingen, Germany

Table 3   *(Continued).*

Protein gene product 9.5 (PGP 9.5) (ubiquitin hydrolase) polyclonal	24 residue synthetic peptide representing amino acids 187-210 from human PGP 9.5	Sheep	1:10,000	PH164CUS01, The Binding Site, Birmingham, UK
Sox8/9/10 monoclonal	Purified bacterially expressed rat Sox10 protein; epitope: N-terminus of Sox10 including high-mobility-group DNA-binding domain[1]	Mouse	1:10 (human) 1:50-1:100 (guinea pig)	M. Wegner / University of Erlangen-Nürnberg / Germany
Sox10 polyclonal	Purified bacterially expressed protein consisting of amino acids 181-233 and 308-400 of rat Sox10 (Maka et al., 2005).	Guinea pig	1:2000	M. Wegner / University of Erlangen-Nürnberg / Germany
S100 polyclonal	Purified S100 protein isolated from cow brain	Rabbit	1:2000	Z0311, DakoCytomation, Hamburg, Germany
S100 monoclonal (clone 15E2E2)	Purified bovine S100 protein	Mouse	1:500	MAB079, Chemicon, Hampshire, UK
GFAP polyclonal	GFAP isolated from cow spinal cord	rabbit	1:200	Z0334, DakoCytomation, Hamburg, Germany
GFAP monoclonal (clone 2.2B10)	Highly enriched glial filaments protein from bovine spinal cord	Rat	1:100-1:200	13-0300, Zytomed, Berlin, Germany
p75NGFR monoclonal (clone NGFR5)	NGFR from A875 melanoma cells (Marano et al., 1987.); epitope: amino acids 1-160	Mouse	undiluted	DLN-09256, Dianova, Hamburg, Germany

* No IR in human ileum and colon.[1] The sequence of rat Sox10 was determined in full and deposited in EMBL/GenBank under accession number AJ001029 (Kuhlbrodt et al 1998).

Table 4.   **Secondary antibodies used in human and guinea pig tissues.**

Antiserum	Dilution	Order number	Supplier
donkey anti-mouse IgG Cy3	1:500	715 165 151	Dianova, Hamburg
donkey anti-mouse IgG Cy2	1:200	711 225 152	Dianova, Hamburg
donkey anti-mouse IgG Cy5	1:500	715 175 151	Dianova, Hamburg
donkey anti-mouse IgG AMCA	1:50	715 155 151	Dianova, Hamburg
donkey anti-rabbit IgG Cy2	1:200	711 225 152	Dianova, Hamburg
donkey anti-rabbit IgG Cy3	1:500	711 165 152	Dianova, Hamburg
donkey anti-rat IgG Cy3	1:500	712 165 153	Dianova, Hamburg
goat anti guinea pig IgG Cy3	1:500	106 165 003	Dianova, Hamburg
Streptavidin Cy3	1:500	016 160 084	Dianova, Hamburg
donkey anti-sheep IgG Cy3	1:500	713 165 147	Dianova, Hamburg
donkey anti-sheep IgG Cy5	1:500	713 175 147	Dianova, Hamburg

All secondary antibodies were purchased from Dianova (Hamburg, Germany). AMCA aminomethyl-coumarin-acetat, Cy2 carbocyanin, Cy3 indocarbocyanin, Cy5 indodicarbocyanin.

2.1.5. Ala-Lys-AMCA labeling of enteric glial cells

Ala-Lys-AMCA dipeptide uptake in glial cells was conducted according to a previously published protocol (Ruhl et al 2005). Briefly, dissected tissues were mounted on small rings made of Sylgard (cf. Table S 9) and placed in a sterile culture dish and incubated in DMEM/F12 supplemented with 10% heat-inactivated horse serum and the fluorescent dipeptide Ala-Lys-AMCA in a final concentration of 25 µM (human) or 5 µM (guinea pig). Culture dishes were placed on a gently rocking horizontal shaker (self made) in a humidified incubator (37 °C; 5 % CO_2) for 4-8 hrs (human) or 3 hrs (guinea pig). Incubations were stopped by repeated washings with ice-cold PBS. Tissues were subsequently fixed and thereafter washed as described above. AMCA-labeled preparations were either immediately mounted and the presence of AMCA-fluorescence was assessed by epifluorescence microscopy, or the preparations were further processed for multiple labeling immunohistochemistry.

2.1.6. Validation of the enteric glial cell marker Sox8/9/10

Whole-mount preparations of MP and SMP from ileum and colon were labeled with antibodies directed against the calcium binding protein S100b, glial fibrillary acidic protein (GFAP), the low affinity nerve growth factor receptor p75 (p75NGFR) and an antibody (Ab) directed against the transcription factors Sox8, 9 and 10 (Sox8/9/10). The latter Ab was generated by one of the authors (Paratore et al 2001, Schmidt et al 2003). Neuronal counterstaining was performed with neuron-specific antibodies, namely anti-HuC/D, anti-neuron specific enolase (NSE), and/or anti-protein gene product 9.5 (PGP 9.5), yielding double- or triple-labeled preparations. In this series, all preparations were evaluated; tissues which were damaged at the dissection or staining process or tissues with insufficient immunostaining were rejected for further assessments. Ala-Lys-AMCA labeled tissues were double-labeled with the anti-Sox8/9/10 Ab.

2.1.7. Morphometric analysis

Quantitative analyses were carried out in tissues that were double-labeled with anti-NSE plus anti-Sox8/9/10 antibodies. From random areas of all human whole-mounts, at least 20 ganglia in the SMP and 10 in the MP were photomicrographed at a magnification of x20. Each field of view was focused separately and documented with a Cy2 followed by a Cy3 filter. False-colored pictures were adjusted for contrast and brightness prior to overlay and quantification.

For guinea pig tissues (SMP and MP) 6-12 photomicrographs were taken from adjacent sites containing at least 20 ganglia at a magnification of x10. The resulting images were processed as described above and merged by multiple image alignment to provide an overview which was used for quantification. The required number of pictures was dependent on size and shape of the individual ganglia.

ENS components that were quantitatively assessed

Glial cells (number and nuclear area) were identified by their clearly discernible Sox8/9/10 positive nuclei. All glial cells within the area of randomly selected ganglia (see above) were counted and expressed as *glial cells/ganglion*. *Glial nuclear area* was compared between SMP and MP of identical regions from the same patients or animals. ***Neuronal cell*** numbers were determined by counting all NSE-positive perikarya in randomly selected ganglia and expressed as *neuronal cells/ganglion*.

Ganglionic area was determined in ganglia which were defined as coherent clusters of at least 2 NSE-positive neurons at the junctions and branching points of primary and secondary nerve fiber strands, respectively. Isolated and disseminated neurons lying on nerve fiber strands were disregarded as proposed by Wedel and co-workers (Wedel et al 1999). Ganglia were defined as 2 separate entities if their borders were separated by a gap of at least two neurons in width. Cavities of the size of at least one single neuronal cell body within the ganglia were subtracted from the computed ganglionic area. ***Glial cell density*** in the ganglia was calculated from glial cell numbers and ganglionic area.

Extraganglionic area was automatically integrated from delineated primary and secondary nerve strands in the MP (cf. Figure 15). Glial cell density in the extraganglionic areas was calculated by counting all glial cells in the extraganglionic area adjacent to at least 10 ganglia, and expressed per proportionate nerve strands of one ganglion.

Quantification of glial cell numbers in SMP nerve strands could technically not be performed: Most SMP nerve strands became seriously damaged during the preparation procedure and undamaged ones could not be satisfactorily photomicrographed in a single plane of focus.

The parameters "***neurons per ganglionic area***", "***glial cells per ganglionic area***", "***glial cells per nerve strand area***" and the ***glia index***, i.e. ratio of EGC:neurons, were derived from the primary measures described above. Since tissue stretch can influence surface area, calculated cell numbers per surface area are biased. Therefore, multiple normalization methods (i.e., cells per ganglion and cells per ganglionic area) were used

to eliminate the effects of the pre-fixation stretching procedures and thus render present results more robust (Karaosmanoglu et al 1996, Parr & Sharkey 1997). In addition, previous reports have suggested that normalization can also help to correct for possible age-dependent changes in the tissue area (Gabella 1989, Hanani et al 2004, Johnson et al 1998, Phillips & Powley 2001, Phillips et al 2004b).

2.1.8. Statistical analysis of morphological studies

Mean scores for each gut region and plexus layer were computed using the medians of each tissue. Two-way analyses of variance (ANOVA) with Holm-Sidak tests for all pairwise multiple comparisons were performed separately for human and guinea pig to determine differences between gut regions and plexus layers. For species differences, unpaired Student's t-test was used to analyze the MP and one-way ANOVA with the Holm-Sidak method to compare all human SMP to guinea pig SMP. For the analysis of glial density and absolute EGC numbers in the ganglionic and extraganglionic area of the MP and gut regions of man and guinea pig, two-way ANOVA with Holm-Sidak in order to test which group(s) differed from the others were used. Differences of glial nuclear area were determined using two-way ANOVA with Holm-Sidak with the factors plexus layer and species.

Whole-mount preparations of all resected regions from CD patients could not always be obtained. Thus, data of each region were pooled and used for further testing. ANOVA with Holm-Sidak tests for all pairwise multiple comparisons was applied to detect if parameters from CD (proximal and distal resection margins, inflamed area) and controls (ileum, ascending colon) differed. Student's t-test was used to explore region specificity of control tissue variables.

Pearson's correlation was applied to test if age had any influence on glial and neuronal cell numbers, ganglionic area, glial and neuronal density in ganglia or the glia index in human specimens. This test was also conducted with data from patients with CD. Student's t-test was utilized to explore gender differences of all parameters obtained from human specimen.

The non-parametric tests ANOVA on ranks with Dunn's method and Mann-Whitney rank sum test was used for non-normally distributed mean scores. Data are visualized as box plots with medians and interquartile ranges. A level of probability $p \leq 0.05$ was considered statistically significant for all analyses. Statistical analyses were performed using the SigmaStat 3.1 software; graphs were created with SigmaPlot 9.01 (Systat Software, Erkrath).

2.2.   Coculture experiments (*in vitro* Studies)

A prerequisite to allow for the direct biochemical and molecular analysis of EGC – which are tightly intermingled with several other cell types in the intestinal wall - was the availability of isolated and purified cultures of EGC. A method developed previously to isolate rodent EGC (Ruhl et al 2001c) was adopted to the human enteric nervous system. Afterwards, interactions of glial cells and epithelial cells as important players of the microenvironment can be assessed using a novel co-culture system.

2.2.1. Isolation of human enteric glial cells

Subjects and tissue specimen

Human ileal and colonic tissue samples were obtained from 21 adult patients (11 females, 10 males) with a median age of 65 yrs (range: 40-89 yrs) undergoing surgery in the Department of Surgery at the Medical Clinic in Freising (cf. Table S 11). Indications for intestinal resections were: colorectal carcinoma (13), diverticulitis (4), multiple colonic polyps (2), benign stenosis of the sigmoid colon (1), and gastric carcinoma (1). Immediately after resection, tissue specimens were placed into sterile, ice-cold, oxygenated (95 % O_2, 5 % CO_2; pH 7.4) Krebs solution (composed of [mmol/l]: NaCl, 117; KCl, 4.7; $MgCl_2$, 1.2, NaH_2PO_4, 1.2, $NaHCO_3$, 25; $CaCl_2$, 2.5; and glucose, 11.5) supplemented with 1 % (v/v) antibiotic-antimycotic solution (containing 100 U/ml penicillin, 100 µg/ml streptomycin, and 250 ng/ml amphotericin B) (cf. Table S 8). Tissue samples were rapidly transported from the operating room to the laboratory where they were further processed. The tissues used for human glial cell isolation comprised only macroscopically normal intestinal segments from uninvolved resection margins. One specimen of jejunum, 6 of ileum, 4 of transverse colon, 4 of descending colon, and 6 of sigmoid colon were examined (cf. Table S 10). Informed consent was obtained from all patients, and the study was approved by the Ethics Committee of the Technical University of Munich (project 1071/04).

The isolation of human enteric glial cells was conducted in a as sterile as possible manner using sterile dissection forceps (Fine Science Tools, Heidelberg), sterile dissection scissors (Fine Science Tools, Heidelberg), and Sylgard-coated (cf. Table S 9) glass dissection dishes (Schott, Mainz) prepared with Ø 0.2 mm insect pins (Fine Science Tools, Heidelberg) that had been sterilized by dry heat for 2 hours at 180 °C. Sterile, ice-cold, oxygenated Krebs' solution supplemented with 1 % (v/v) antibiotic-

antimycotic solution was used throughout the dissection procedure and was changed every 10 min to ensure tissue viability and to minimize microbial growth. Sterile surgical gloves (Gammex PF; Ansell, Brussels, Belgium), a surgeon-face mask (BEEM-Visma Plus; B Braun, Melsungen) and a clean lab coat was worn to minimize external contamination of the tissue.

For cell isolation, all dissection steps are performed according to the description above (cf. 2.1.2) until the muscle layer containing the MP and the submucous plexus (SMP) layer are separated. In this case the submucosa and adherent mucosa were removed from the dish and the muscle layer was pinned flat in the dissection dish under maximal stretch with the serosal side up. Adherent visceral fat and connective tissue was removed and discarded. A piece of 2 x 3 cm was cut out of the MP layer and serosa and some of the longitudinal muscle layer were carefully dissected off using fine dissection instruments (11252-20; 15396-02; Fine Science Tools, Heidelberg) and discarded. The *myenteric plexus* is more tightly attached to the longitudinal muscle layer than to the circular muscle and was peeled off with the remaining longitudinal muscle strips. The muscle strips with adherent myenteric plexus were cut into pieces of about 5 mm^2 and put into 15 ml tubes (188271; Greiner Bio-One, Frickenhausen) containing 10 ml of dissociation solution on ice (cf. Table S 8). For the isolation of glial cells from the SMP, the mucosa was peeled off from a 2 x 3 cm piece of the SMP layer separated as described above. For this procedure, the tissue was mounted in a dissection dish under maximal stretch. After removal of the mucosa with fine forceps (11252-20; Fine Science Tools, Heidelberg), the SMP layer was cut into pieces of about 5 mm^2 and put into 15 ml tubes (188271; Greiner Bio-One, Frickenhausen) containing 10 ml of dissociation solution on ice (cf. Table S 8).

The pieces of tissue were digested for 30-45 min in a shaking water bath (1083; GFL - Gesellschaft für Labortechnik, Burgwedel) at 37 °C in Hanks Balanced Salt Solution (HBSS) (pH 7.4) containing 2350 mg/l HEPES, 2500 mg/l collagenase (type IA), 2000 mg/l protease (type IX derived from *Bacillus polymyxa*), 25 mg/l deoxyribonucelase I (DN-25), and 300 mg/l bovine serum albumin (fraction V) (modified from (Yau et al 1989)). After removal of the enzyme solution by two centrifugation steps (250 x g at 4 °C for 2 min and 5 min, respectively), the cells were seeded in three 25 cm^2 tissue culture flasks (Nunc, Wiesbaden) each containing 3 ml of DMEM/F12 supplemented with 20 % (v/v) heat-inactivated FBS, 2 % (v/v) AA (containing 100 U/ml penicillin, 100 µg/ml streptomycin, and 250 ng/ml amphotericin B), and additionally 1 %

(v/v) amphotericin B (2.5 mg/l). The cells were maintained in culture at 37 °C in a humidified 5 % CO_2 air atmosphere. Cell culture medium was changed 24 to 48 hours after seeding depending on how many cells had settled down on the bottom of the culture vessel, and then 3-4 times a week. In the first week, the antimitotic agent AraC (Sigma-Aldrich, Steinheim) was additionally added at a concentration of 10 µmol/l. At the beginning of the second week, the amphotericin B was omitted, and AA was reduced to 1 % (v/v) from the third week onwards. To stimulate glial cell growth, culture medium was supplemented with 1 µmol/l of forskolin (Sigma-Aldrich, Steinheim) and 500 µg/ml of BPE (Linaris, Wertheim) after removal of AraC based on the published potential of this treatment to stimulate the growth of Schwann cell in tissue culture (Jessen & Mirsky 1991, Raff et al 1978). Additionally, well growing cultures were used to generate glia-conditioned culture medium: culture medium was incubated with those cells for 4-8 hours after the medium change every other day, then taken off, filtered (0.2 µm; Sartorius, Göttingen) and used for slow growing cultures (Takahashi & Okada 1970).

2.2.2. Isolation of rat enteric glial cells

Enteric glial cells used in this study were generated as previously described (Ruhl et al 2001c). Briefly, the entire jejunum was removed from adult rats under sterile conditions, cut into 4-6 cm segments, which were opened along the mesentery and pinned with the serosal side up. The MP with the longitudinal muscle layer was peeled off from the circular muscle using dissection forceps, cut into about 5 mm^2 pieces and placed in Dulbecco's modified Eagle's medium (DMEM) containing 6 U/ml of dispase at 37 °C for 30-60 min. Dissociated cells were seeded into 75 cm^2 flasks and maintained in DMEM supplemented with 10% FBS, 1% AA solution, and the antimitotic agent AraC at a concentration of 10 µmol /l. After 2 weeks, Ara was replaced with BPE (500 µg/ml) and forskolin (1 µmol/l) (Jessen & Mirsky 1991, Raff et al 1978).

2.2.3. Complement lysis of enteric glial cells

After 3-4 weeks, depending on seeding density and growth rate of the primary cell cultures, antibody-mediated complement-lysis was used to eliminate faster growing fibroblasts from the primary cultures following a protocol initially described by Brockes (Brockes et al 1979). The cells were detached from the tissue culture flask with trypsin/EDTA, centrifuged (see 2.2.6) and the cell pellet in the 15 ml centrifugation tube

(188271; Greiner Bio-One, Frickenhausen) was mixed with 1 ml of a 1:1000 dilution of a monoclonal mouse anti-human CD90 antibody (Thy-1.1; BD Biosciences, Heidelberg). For each 10^6 cells 1 µl of anti-human CD90 antibody was used. If rat cultures were purified, mouse-anti-rat Thy-1.1 diluted in culture medium was used. For most of the cases, 2 ml of the antibody dilution was sufficient. The mixture was thoroughly triturated several times using a 1 ml syringe (Dispomed Witt, Gelnhausen) with a 20-gage needle (Heiland Medical, Wien, Austria) to break up cell clots and facilitate access of the antibody to its epitope. The suspended cells were incubated with the antibody for 30 min at 37 °C in a shaking water bath (1083; GFL - Gesellschaft für Labortechnik, Burgwedel). CD90 is a glycophosphatidylinositol anchored conserved cell surface protein found on fibroblasts, which therefore can be specifically tagged with an antibody directed against this surface marker. After 30 min of incubation, 200 µl of guinea pig complement (Cedarlane, Harnby, Canada) (cf. Table S 8) was added per µl of the anti-human CD90 dilution. The antibody tagged cells can be lysed by binding of complement and the subsequent initiation of cell lysis. The mixture was shaken for another 20 min at 37 °C. Then, excessive antibody and guinea pig complement were removed by centrifugation (250 x g for 5 min at 4 °C), and the cells were resuspended in culture medium supplemented with forskolin plus BPE and seeded in 25 cm² or 75 cm² flasks, depending on cell density. The cells were incubated at 37 °C in a humidified 5 % CO_2 air atmosphere and culture medium was changed 24 hours after complement lysis. When the cultures had once again grown to confluence, the supplements were omitted from the culture medium.

2.2.4. Assessment of enteric glial cell culture purity

Immunocytochemistry and morphology

Primary EGC cultures were morphologically and immunohistochemically characterized. Morphological assessment was performed with a phase-contrast microscope (DM IL; Leica Microsystems, Wetzlar). Identification and confirmation of the homogeneity of EGC cultures were performed with polyclonal antibodies against the cytoskeleton intermediate-filament protein GFAP (Z0334; DakoCytomation, Hamburg), the calcium binding protein S100b (Z0311; DakoCytomation, Hamburg), the nuclear stain Hoechst 33258 (861405; Sigma-Aldrich, Steinheim), and the transcription factors Sox8/9/10 (generous gift from M. Wegner; University of Erlangen-Nürnberg, Erlangen; cf. Table 3). For immunohistochemistry, cells at 80-90 % confluence were suspended with trypsin/EDTA and seeded on 24 x 24 mm cover slips (Menzel-Gläser, Braunschweig)

placed in sterile tissue culture dishes (Ø 60 mm; Greiner Bio-One, Frickenhausen) at a density of 10,000 cells per cm^2. The cells were maintained in culture for 24-72 hours until they reached subconfluence which was depending on growth rate. Within this period of time, culture medium was changed only 24 hours after seeding. The culture medium was carefully removed after the proliferation period, and the cells were rinsed with prewarmed PBS (cf. Table S 8) and fixed with -20 °C methanol (Mallinckrodt Baker, Griesheim) for 30 min. The following immunohistochemical staining procedure was done under constant agitation on a wave shaker (Polymax 1040; Heidolph Instruments, Schwabach) at room temperature. After three 10 min washing steps with PBS (4 °C), 500 µl of blocking solution (cf. Table S 8) were carefully trickled on the cover slip, followed by incubation for 30 min. Then, the primary and the secondary antibodies were applied for 2 and 1 hour, respectively, with 3 x 10 min washing steps in between. If more than one primary or secondary antibody was used for one staining procedure, they were mixed before use and applied simultaneously. Finally, the cover slips were rinsed 3 x 10 min before mounting them carefully on microscopy slides (Menzel-Gläser, Braunschweig) using fine forceps (11252-20; Fine Science Tools, Heidelberg) to grab and turn the cover slip. A self-made anti-fading mounting solution was used (cf. Table S 8). In order to show immunoreactivity of the Sox8/9/10 antibody to be glial specific and to demonstrate the purity of EGC cultures, Caco-2 cells and EGC were simultaneously seeded on cover slips and stained with the herein described protocol. Note that both cell types could make cellular contact in this type of coculture.

Metaphase spreads of EGC chromosomes

Metaphase spreads for karyotyping of rat EGC cultures were prepared to verify species specificity and to exclude cross contamination. A well proliferating EGC culture in a 75 cm^2 flask was incubated for 30-60 min with 10 µl of colcemid solution (Seromed, Berlin) per ml of medium to stop the cell cycle in the metaphase. Colcemid solution was prepared with 10 mg of colcemid/ml H_2O (Seromed Biochrom, Berlin) diluted in PBS buffer to a final concentration of 10 µg/ml. The cells were detached from the bottom of the flask with 4.5 ml of 0.05 % (v/v) trypsin/0.02 % (v/v) EDTA diluted in PBS and placed in a humidified incubator (95 % CO_2/5 % O_2) for 5 min. The cell suspension was transferred to a 50 ml tube and spun down for 10 min at 200 x g. The supernatant was taken off and the cell pellet was resuspended in 10 ml of prewarmed, hypotonic 0.075 M KCl solution and incubated in a waterbath at 37 °C for 15 min. Then 0.5 ml of fixative – a mixture of ice-cold methanol/glacial acetic acid 3:1 (v/v) – was added to the 10 ml and the suspension was centrifuged a second time for 10 min at 200 x g. After the

separation, the supernatant was discarded and the pellet was carefully resuspended with 10 ml of ice-cold fixative. The cells were fixed at -20 °C for 25 min. Afterwards, the pellet was washed three consecutive times with 10 ml of fixative. After the final centrifugation step, the supernatant was removed and the cells were resuspended in 2-5 ml of fixative. The metaphase preparations were fixed on glass slides according to the following protocol: Microscopy slides were cleaned with 70 % ethanol and prewarmed in the humidified atmosphere of a 55 °C waterbath. The chromosome solution was trickled on the prepared glass slides to spread the metaphase chromosomes, and the spreading chromosomes were immediately dried at 55 °C for 1 min. After fixation, the metaphase preparations were stained with 0.2 µg/ml DAPI or 0.8 µl/ml of a 1 mmol 7-Amino-Actinomycin D (7-AAD) solution mixed with 0.2 µg/ml DAPI, both diluted in PBS for 10 min. The preparation was washed in 4x SSC/ 0.2% Tween-20 or PBS. Glass slides were dried and cover slips were mounted with Vectashield (Linaris, Wertheim). Photomicrographs were acquired with a color CCD camera connected to a phase contrast microscope Axiovert 40-C (Zeiss).

2.2.5. Intestinal epithelial cell lines

The following intestinal epithelial cell (IEC) lines were used in this project (cf. Table S 5): **Caco-2** cells were purchased from European Collection of Cell Cultures (86010202; ECACC, Salisbury, UK). The adherent epithelial cell line Caco-2 was isolated from a primary colonic tumor in a 72-year-old Caucasian male using the explant culture technique. Upon reaching confluence, the human colonic adenocarcinoma cells form polarized monolayers and express characteristics of enterocytic differentiation (Delie & Rubas 1997, Hidalgo et al 1989, Jumarie & Malo 1991).

HT-29 cells were from American Type Culture Collection (HTB-38; Rockville, MD, USA). The adherent epithelial cell line HT-29 was isolated in 1964 by J. Fogh from a primary colonic tumor in a 44 year old Caucasian female using the explant culture technique (Fogh 1975). In post-confluent HT-29 cultures, unpolarized and undifferentiated cells make up more than 95% of the culture with a minority (<5%) of differentiated cell types, including enterocytes and mucus secreting goblet cells (Lesuffleur et al 1990)

IEC-6 cells were purchased from European Collection of Cell Cultures (88071401; ECACC, Salisbury, UK). The adherent epithelial cell line was isolated from rat small intestine. The cells grow as monolayers and have a limited population doubling capability (Quaroni et al 1979). Characteristics specific for intestinal epithelium like microvilli and tight junctions are expressed (Quaroni et al 1979).

T84 cells were purchased from European Collection of Cell Cultures (88021101; ECACC; Salisbury, UK). The adherent epithelial cell line was derived from a lung metastasis of colon carcinoma in a 72 year old male (Dharmsathaphorn et al 1984, Murakami & Masui 1980). Cells grow to confluence as monolayers with microvilli expressed on the apical surface and tight junctions and desmosomes between adjacent cells (Dharmsathaphorn et al 1984).

Primary human and rat EGC and the human epithelial cell lines Caco-2, HT-29 and T84 were cultured in Dulbecco's modified Eagle's medium/nutrient mixture F-12 Ham (DMEM/F12; Sigma-Aldrich, Steinheim) supplemented with 10 % (v/v) heat inactivated fetal bovine serum (FBS; Invitrogen, Karlsruhe) and 1 % (v/v) antibiotic-antimycotic solution (AA; CCPro, Neustadt/W.) containing 100 U/ml penicillin, 100 µg/ml streptomycin, and 250 ng/ml amphotericin B. In the following, this is also referred to as culture medium. The rat epithelial cell line IEC-6 was cultured in Dulbecco's modified Eagle's medium (DMEM; Biochrom, Berlin) with 4.5 g/l glucose supplemented with 10 % (v/v) FBS and 1 % (v/v). Variations of these compositions are stated in the text. All cells were grown in $25\,cm^2$ and/or $75\,cm^2$ tissue culture flasks (Greiner Bio-One, Frickenhausen) maintained in culture at 37 °C in a humidified 5 % CO_2 air atmosphere.

2.2.6. Cell culture techniques

Resuscitation of frozen cells

Cell cultures which were cryopreserved in a deep freezer at -80 °C or obtained from a culture collection, such as ECACC, were thawed in a shaking water bath (1083; GFL - Gesellschaft für Labortechnik, Burgwedel) at 37 °C. Only the lower half of the tube was submerged until a small amount of ice remained in the vial. Then the tube was immediately transferred to a class II biological safety cabinet (Holten Lamin Air S 2010, type 1.2; Heto-Holten, Allerød, Denmark). The cells were pipetted into a 15 ml centrifuge tube (Greiner Bio-One, Frickenhausen) prepared with 5 ml of pre-warmed (37 °C) culture medium using a 5 ml serological pipette. DMSO is a toxic component of freezing medium (cf. Table S 8) which is diluted by this procedure. The tube with the cells was then centrifugated with 250 × g for 5 min at 4 °C (Z 513 K; Hermle Labortechnik, Wehingen). Afterwards, the supernatant was carefully sucked off with a glass Pasteur pipette (Brand, Wertheim) attached to a vacuum pump (KNF Neuberger, Freiburg), and the cell pellet was carefully resuspended in 3 ml pre-warmed culture medium. The cell suspension was transferred into a $25\,cm^2$ cell culture flask (Greiner

Bio-One, Frickenhausen) and cultured at 37 °C in a humidified CO_2 incubator (Binder, Tuttlingen) with a 5 % CO_2 atmosphere. After 24 hours, the cells were examined with a phase contrast microscope (DM IL; Leica Microsystems, Wetzlar) and subcultured as necessary.

Subculture of adherent cells

The cells were examined daily and always prior to subcultivation with a phase contrast microscope (DM IL; Leica Microsystems, Wetzlar) to check the general appearance of the culture and to look for signs of microbial contamination. When cells reached 80% to 90% confluency, they were subcultured using enzymatic dissociation. Culture medium was removed from 25 cm^2 (or 75 cm^2) cell culture flasks (Greiner Bio-One, Frickenhausen), and the cells were gently rinsed with prewarmed sterile PBS (cf. Table S 8) using a volume equivalent to half the volume of culture medium. The wash solution was then removed and discarded. Trypsin 10× or trypsin/EDTA 10× (CCPro, Neustadt/W.) was diluted with deionized H_2O (NANOpure Diamond; Barnstead Int., Dubuque, IA, USA) to 1× and pipetted onto the washed cells using 1 ml per 25 cm^2 of surface area. The flask was carefully rotated to cover the monolayer with trypsin (0.25 %) or trypsin (0.05%)/EDTA (0.02 %) and placed in the incubator for 2 to 10 min depending on the type of cell culture. After the incubation period, the flasks were gently rocked under microscopic control or tapped on the side of the flask to ensure that all cells were detached and floating. The enzymatic dissociation was immediately stopped by addition of 1 ml (or 3 ml) fresh culture medium supplemented with 10 % (v/v) FBS to inactivate the trypsin. The cells were vigorously washed from the bottom of the cell culture vessel with a serological pipette and transferred into a 15 ml centrifuge tube (Greiner Bio-One, Frickenhausen). At this point, an aliquot of 100 µl was transferred into a 0.5 µl tube and a cell count was performed if necessary. The enzymatic dissociation solution was separated from the remaining cell suspension by centrifugation (250 x g for 5 min at 4 °C) and removal of the supernatant. Subsequently, the cells were resuspended in pre-warmed culture medium and the required number of cells was seeded in new labeled 25 cm^2 (or 75 cm^2) cell culture flasks (Greiner Bio-One, Frickenhausen) containing pre-warmed medium. Alternatively, the cell suspension was split among a number of culture vessels of equivalent surface area with a ratio of 1:2 to 1:10 depending on the growth characteristics of the cell culture. The culture vessels contained a final volume of about 0.2 ml per square centimeter of growth area. The cells were maintained in culture at 37 °C in a humidified 5 % CO_2 atmosphere. Culture

medium was changed 24 hours after seeding and then three times a week in the following period until they again reached 80 % to 90 % confluency.

Cell Quantification

In order to use defined cell numbers for coculture experiments, cryopreservation and subculture, it was necessary to quantify the number of cells prior to use. An adherent cell culture was brought into suspension using trypsin/EDTA as described above and resuspended in fresh medium. A hemacytometer (Sigma-Aldrich, Steinheim) was cleaned with 70 % ethanol. The coverslip was moistened by breathing onto it and then slid over the counting chamber back and forth using slight pressure until Newton's refractions rings appeared. 20 µl of a 100 µl aliquot taken from the cell suspension was carefully filled into both sides of the hemacytometer. The number of viable cells which were seen as bright dots was counted under a phase contrast microscope (DM IL; Leica Microsystems, Wetzlar). In detail, all viable cells in the 1 mm center square and the four 1 mm corner squares were counted and an average value was calculated. Only cells on top and right touching the middle line of the perimeter of each square were included in the cell counts. The number of viable cells per ml and the total cell number were calculated using the equations below:

Cells per ml = (average count per 1 mm square) x 10^4 (chamber conversion factor)

Total cell number = (cells per ml) x (original or predilution volume)

The chamber conversion factor of 10^4 was derived from the total volume of chamber square: since each 1 mm square had a depth of 0.1 mm, the total volume was 0.1 mm^3 or 10^{-4} mm^3.

Cryopreservation of Cells

Cryogenic preservation was used to maintain backups and preserve cells for experiments to start with always identical passage numbers, which is an important indicator for the age of a cell culture. Passage number refers to the number of times the cells have been subcultured; ideally taking 1:2 splits into account.

Cells which had to be frozen were detached from the cell culture flask when they had reached 80 % to 90 % confluency using enzymatic dissociation, and a cell count was performed. After the dissociation solution has been removed by a centrifugation step, the supernatant was discarded and the cell pellet at the bottom of the tube was resuspended in a calculated volume of freezing medium (DMEM/F12 containing 20 % (v/v) FBS and 10 % (v/v) DMSO; cf. Table S 8). A final concentration of 1-2x10^6 cells per ml was obtained. Aliquots of 1 ml of the cell suspension were pipetted into 2 ml cryo

tubes (Greiner Bio-One, Frickenhausen) that had been labeled with cell culture name, passage number, cell concentration and date. DMSO is an often used, but at room temperature toxic component of freezing medium. All procedures involving DMSO were performed quickly and on ice to minimize toxic effects and ensure cell viability. The cells were stored at -80 °C in a deep freezer (GFL - Gesellschaft für Labortechnik, Burgwedel) and the location was databased using the BOXIT software (BOXIT LabSoftware, version 2.0; www.boxit-labstorage.de).

2.2.7. Coculture procedures

A cell culture system consisting of EGC cocultured with IEC was utilized to identify the interactions between both cell types. Using the Transwell® system, IEC and EGC can be assessed in coculture without making direct cell contact (Figure 5), whereas both cell types could make direct cell contact when cultured on coverslips (see above 2.2.4). For coculture experiments rat EGC were used which were generated by the method described above (cf. 2.2.2) (Ruhl et al 2001c).

Appropriate intestinal epithelial cell lines for the coculture system were selected in preliminary experiments based on growth characteristics, culture conditions and absolute transepithelial electrical resistance (TER) values of mature monolayers. Therefore, all IEC lines were grown on permeable filter supports to assess and compare their growth characteristics and properties as well as their suitability for coculture experiments (Transwell®, Coring Int., Corning, NY, USA). The formation of functional epithelial monolayers was monitored by measuring TER with a voltohmmeter (Millicell-ERS, Millipore, Eschborn).

The selected epithelial cell line T84 originates from human colon carcinoma and grows as polarized monolayers (Dharmsathaphorn et al 1984). It is an established model system for the analysis of the (patho-)-physiology of intestinal epithelial cells (Hidalgo et al 1989, Madara et al 1987).

T84 were seeded in the basolateral compartment of Transwell® filter supports (polyester membrane, 0.4 µm pore size) in 12-well plates at a density of 50,000 cells/insert as a monoculture or in coculture with EGC at a density of 20,000 or 40,000 cells/insert in the basolateral compartment. A scheme of the Transwell® system is given in Figure 5.
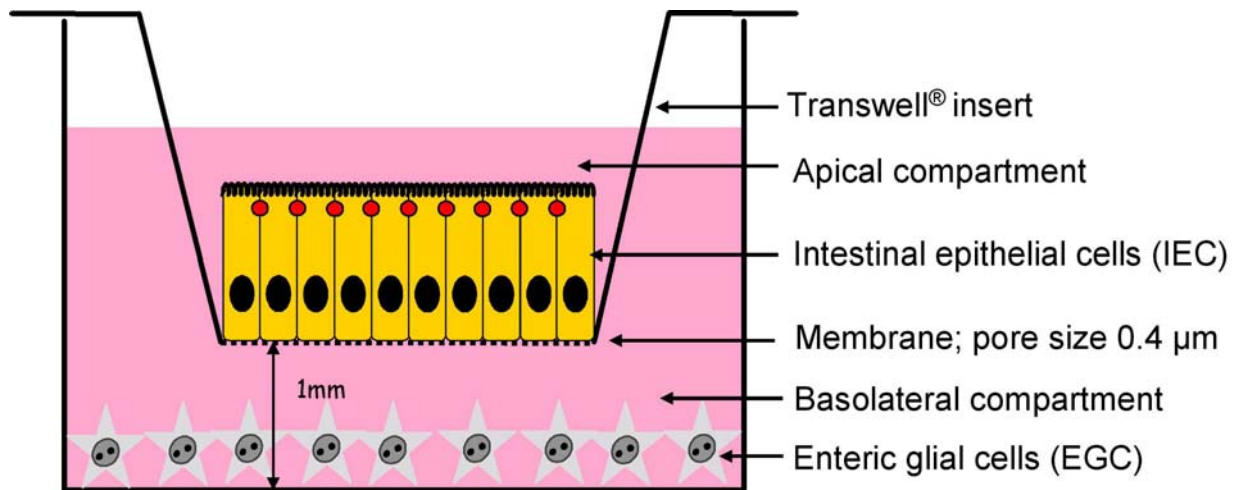
Figure 5. Scheme of Transwell® Systems. Intestinal epithelial cells (IEC) are cultured in the apical compartment on a porous membrane and enteric glial cells (EGC) in the basolateral compartment on the bottom of the well. The scheme shows only one out of six or twelve wells of the microplates used in this study.

The upper and the lower compartments contained 1.5 and 0.8 ml of culture medium, respectively. Medium was changed every other day. To simulate inflammatory conditions, mature IEC in the presence or absence of EGC were treated for 24 h with the proinflammatory cytokines TNFα (1, 10, 100 ng/ml), IL-1β (1, 10, 100 ng/ml), IFNγ (10 ng/ml) or IL-13 (10 ng/ml) (all from R&D Systems, Wiesbaden). Subsequently, the integrity of IEC monolayers was determined by assessing the transepithelial electrical resistance (TER; for details of the method, see below) over a period of 48hrs after cytokine treatment (Figure 7).

Additionally, one series with TNFα (10 ng/ml) treatment was repeated with an antibody against glial cell line-derived neurotrophic factor (GDNF). Anti-GDNF (R&D Systems, Wiesbaden) was added to the culture medium at a concentration of 50 mg/ml 48 hrs prior to the assessment of the basal TER (cf. Figure 7) for both groups cocultured from day -2 on and a second time to all groups at day 0 with the TNFα treatment. A parallel experiment with only the TNFα treatment served as control.

In another series of experiments, RNA extracts were collected from EGC grown either alone or in coculture with T84 cells after treatment with TNFα and IL-1β in various concentrations for 24 h. RNA was extracted only from EGC right after the end of the cytokine treatment.

2.2.8. Measurement of TER and permeability

The transepithelial electrical resistance (TER) of the filter-grown intestinal epithelial cell (IEC) monolayers was measured using a Millicell-ERS voltohmmeter (Millipore, Eschborn). The electrodes were soaked in 12 ml of 80 % ethanol for 15 min in a 15 ml centrifuge tube, dried for 30 sec in the safety cabinet and equilibrated with 7 ml of DMEM/F12 for another 15 min prior to use. Cell culture medium was changed and the cells were incubated for 1 h under normal conditions (37 °C, 5% CO_2) to exclude effects which originate from equilibration of fresh culture medium. The measurement of TER was performed at 37°C on a thermal plate heated by water circulation (both self-made) to avoid alteration in resistance due to temperature changes (Cereijido et al 1983, Matter & Balda 2003). Each Transwell® insert was measured three consecutive times at different positions and the mean value was used for subsequent calculations. TER value was calculated using the following equation:

$$\text{TER } (\Omega \text{ cm}^2) = (R_{\text{cell monolayer}} - R_{\text{filter w/o cells}}) \times A \ (\Omega \text{ cm}^2)$$

where $R_{\text{cell monolayer}}$ is the resistance measured, $R_{\text{filter w/o cells}}$ is the resistance of control filters without cells (~110 Ω) and A is the surface of Transwell® insert (1.12 cm^2).

Additionally, cell layer integrity was visually controlled with an inverted phase contrast microscope (Leica DM IL, Leica Microsystems, Wetzlar).

Because TER reflects the epithelial barrier to the flux of ions only, transepithelial macromolecular flux was assessed employing the fluorescent tracers fluorescein sulfonic acid (FSA; MW 478) and fluorescein dextran (FD; MW 70,000) (Sanders et al 1995). Before each measurement, cell culture medium in the Transwell® system was replaced by DMEM/F12 in the basolateral compartment and DMEM/F12 supplemented with FSA (0.1 mg/ml) or FD (1 mg/ml) in the apical part. Working solutions were diluted from stock solutions of 10 mg FSA or FD per ml DMEM/F12. After a 2 h incubation period (37°C, 5% CO_2), three 100 µl samples were taken from the basolateral compartment of each well, transferred in a 96-well microplate (655180; Greiner Bio-One, Frickenhausen) and analyzed in duplicate with a fluorescence microplate reader (Varioskan; Thermo Electron Corporation, Dreieich). To exclude interference of the cell culture medium used with the relative fluorescence of the macromolecular markers and to identify the appropriate marker concentration, standard concentration curves were established. For this, the markers were dissolved in HBSS, H_2O or DMEM/F12, and a dilution series was generated.

Since the cell culture medium (DMEM/F12) was not autoflorescent, it was used for the coculture experiments. Culture medium was changed after each measurement.

Experimental protocol

IEC monolayers were cultured alone or in combination with EGC in the basolateral compartment according to the protocol given in the schematic below (Figure 6A).
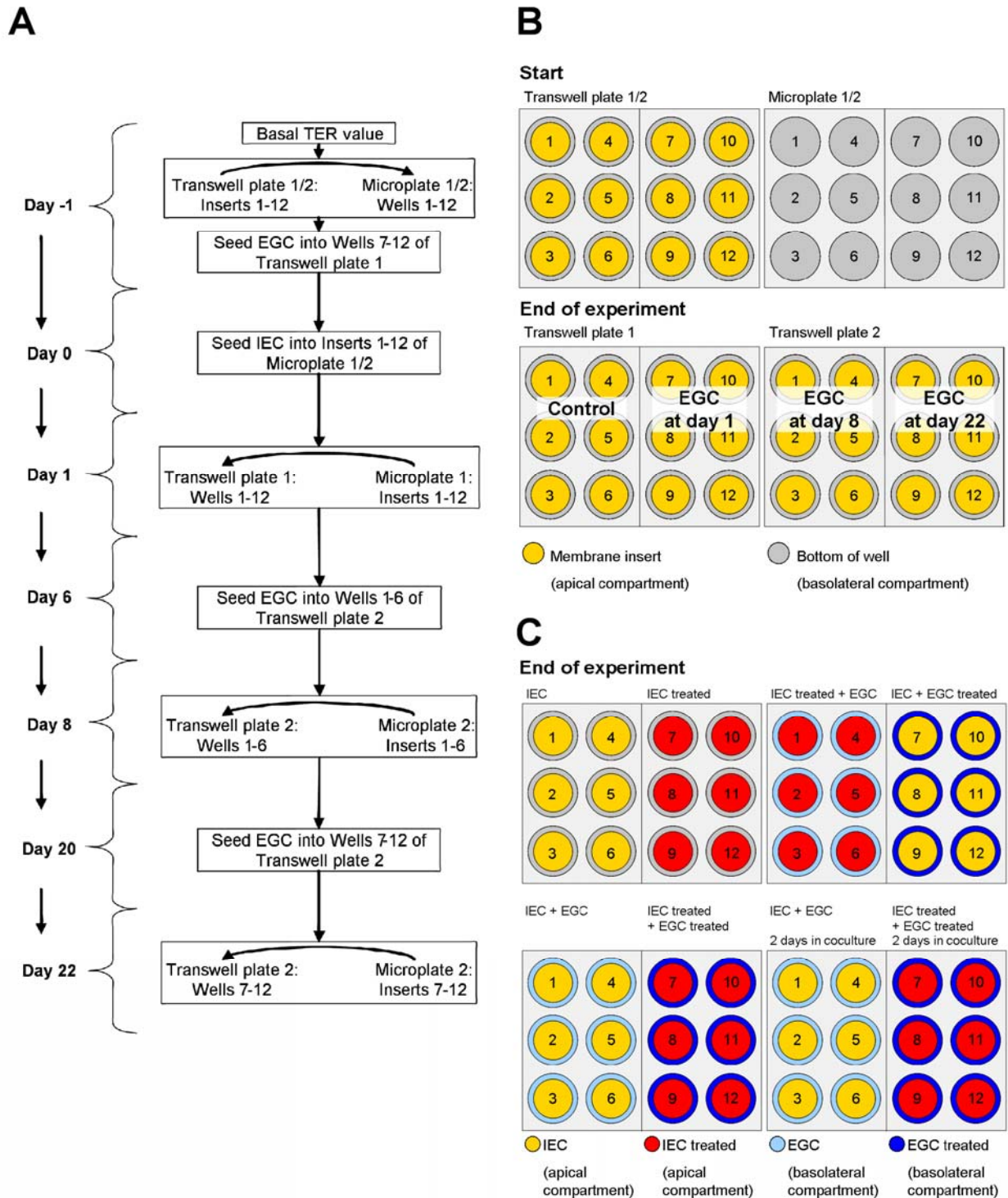
Figure 6. Schematic and flow of coculture experiments. (A) Flow chart of the experimental protocol for the coculture of intestinal epithelial cells (IEC) and enteric glial cells (EGC). (B) Layout of the 12 well plates at the start and end of the experiment. (C) Layout of the 12 well plates at the end of the cytokine treatment.

For this experimental series, various IEC cell lines (T84, Caco-2, HT-29, IEC-6) and EGC (PK 29/6) grown to 75 % confluence were used at the beginning of the experiment. The Transwell® inserts were incubated with cell culture medium for 2 h to equilibrate the membrane before the resistance of control filters without cells was measured (=basal TER). Culture medium (DMEM/F12 + 10 % FBS + 1 % AA) was changed daily, after each TER measurement. Cell seeding densities were 50,000 IEC cells/insert and 20,000 EGC/well (Figure 6B). A sterile forceps was used to transfer membrane inserts had to be transferred from a Transwell® plate to a microplate and back. On days 1, 8 and 22, basal TER was measured one hour after transferring IEC inserts into EGC containing wells to allow for equilibration of the newly added cell culture medium.

2.2.9. Experimental protocol for cytokine treatment

IEC monolayers alone or in coculture with EGC were treated with proinflammatory cytokines such as TNFα, IL-1β, IL-13 and IFNγ to mimic inflammatory conditions in the experiments. A schematic of the Transwell® layout at the end of the experimental period with the maximum of 8 different groups is given in Figure 6C.
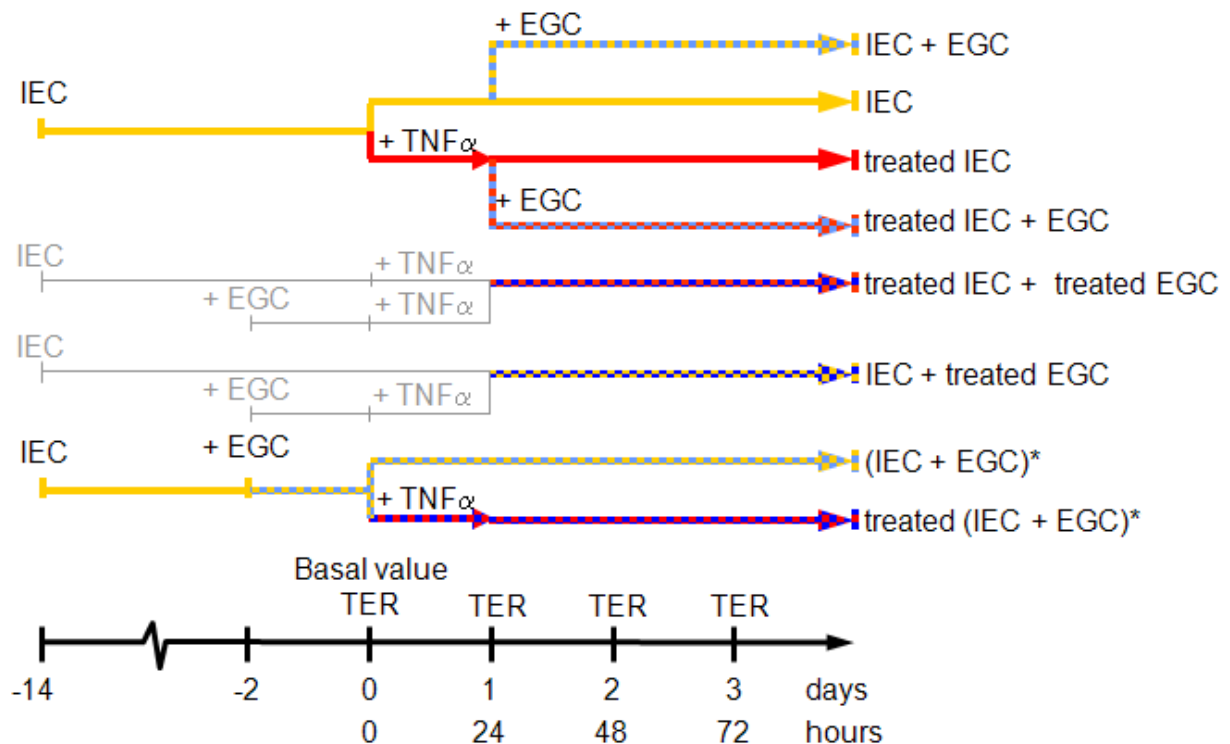
Figure 7. Time schedule for the coculture of intestinal epithelial cells (IEC) and enteric glial cells (EGC) under experimental inflammatory conditions. Cells were treated with different cytokines for 24 h (TNFα is exemplary shown). A maximum of eight different groups was analyzed. *Brackets indicate cells cocultured prior to experiment.

For these experiments, only T84 cells were used, because of their relative higher TER values compared to all other epithelial cell lines used (cf. results 3.2.2). This allows detecting also small differences in TER in more detail.

IEC (T84) and EGC (PK 29/6) grown to 75 % confluence were used at the beginning of the experiment. T84 cells were seeded at a density of 50,000 cells/insert 14 days prior to measurement of the basal value at day 0 (Figure 7). Culture medium was changed every other day. EGC were grown for 3 days prior to day 0 at a density of 40,000 cells/well. Some IEC inserts were put together with EGC at day -2 according to the time schedule shown in Figure 7.

After the measurement of the basal TER value (day 0), the medium was replaced by cell culture medium supplemented with a cytokine (TNFα, IL-1β, IFNγ or IL-13), and cultures were incubated for further 24 hrs. After the incubation period on day 1, culture medium was changed to remove the cytokine, and some IEC were transferred into EGC wells according to the protocol (Figure 7). TER values were re-assessed 1 h thereafter. Macromolecular fluxes were measured right after TER measurements on days 1 and 3.

2.3. Molecular experiments (*in vitro* Studies)

Alterations of TER values of IEC monolayers may be mediated by glial synthesis and release of small molecules, because EGC do not make direct cell contact. Therefore, EGC cultured with or without IEC were employed and incubated with the proinflammatory cytokines IL-1β and TNF-α to mimic inflammatory conditions. To analyze factors potentially responsible for glial-induced alterations of TER values in the Transwell® system, RNA from EGC were extracted and quantified.

2.3.1. RNA extraction and RT-PCR

Total RNA was extracted from EGC cultured in 12-well plates using the FastRNA® Pro Green Kit (Qbiogene, Carlsbad, CA, USA) and the FastPrep® Instrument FP120 (Qbiogene, Carlsbad, CA, USA). Briefly, after homogenization with the FastPrep® Instrument, the RNA is purified and isolated by chloroform extraction and ethanol precipitation. In detail, cell cultures were rinsed with PBS and the 12-well plates were put on ice. Into each single well 1 ml RNApro™ Solution was pipetted to detach the cells before the suspension was transferred to green-cap tubes™ containing Lysing Matrix D™ and processed in the FastPrep® Instrument for 40 s at a setting of 4.0 to release total cellular RNA, DNA and proteins.

Afterwards, the tubes were centrifuged at 12,000 x g at 4 °C for 5 min (Microliter centrifuge, 5415 C, Eppendorf, Hamburg, placed in a cold storage) and the liquid supernatant (~750 µl) was carefully transferred into new 1.5 ml microcentrifuge tubes (Eppendorf, Hamburg). The samples were incubated at room temperature for 5 min to increase the RNA yield. To each tube 300 µl of chloroform (Mallinckrodt Baker, Griesheim) was added before they were vortexed for 10 s and incubated at room temperature for 5 min to permit nucleoprotein dissociation and increase RNA purity. Subsequently, the tubes were centrifuged at 12,000 x g at 4 °C for 5 min and the upper phases were transferred into fresh microcentrifuge tubes without disturbing the white interphases. Five hundred µl of -20 °C absolute ethanol (Mallinckrodt Baker, Griesheim) were then added into every tube, mixed by inversion (5x) and stored at -20 °C for 30 min. A final centrifugation step (12,000 x g at 4 °C for 15 min) was carried out to remove the supernatant. The resulting pellets were carefully washed with 75 % ethanol prepared with DEPC-treated water, the ethanol was decanted and the RNA pellets were air dried at room temperature. Finally, the RNA was resuspended in 100 µl DEPC-H_2O and incubated for 5 min at room temperature before determination of RNA concentration and storage.

To quantify the amount of total RNA extracted, optical density (OD) was determined in duplicate of 1:50 dilutions of the final RNA preparation at 260 nm using a UV spectrophotometer (GeneQuant pro, Biochrom, Cambridge, UK). RNA integrity was determined by the OD260/OD280 absorption ratio. Total RNA was stored at -80 °C until analysis.

Real time polymerase chain reaction (RT-PCR) was performed by a one-step method using SuperScript™ III Platinum® SYBR® Green One-Step qRT-PCR Kit (Invitrogen, Karlsruhe). Total RNA was transcribed and amplified from 190 ng total RNA. The reaction was performed in 10 µl with 0.5 µl SuperScript™ III Reverse Transcriptase/Platinum® *Taq* DNA polymerase Mix, 5 µl 2X SYBR® Green Reaction Mix, 0.5 µl forward primer (100pmol) and 0.5 µl reverse primer (100 pmol). A Rotor-Gene™ 3000 Real Time Thermal Cycler (Corbett Research, Sidney, Australia) was used for all RT-PCR experiments. The reverse transcription step was performed at 55 °C for 10 min followed by a denaturation step at 95 °C for 5 min. Amplification was carried out for 40 cycles of 95 °C for 15 s; 60 °C for 30 s; and 68 °C for 20 s. Amplified RT-PCR products underwent a melting curve analysis to specify the integrity of amplification and finally a cooling step was performed.

The threshold cycle (C_T) values were acquired by the 'second derivate maximum method' of the rotor-gene software, version 6 (Corbett Research, Sidney, Australia). The C_T is defined as the fractional cycle number at which the amount of amplified target reaches a defined threshold (Livak & Schmittgen 2001). The C_T indicates the transition from background ("noise") to the exponential phase of the amplification curve. At this point, there are identical amounts of newly synthesized DNA in each reaction tube.

2.3.2. Normalization and quantification of RT-PCR data

A relative gene expression analysis was performed using the delta delta C_T ($2^{-\Delta\Delta CT}$) method (Livak & Schmittgen 2001). The C_T values of target gene expression were normalized to the mean C_T derived from the reference or house-keeping genes actin beta (ACTB) and histone 3 (HIS3H3) described by the following equation:

$$\Delta C_T = C_T \text{ (target gene)} - C_T \text{ (mean reference genes)}.$$

Each ΔC_T value was normalized per target gene. For this, the mean expression C_T of the control group was used:

$$\Delta\Delta C_T = \Delta C_T \text{ (cytokine treated EGC)} - \text{mean } \Delta C_T \text{ (control group)}.$$

Positive $\Delta\Delta C_T$ values represent a down-regulation and negative $\Delta\Delta C_T$ values an up-regulation of target gene expression.

2.3.3. DNA gel electrophoresis

RT-PCR product specificity was verified by agarose gel electrophoresis (Sambrook et al 1989). Briefly, to get a 2 % agarose gel 0.66 g of agarose (UltraPure™, 15510027; Invitrogen, Karlsruhe) were added to 33 ml 1× TAE electrophoresis buffer (see Table S 8) and heated in a microwave oven (ER-654MD; Goldstar) until the agarose was completely dissolved. The solution was cooled to about 60 °C, 3.75 µl ethidium bromide solution (from a 10 mg/ml stock solution in water; E1510; Sigma-Aldrich, Steinheim) was added and mixed thoroughly. The gel was immediately poured into the mold of an electrophoresis unit (Mini D; LTF Labortechnik, Wasserburg am Bodensee) and a 12-teeth comb was inserted. After 30-45 min at room temperature, the gel was completely solidified. The comb and the sealing were carefully removed and the mold was mounted in the electrophoresis tank. Then, electrophoresis buffer was added to just completely cover the gel and the DNA samples (5 µl) mixed with gel-loading buffer (1.5 µl; see Table S 8), were slowly loaded into the slots of the submerged gel using a microliter pipette (Transferpette®, 704102, Brand, Wertheim).

To determine DNA fragment length, a DNA ladder (Low Molecular Weight DNA Ladder, N3233S, New England Biolabs, Ipswich, MA, USA) was used as a reference. The lid of the gel tank was closed and the electrical leads were attached so that the DNA would migrate towards the anode (red lead). A voltage of 130 V was applied for 60 min using an electrophoresis power supply (EPS 300; Pharmacia Biotech, Freiburg). After the electrophoretical separation of the DNA fragments, the gel was examined by ultraviolet light (wavelength 302 nm) and photographed using a MultiDoc-It Imaging System M20 equipped with a 5.1 megapixel color digicam, UV-Transilluminator M-20 and Doc-It 1D software for gel analysis (all parts from LTF Labortechnik, Wasserburg am Bodensee).

2.3.4. Oligonucleotide primers

Primer pairs were designed to be exon-spanning in the highly conserved coding region (CDS) of the appropriate coding sequence rat to distinguish between cDNA amplification products and genomic DNA. For this purpose, the modules *Primer* and *PrimePair* of the HUSAR Sequence Analysis Package software, version 4.1 (http://genome.dkfz-heidelberg.de/biounit/) (HUSAR, DKFZ, Heidelberg) or Primer3 software, version 1.0 (http://frodo.wi.mit.edu/) were used. Primer design and optimization were carried out with regard to self-priming formation, primer dimer formation and primer melting temperature. All oligonucleotide primers were synthesized by MWG (Ebersberg). Detailed information is given in Table 5.

Table 5.   Primers used for RT-PCR.

Gene	Primer	Sequence (5'→3')	Product length (bp)a	Locationb	NCBI Accession Numberc
ACTBd	Sense	AAC TCC ATC ATG AAG TGT GAC G	234	838-859	NM_031144
	Antisense	GAT CCA CAT CTG CTG AAA GG		1052-1071	
FGF2	Sense	AGC GGC TCT ACT GCA AGA AC	183	618-637	NM_019305
	Antisense	GCC GTC CAT CTT CCT TCA TAG C		779-800	
GDNF	Sense	GCT GAG CAG TGA CTC AAA TAT G	191	138-159	NM_019139
	Antisense	CTC TCC GAC CTT TTC CTC TG		309-328	
GFAP	Sense	GCT CCA GGA TGA AAC CAA CC	171	456-465	NM_017009
	Antisense	AGT TCC CGA ACC TCC TCC TC		607-626	
GFRA1	Sense	CTC CAG TCC AGA CCA CCA CT	163	1329-1348	NM_012959
	Antisense	TGT GTG CTA CCC GAC ACA TT		1472-1491	
GFRA2	Sense	TCA GGG ACT TCA CGG AAA AC	197	1136-1155	NM_012750
	Antisense	AGA TGT GCA GGT GGT GAT GA		1313-1332	
HIST3H3d	Sense	ACT CGC TAC AAA AGC CGC TC	232	60-79	NM_003493
	Antisense	ACT TGC CTC CTG CAA AGC AC		272-291	
IFNGR	Sense	CAA TAG TTG TCC CGG CAC TT	151	761-780	NM_053783
	Antisense	CAC GAC GTG ACA AGG GAG TA		892-911	
IL10	Sense	CAC TTC CCA GTC AGC CAG AC	196	138-157	NM_012854
	Antisense	GGG GCA TCA CTT CTA CCA GG		314-333	
IL13RA1	Sense	ATT CGT GCA GTG GAA GAA CC	163	720-739	NM_145789
	Antisense	ACT TGC ACC TCC ATG TTT TC		863-882	

Table 5.   (Continued).

			a	b	c
IL1R1	Sense	TGC CGA GGC TTG TGA CAT CT	208	326-345	NM_013123
	Antisense	GTG CCG CCA TGC ATT TCG TT		514-533	
IL1R2	Sense	CAT GGG AGA TGC AGG CTA TT	188	753-772	NM_053953
	Antisense	ACA CCT TGC ACG GGA CTA T		922-940	
IL1RAP	Sense	GTC ACC CCT GAG GAT CTG AA	199	1063-1082	NM_012968
	Antisense	GGA CCA TCT CCA GCC AGT AA		1242-1261	
NES	Sense	ACT CTC GGT TGC AGA CAC CT	161	1059-1078	NM_012987
	Antisense	GGT ATT AGG CAA GGG GGA AGG		1199-1219	
NGF	Sense	GCA GAC CCG CAA CAT TAC TG	205	384-403	XM_227525
	Antisense	GAA TTC GCC CCT GTG GAA G		570-588	
NGFR	Sense	TGG GCT GAT GCT GAA TGC GA	245	550-569	NM_012610
	Antisense	ACG ACC ACA GCA GCC AAG AT		775-794	
NTF3	Sense	CGC GGA GCA TAA GAG TCAC	213	420-438	NM_031073
	Antisense	TCA TCA ATA CCC CTG CAA CC		613-632	
NTRK1	Sense	CCA AGT CAG CGT CTC CTT C	195	901-919	NM_021589
	Antisense	CGC ATG GTC TCA TTG GTC		1078-1095	
NTRK2	Sense	AGC ACG AGC ACA TTG TCA AG	228	2448-2467	NM_012731
	Antisense	AGT GTT GGG ATG CCA GGT AG		2656-2675	
NTRK3	Sense	TCC GAG AAG GAG ACA ATG CT	170	713-732	NM_019248
	Antisense	GTC TTC GCT CGT CAC ATT CA		863-882	
RET	Sense	CTG GAG CCA ACA AGG AGA AG	174	756-775	NM_012643
	Antisense	CCA CAT CTG CAT CAA ACA CC		910-929	
TNFRSF1A	Sense	ACC AAG TGC CAC AAA GGA AC	212	415-434	NM_013091
	Antisense	TTC TTC TTG CAG CCA CAC AC		607-626	

ACTB, beta actin; FGF2, fibroblast growth factor 2; GDNF, glial cell line-derived neurotrophic factor; GFAP, glial fibrillary acidic protein; GFRA1, GDNF family receptor alpha 1; GFRA2, GDNF family receptor alpha 2; HIST3H3, histone 3, H3; IFNGR1, interferon gamma receptor 1; IL10, interleukin 10; IL13RA1, interleukin 13 receptor, alpha 1; IL1R1, interleukin 1 receptor, type I; IL1R2, interleukin 1 receptor, type II; IL1RAP, interleukin 1 receptor accessory protein; NES, nestin; NGF, nerve growth factor; NGFR, nerve growth factor receptor; NTF3, neurotrophin 3; NTRK1, neurotrophic tyrosine kinase, receptor, type 1; NTRK2, neurotrophic tyrosine kinase, receptor, type 2; NTRK3, neurotrophic tyrosine kinase, receptor, type 3; TNFRSF1A, tumor necrosis factor receptor superfamily, member 1A; RET, ret proto-oncogene.
[a] Expected product length in base pairs.
[b] Location in coding sequence
[c] Genebank accession number of cDNA and corresponding gene, available at http://www.ncbi.nlm.nih.gov.
[d] Primer sequences were kindly provided by PD Dr. Michael W. Pfaffl from the Department of Physiology, Technische Universität München (Freising-Weihenstephan).

2.4.   Statistical analysis of *in vitro* studies

Relative gene expression data generated by RT-PCR were analyzed by one-way ANOVA using normalized mRNA expression results ($\Delta\Delta C_T$) to compare treatment groups vs. control. For analysis of TER values, the mean of three replicate measurements of each well was used. Unless stated otherwise, the mean of $n = 6$ wells was used for statistical analysis. At the first time point (t = 0), a basal value was measured and set to 100 %. Relative TER changes at consecutive time points were computed from the absolute measures in relation to the basal value. For each time

point, one-way ANOVA with the Holm-Sidak method for pairwise multiple comparison procedures of different treatment groups was applied.

The non-parametric test ANOVA on ranks with Student-Newman-Keuls was used for non-normally distributed values. Two-way ANOVA was used to analyze the effect of anti-GDNF antibody using cytokine treatment as the first and the antibody application as the second factor.

Relative changes of TER values measured in coculture experiments are visualized as line plots with mean ± standard error of means (SEM). Because 2 different tests were performed (ANOVA and ANOVA on ranks), but only one type of graphical presentation is used to display cytokine effects in treated cocultures - namely line plots -, there is some minor inaccuracy in the plotted data points for non parametric tests. Nevertheless the statistical test (ANOVA and ANOVA on ranks, respectively) and its result for this data are correct. A level of probability of $p \leq 0.05$ was considered significant for all analyses except for multiple comparison procedures where adjusted p-values were applied. All data were analyzed using the SigmaStat 3.1 software and graphs were created with SigmaPlot 9.01 (Systat Software, Erkrath).

3.   Results

3.1.   Morphological analyses (*ex vivo* studies)

Sox8/9/10-IR selectively and specifically occurs in all glial cell nuclei in the adult ENS

With the antibody selected for this study, abundant Sox8/9/10-IR was detectable in all studied regions of the adult human and guinea pig ENS and strictly localized to the glial nuclei in ganglia, interganglionic nerve fiber strands and nerve fibers innervating muscle, blood vessels and the epithelium (Figure 8).

In contrast, the well-established glial marker S100b displayed a cytoplasmatic staining pattern with IR in both enteric glial cell bodies and processes sparing the adjacent neuronal cell bodies, whereas glial marker p75NGFR labeled EGC cell bodies and processes, but also neuronal fiber-like structures. S100b and p75NGFR-IR was very intense in the human SMP and occurred in identical glial structures (Figure 8L). In the MP, p75NGFR-IR was consistently homogeneous, whereas the anti-S100b Ab yielded only irregular staining of large ganglia and fiber tracts, most likely due to limited antibody-penetration into these structures. GFAP, which is another well-established cytoplasmatic marker of glial cell bodies and processes in the CNS, displayed its typical fibrillary staining pattern, but was patchy and irregular in the human MP (Figure 8G). S100b and GFAP-IR were 100% co-localized with Sox8/9/10, so all S100b and GFAP immunoreactive structures contained Sox8/9/10 immunopositive nuclei (Figure 8F and I). Unfortunately, double-labeling studies could not be performed with Sox8/9/10 and p75NGFR since the respective antibodies were raised in the same species (mouse). The reporter peptide Ala-Lys-AMCA was detectable in all glial cell bodies in the ENS, and counterstaining with Sox8/9/10 demonstrated a total overlap of Ala-Lys-AMCA uptake and Sox8/9/10-IR, indicating that Sox8/9/10 is indeed a pan-glial marker in the ENS (Figure 8O). Additionally, immunoreactivity of Sox8/9/10 antibody was blocked by pre-incubation with a Sox10 fusion protein (Figure 9). The Sox10 polyclonal antibody showed no immunoreactivity in human ileum and colon. The characteristic staining patterns of all antibodies employed in the current study are listed in Table 3.

Anti-NSE, anti-HuC/D and anti-PGP 9.5 are pan-neuronal markers with different characteristics in the human and guinea pig ENS

Using the antibody selected for the current study, NSE-IR could be detected in neuronal cell bodies and processes as well as interganglionic nerve fiber strands but not cell

nuclei in man and guinea pig (Figure 10). In the human ENS, individual neurons could be clearly identified by their intense stained cell bodies, yet staining intensity varied considerably. In contrast, neuronal cell borders were not discernible in NSE-immunostained guinea pig tissues so that individual neurons were mainly identified by their unlabeled nuclei. HuC/D-IR was homogeneously distributed in neuronal nuclei and to a lesser extent in neuronal cell bodies throughout the human ENS, but did not occur in any neuronal processes or interganglionic connectives, whereas PGP 9.5-IR was found both in neuronal cell bodies and processes (Figure 10). In guinea pig tissues, HuC/D-IR was primarily located in the cytoplasm resulting in less well discernible cell borders than in the human ENS (Figure 10), and strong PGP 9.5-IR in nerve fiber tracts hampered the identification of individual neurons.

Since NSE, HuC/D and PGP 9.5 appeared to be co-localized in all enteric neurons (Figure 10), the anti-NSE Ab was selected as the most appropriate tool to label enteric neurons which at the same time could be used in combination with the anti-Sox8/9/10 Ab for the subsequent quantitative studies in both human and guinea pig tissues.

Double-labeling with anti-Sox8/9/10 and anti-NSE allows for reliable quantification of EGC and neurons throughout all plexus layers and studied regions in the human and guinea pig ENS

In human tissues, glial Sox8/9/10-IR and neuronal NSE-IR was abundant in all plexus layers from ileum, as well as ascending and sigmoid colon (Figure 11). Sox8/9/10-IR was remarkably homogeneous without any differences in staining intensity between ganglionic and extraganglionic areas throughout all plexus layers. In contrast, staining intensity using the anti-NSE Ab was highly variable with greater intensity in the inner, intermediate and external SMP as compared to the MP, and, overall, ganglia appearing brighter than nerve fiber strands in both the human SMP and MP (Figure 11).

Labeling of the SMP and MP of guinea pig ileum as well as proximal and distal colon with anti-Sox8/9/10 and anti-NSE antibodies resulted in a homogeneous staining of all glial nuclei and all neurons with a cytoplasmatic NSE staining pattern that excluded the cell nuclei (Figure 11). Separate cell bodies could not be discriminated in nerve fibers, except to some extent in both plexus layers in the distal colon. The dark, non-stained cell nuclei were used to guide the identification of individual neurons and their subsequent quantification. The staining intensity was higher in the SMP, being best in the proximal and distal colon and less optimal in the ileum. To compensate for this difference in staining quality a lower Ab dilution factor for ileal tissues was employed.

Human
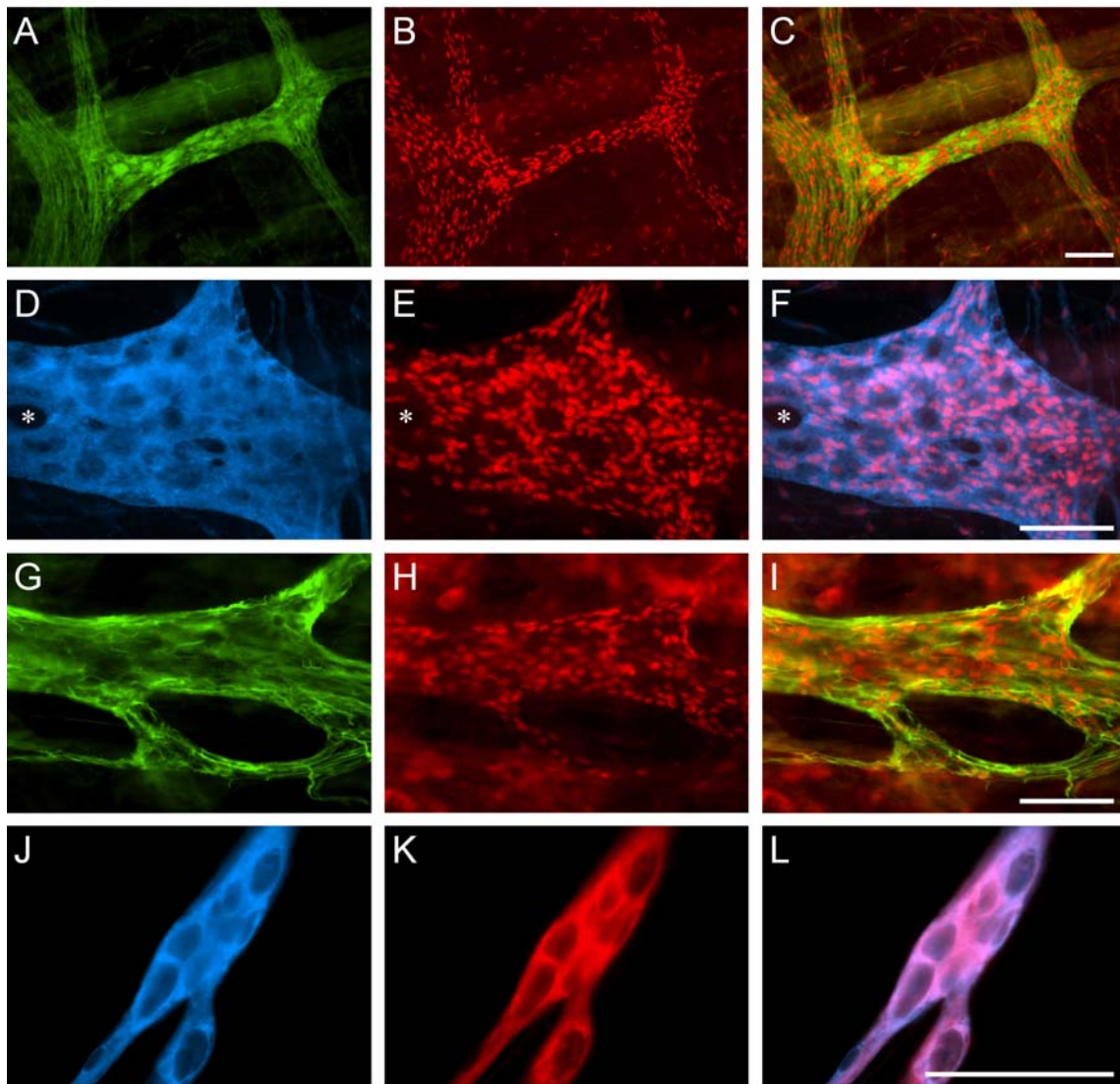
Guinea pig
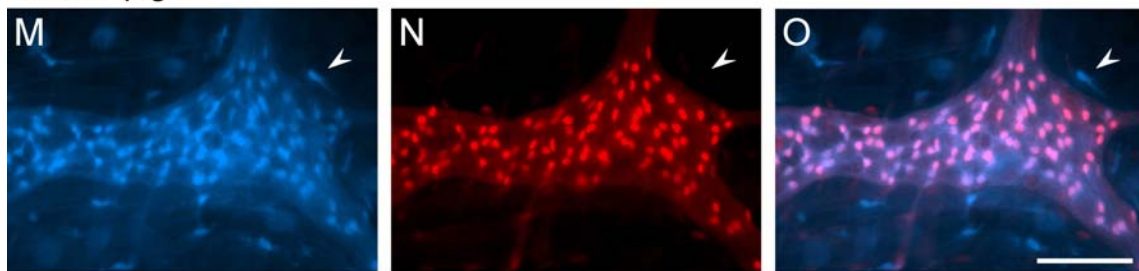
Figure 8. Immunohistochemical staining patterns of various glial markers in whole-mount preparations of the human and guinea pig enteric nervous system (ENS): Only Sox8/9/10-immunoreactivity (IR) specifically occurs in all glial cell nuclei. (A-C) Myenteric plexus (MP) from human ileum stained for NSE (Cy2; green) and Sox8/9/10 (Cy3; red.) (D-F) Myenteric ganglion from human ileum double-labeled with the calcium-binding protein S100b (Cy2; blue) and the transcription factors Sox8/9/10 (Cy3; red). A cavity in the ganglion is marked with an asterisk. (G-I) MP ganglia from human ileum double-labeled with antibodies directed against glial fibrillary acidic protein (GFAP) (Cy2; green) and Sox8/9/10 (Cy3; red). (J-L) Ganglion from the inner submucous plexus (SMP) of human ascending colon was stained for S100b (J; Cy2) and the low-affinity nerve growth factor receptor p75 (p75NGFR) (K; Cy3). (M-O) Guinea pig MP stained with the dipeptide β-Ala-Lys-Nε-7-amino-4-methyl-coumarin-3-acetic acid (Ala-Lys-AMCA) and anti-Sox8/9/10 (Cy3). (M) Ala-Lys-AMCA-uptake (blue) occurred in glial cells and some macrophages outside the ENS. A macrophage is indicated by an arrowhead. Sox8/9/10 is restricted to glial nuclei and shows perfect co-localization with Ala-Lys-AMCA uptake in all glial cells. All merged images are displayed in the right column. Original magnifications A-C 10X; D-I, M-O 20X; J-L 40X; scale bars = 100 μm.
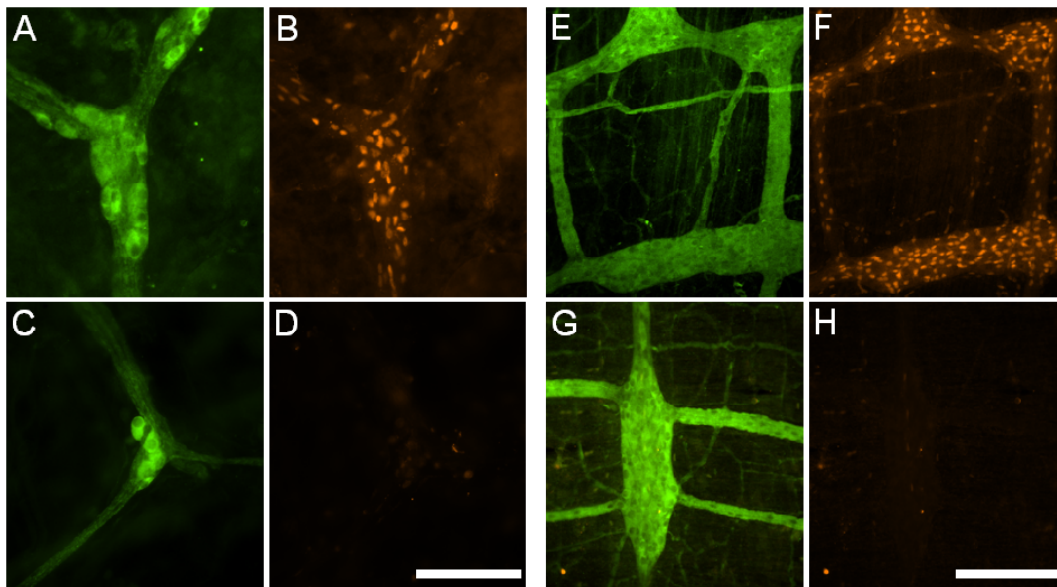
Figure 9. Blocking of Sox8/9/10 immunoreactivity. (A-D) Immunohistochemical visualization of specific Sox8/9/10 staining in glial cells of the human enteric nervous system. (A-B) Whole-mount preparations of the inner submucous plexus of human sigmoid colon were stained for NSE (Cy2; green) and Sox8/9/10 (Cy3;orange). (C,D) Incubation of the Sox8/9/10 antibody (Cy3; orange) with a Sox10 fusion protein fully abolished Sox8/9/10 staining of enteric glial cells in double-labeled preparations using NSE (Cy2; green) as a neuronal marker. Original magnification (A,B) 20X, (C,D) 40X; scale bar = 100 µm. (A,B) Whole-mount preparations of the myenteric plexus from guinea pig ileum were double-labeled with NSE (Cy2; green) and Sox8/9/10 (Cy3; orange). (C,D) Incubation of the Sox8/9/10 antibody (Cy3; orange) with a Sox10 fusion protein fully abolished Sox8/9/10 staining of all enteric glial cells in double-labeled preparations. Original magnification 20X; scale bar = 200 µm.
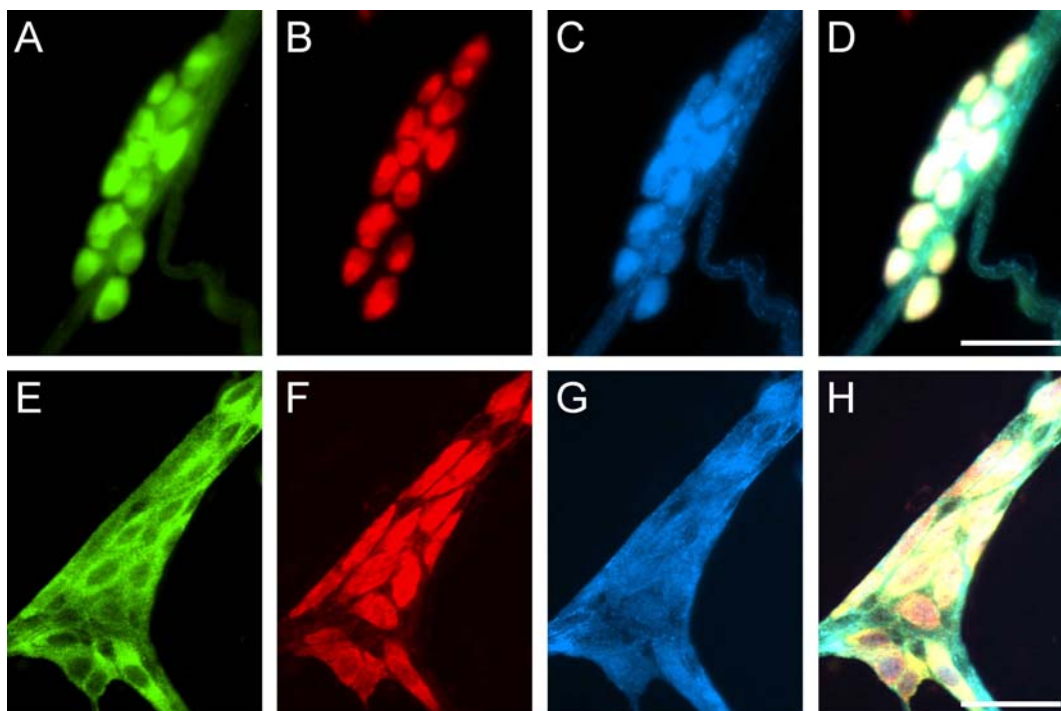
Figure 10. Characterization of neuronal counterstaining: Anti-NSE, anti-HuC/D and anti-PGP 9.5 are pan-neuronal markers with different characteristics in the human and guinea pig ENS. Whole-mount preparations of the inner submucous plexus (SMP) from human ascending colon (A-D) and SMP from guinea pig proximal colon (E-H) were triple-labeled with antibodies directed against neuron specific enolase (NSE) (Cy2; green), HuC/HuD neuronal proteins (HuC/D) (Cy3; red) and the ubiquitin hydrolase protein gene product 9.5 (PGP 9.5) (Cy5; blue). (D,H) Overlaying pictures A to C and E to G shows co-localization of NSE, HuC/D and PGP 9.5 in all enteric neurons. Original magnification: 40X; scale bars = 100 µm.
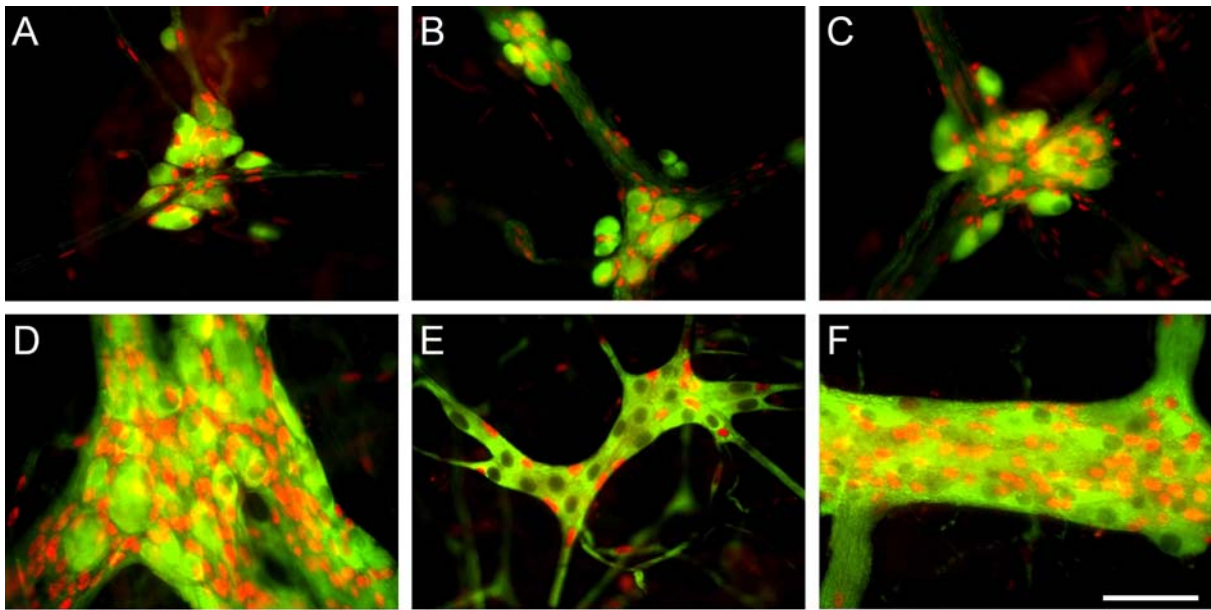
Figure 11. Immunohistochemical visualization of the different plexus layers in the human and guinea pig ENS. Whole-mount preparations of the inner (A), intermediate (B) and external (C) submucous plexus (SMP) and the myenteric plexus (MP) (D) of human ileum as well as the SMP (E) and MP (F) of guinea pig ileum were stained with an antibody directed against the transcription factors Sox8/9/10 (red) which labeled all glial nuclei, and the pan-neuronal marker neuron specific enolase (NSE; green) which exhibited a cytoplasmatic staining pattern and also labeled nerve fibers. Original magnification 40X, scale bars = 50 µm.

3.1.1. Quantitative assessment of ENS components

Glial and neuronal numbers and ganglionic area in the human and guinea pig ENS

In man and guinea pig, the ganglia of the MP were significantly larger and contained significantly more glial cells as well as neurons than the SMP ganglia ($p < 0.001$; Figure 12). The median number of glial cells per ganglion in man ranged between 8-20 in the SMP and 272-488 in the MP; in guinea pig, the corresponding numbers were 6-15 for the SMP and 104-126 for the MP (Figure 12A). There were between 5-13 neurons per ganglion in the human SMP and 48-76 in the MP; ganglia in the guinea pig ENS contained 8-20 and 68-76 neurons in the SMP and MP, respectively (Figure 12B). The median of the ganglionic area in man varied between 1.8-5.8 x 10^{-3} mm^2 in the SMP and 75.5-124.6 x 10^{-3} mm^2 in the MP; corresponding data for guinea pig were 4.7-12.9 x 10^{-3} mm^2 and 49.8-74.9 x 10^{-3} mm^2 for the SMP and MP, respectively (Figure 12C). There were significantly less neurons per ganglion in the MP of human ileum compared to ascending colon and sigmoid colon ($p < 0.01$; Figure 12B). Regarding ganglionic area, no regional differences were seen in the human ENS, whereas in guinea pig the proximal colon differed from ileum and distal colon ($p < 0.01$; Figure 12C). Comparing absolute ganglionic cell numbers between man and guinea pig, there were significantly

more glial cells in the human MP (p<0.01), while neuronal cell counts were identical between man and guinea pig (Figure 12A,B). In contrast to most regions, the SMP ganglia in human ileum and sigmoid colon were smaller than in the corresponding guinea pig regions, whereas those from the MP were larger (Figure 12C). Due to high variability in ganglionic size, these observations reached statistical significance only for the sigmoid colon (p<0.02).

Glial and neuronal density and glia index in the human and guinea pig ENS

In human tissues, the number of glial cells per mm^2 ganglionic area ranged from 3098 to 5956 in the SMP and from 3781 to 4210 in the MP. Ganglia from the guinea pig ENS contained 1264-1583 in the SMP and 1741-2176 glial cells per mm^2 in the MP (Figure 13A). Although there were substantial differences in glial density between the different plexus layers and regions in the human intestine, no statistically significant differences could be detected due to high variability within each layer and region. The only exception was the intermediate SMP from human ileum with significantly higher glial density compared to the colonic regions (p<0.05; Figure 13A). In guinea pig, significant regional differences existed between the MP in the proximal and distal colon (p<0.005). In all guinea pig gut regions, myenteric glial density was significantly higher than submucous glial density (p≤0.002).

The number of neurons per mm^2 ganglionic area ranged from 2166 to 3200 in the human SMP and from 658 to 693 in the human MP. In guinea pig tissues, the respective medians were between 1606-1625 in the SMP and 958-1329 in the MP (Figure 13B). Accordingly, neuronal density was significantly lower in myenteric compared to submucous ganglia of the human ENS (p<0.001); this was similar in guinea pig with the exception of the distal colon (p≤0.002). Regional differences in the human ENS existed between the intermediate SMP from ileum and ascending colon as well as between the external SMP from ascending and sigmoid colon (p<0.01; Figure 13B).

The medians of the glia:neuron ration — i.e. the glia index — ranged from 1.4 to 1.9 and 6.0-6.3 in the human SMP and MP, respectively; in the guinea pig ENS, the glia index was 0.7-0.9 in submucous and 1.7-1.8 in myenteric ganglia (Figure 13C). Overall, the glia index in the MP was considerably higher than in the SMP in all human and guinea pig intestinal regions (p<0.001).

Comparing human to guinea pig tissues, glial density was consistently higher in the human ENS, irrespective of intestinal region or plexus layer (Figure 13A and Figure 14). In contrast, neuronal density was higher in most layers of the human SMP compared to

the guinea pig SMP (with the exception of ascending colon external SMP), but lower in the human MP (Figure 13B). The glia index was consistently higher in the human MP and most human SMP layers when compared to the respective guinea pig plexus layers (with the exception of the inner SMP from ileum and ascending colon) (Figure 13C and Figure 14).

Glial density markedly differs between intra- vs. extraganglionic areas in human and guinea pig MP

Glial density was significantly higher in the human *vs.* guinea pig MP in all studied regions (Figure 13 and Figure 15). In contrast, comparing intra- and extraganglionic areas from all studied regions, glial density was significantly higher in the intraganglionic area only in guinea pig tissues (p<0.001; Figure 15A). In addition, glial density was lower in the guinea pig myenteric ganglia in the proximal colon than in the ileum (p<0.02) or distal colon (p<0.001), whereas in human tissues there were no differences in glial density between ganglionic and extraganglionic areas. Visual assessment revealed that the interganglionic nerve strands that primarily constitute the extraganglionic area are conspicuously broader in the human *vs.* guinea pig ENS which may potentially account for the lack of difference (Figure 13B). In terms of absolute numbers, there were overall more glial cells in the human than in the guinea pig ENS when both intra- and extraganglionic area were taken together (data not shown).

Glial nuclei are substantially larger in the MP than in the SMP

The size of glial cell nuclei differed significantly between the inner SMP and MP in human as well as between SMP and MP in guinea pig ileum (p<0.001; Figure 16). Species differences existed only between human inner SMP and guinea pig SMP (p≤0.001).

Effect of gender and ageing on the human ENS

In nine out of 12 groups comprising the three SMPs and the MP from all regions sampled it was tested whether gender had an effect on the studied parameters. The glia index was significantly higher in the intermediate SMP in male persons (2.0 ± 0.2 vs. 1.4 ± 0.1; p=0.007). No other gender differences were found. Potential age effects on glial and neuronal numbers in the human ENS were also analyzed: for the SMP, no significant correlation between patient age and glial and neuronal ganglionic cell numbers, density, ganglionic area, or the glia index could be detected. In contrast, in ileum MP ganglionic area increased with age (p<0.05; data not shown).

Figure 12. Glial and neuronal numbers and ganglionic area in the human and guinea pig ENS.
Whole-mount preparations of the inner, intermediate and external submucous plexus (SMP) and the myenteric plexus (MP) of ileum, ascending and sigmoid colon in man, as well as the corresponding guinea pig plexus layers and regions were double labeled with anti-Sox8/9/10 and anti-NSE antibodies and appropriate secondary antibodies coupled with Cy3 and Cy2, respectively. EGC and neurons were counted and expressed per ganglion (A, B); the analyzed ganglionic area was multiplied by a factor of x1000 and is given as area per mm^2 (C). The boxes represent the median (n=6 preparations) and interquartile ranges. L Significant difference between plexus layers of the respective gut region of man or guinea pig; $p<0.001$; R significant difference between gut regions of man and guinea pig; two-way ANOVA using the Holm-Sidak method; $p<0.01$; S significant difference between the MP (Student's t-test; $p<0.001$, A; $p<0.02$, C) or SMP (one-way ANOVA with the Holm-Sidak method, testing all human SMP against the guinea pig SMP; $p<0.01$, A,B; $p<0.001$, C) of man and guinea pig. Low case letters indicate Mann-Whitney rank sum test ($p<0.01$) or Dunn's method for ANOVA post-hoc tests ($p<0.05$).
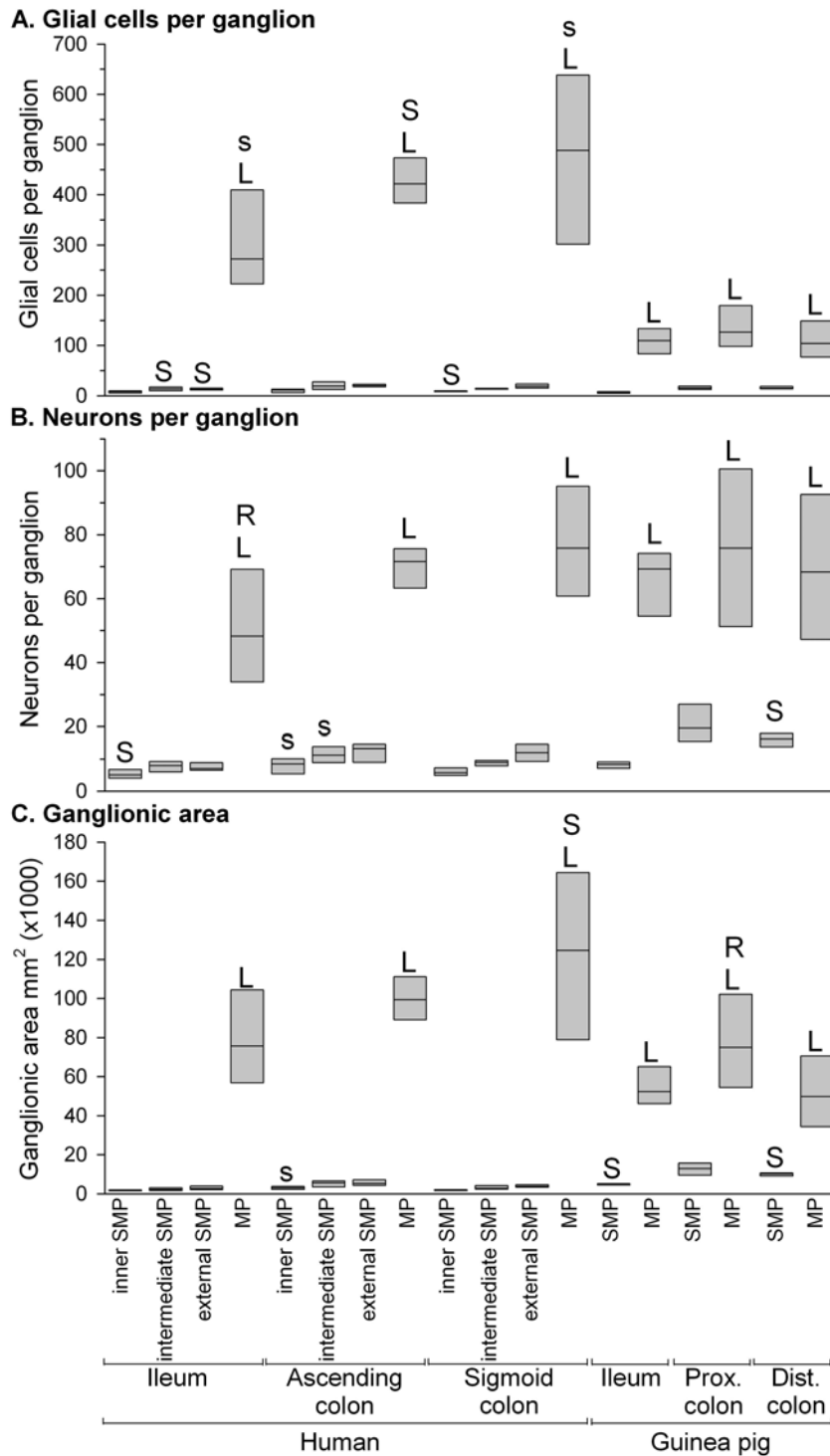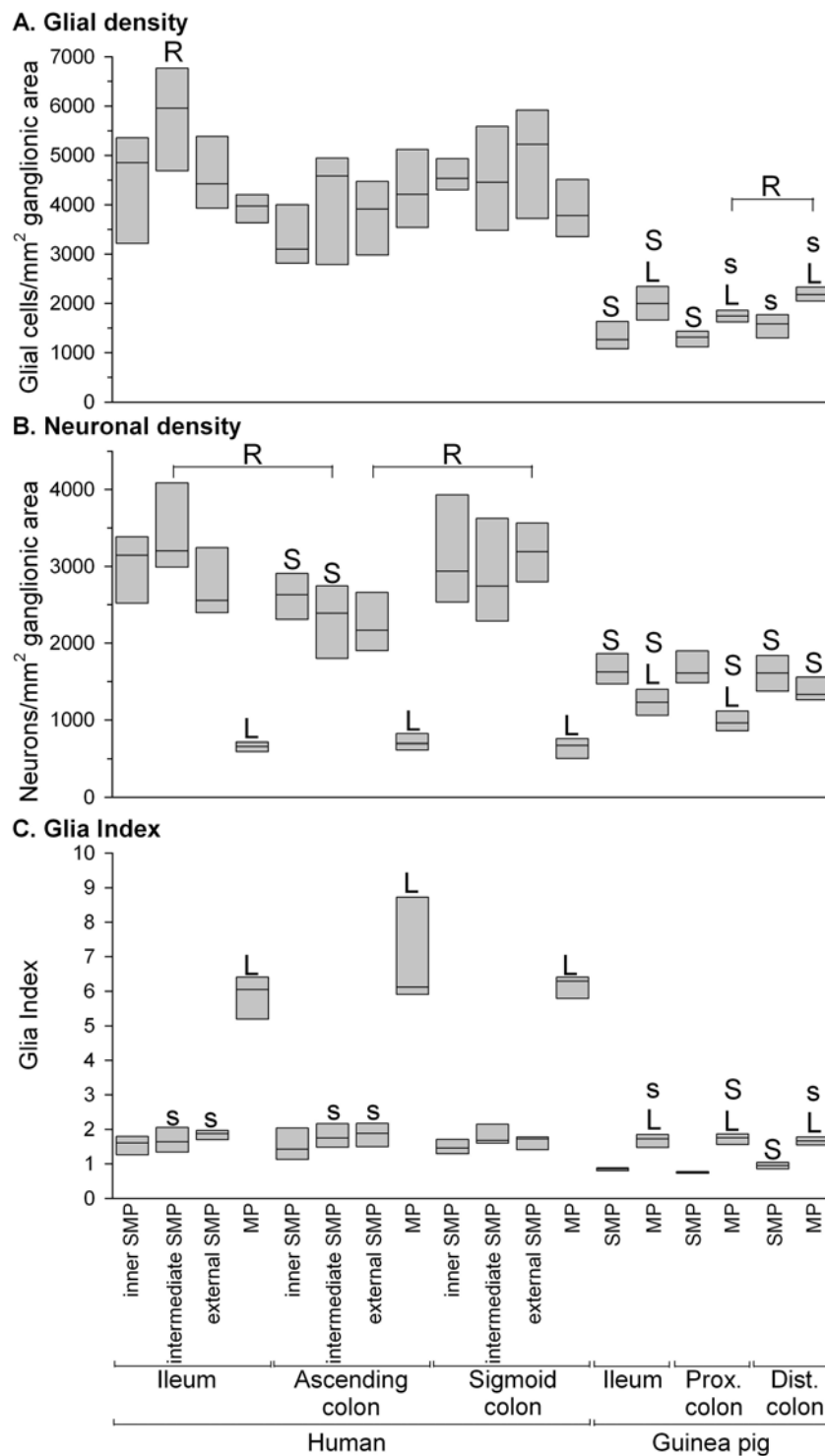
Figure 13. Glial and neuronal density and glia index in the human and guinea pig ENS. Whole-mount preparations of the inner, intermediate and external submucous plexus (SMP) and the myenteric plexus (MP) of ileum, ascending and sigmoid colon in man, as well as the corresponding guinea pig plexus layers and regions were double labeled with anti-Sox8/9/10 and anti-NSE antibodies and appropriate secondary antibodies coupled with the fluorophores Cy3 and Cy2, respectively. EGC and neuronal cell density per ganglionic area (A, B) and the glia index (i.e. glia:neuron ratio) (C) were computed for each tissue. The boxes represent the median (n=6 preparations) and interquartile ranges. L Significant difference between plexus layers of the respective gut region of man or guinea pig; p≤0.002 (A,B); p<0.001 (C); R significant difference between gut regions of man and guinea pig; two-way ANOVA using the Holm-Sidak method; p<0.05 (A); p<0.01 (B); S significant difference between the MP (Student's *t*-test; p<0.001, A; p<0.01, B) or SMP (one-way ANOVA with the Holm-Sidak method, testing all human SMP against the guinea pig SMP; p<0.001, A; p<0.05, B; p<0.002, C) of man and guinea pig. Low case letters indicate Mann-Whitney rank sum test (p≤0.002; A,C) or Dunn's method for ANOVA post-hoc tests (p<0.05).
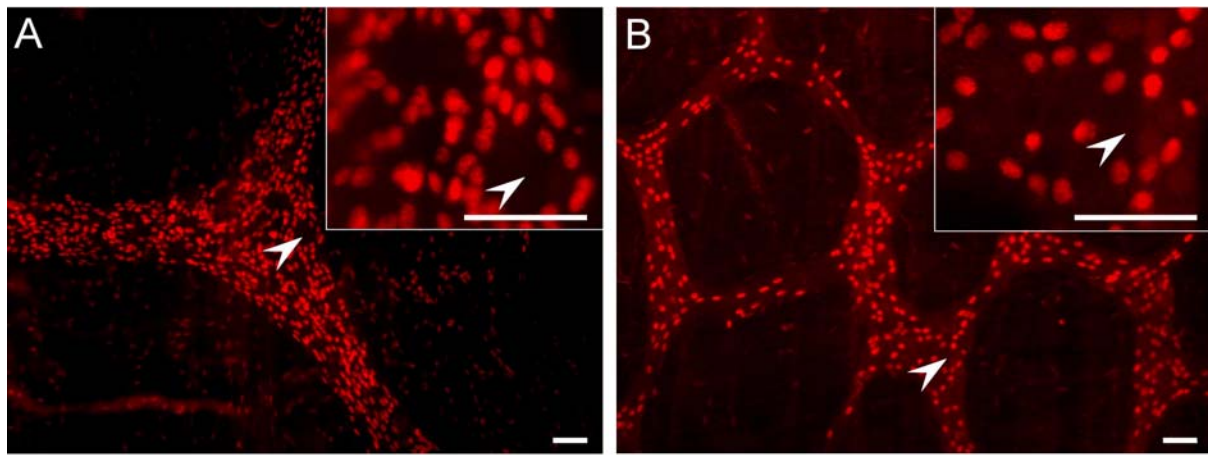
Figure 14. Immunohistochemical visualization of species-dependent differences in the enteric glia index. Human (A) and guinea pig (B) distal colon MP whole-mount preparations were labeled with the anti-Sox8/9/10 antibody. The arrowheads mark the position of a neuronal cell body encircled by glial cell nuclei; the inserts depict the respective area at higher magnification. The human ENS exhibits a higher glial cell density and a higher number of glial cells per neuron resulting in a substantially higher glia index (cf. Fig.5). Original magnification: 10x, insert: 40x; scale bars = 50 µm.
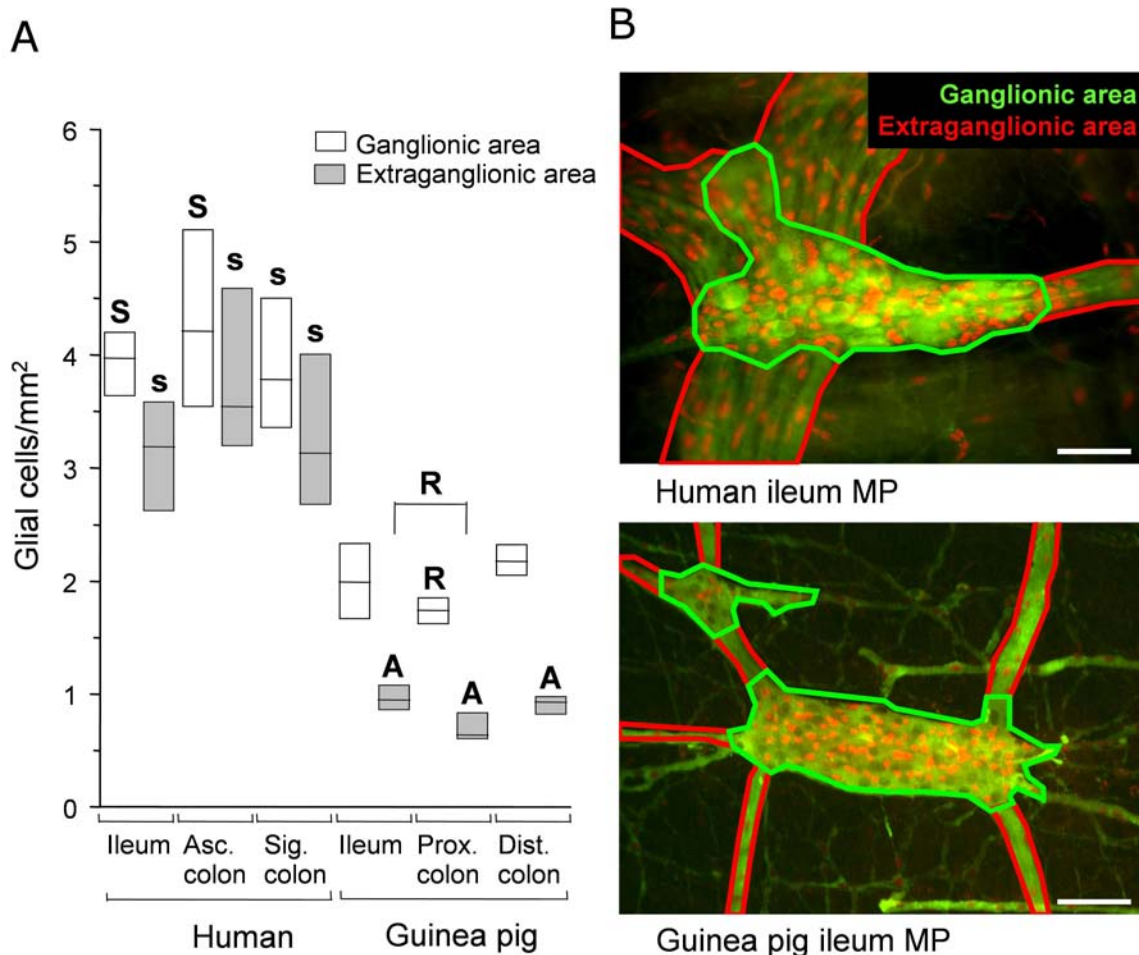
Figure 15. Glial density in the ganglia and extraganglionic area of human and guinea pig myenteric plexus. (A) MP whole-mounts from human and guinea pig intestinal tissues were immunostained with anti-Sox8/9/10 and anti-NSE antibodies, and glial cells were counted both in the ganglia and interganglionic nerve strands. Boxes represent the median (n=6 preparations) and interquartile ranges of glial cell density. A Significant difference between ganglionic and extraganglionic area of the respective gut region of man or guinea pig; $p<0.001$; R significant difference between gut regions of guinea pig; two-way ANOVA with the Holm-Sidak method; $p<0.02$; S significant differences between the ganglionic and extraganglionic area of man and guinea pig were analyzed using Student's *t*-

test (p≤0.001) or Mann-Whitney rank sum test (p=0.002) for non-normally distributed mean scores (indicated with low case letters). (B) Immunohistochemical visualization of representative ganglionic vs. extraganglionic areas in whole-mount preparations of human (top) and guinea pig (bottom) ileum myenteric plexus (MP). Tissues were double-labeled with anti-Sox8/9/10 and anti-NSE antibodies and photomicrographed at identical magnification. Ganglionic (red) and extraganglionic (green) areas used for quantification are highlighted.
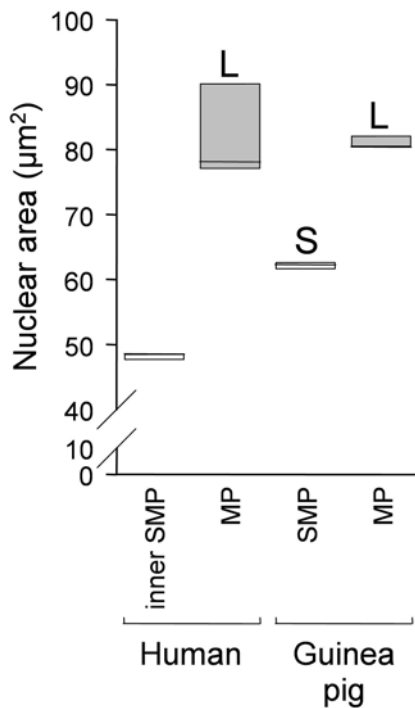
Figure 16. Nuclear area of human and guinea pig EGC stained with the anti-Sox8/9/10 antibody. Whole-mount preparations from the inner submucous plexus (SMP) and SMP, respectively, and from the myenteric plexus (MP) of human and guinea pig ileum were assessed, and 25 cells from 5 ganglia of each preparation (n=3) were quantified. The boxes represent the median and interquartile ranges. L Significant difference between plexus layers of man and guinea pig; p<0.001; S significant differences between the respective plexus layers of man and guinea pig; two-way ANOVA with Holm-Sidak for multiple comparison procedures; p≤0.001.

3.1.2. Quantitative description of the ENS in Crohn's disease

Whole-mount preparations of the MP from the uninvolved proximal and distal resection margin as well as from affected gut regions (ileum and colon) of patients with CD were labeled with antibodies against Sox8/9/10 as the glial marker and neuron specific antibodies against NSE (Figure 17). As in controls, Sox8/9/10 marked all EGC nuclei within ganglia as well as glial nuclei associated with large nerve fiber tracts and neuronal fibers ramifying into the muscle coat. NSE showed a similar cytoplasmic staining pattern as in control tissues. It was noted, that labeling quality was similar in all regions. Variability of staining intensity between CD tissues was comparable to control tissues. Also, no conspicuous differences between affected and macroscopically un-involved proximal and distal CD regions, and controls were detected. Dissection was sometimes complicated by hyperplastic or fibrotic tissue areas so that the ENS could not be totally freed from muscle fibers which interfered with staining quality. Antibodies could not always fully penetrate the tissues. Whole-mount preparations of specimens from inflamed regions of CD patients undergoing surgery because of fibrostenotic strictures were technically not feasible and massive hyperplasia of the muscle layer obscured the epitopes for the antibodies so that lack of immunoreactivity was the consequence. Regarding the SMP, whole-mount preparations of this plexus layer from patients with affected CD could not be obtained due to impaired tissue structure. Therefore, only tissues containing the MP were analyzed.
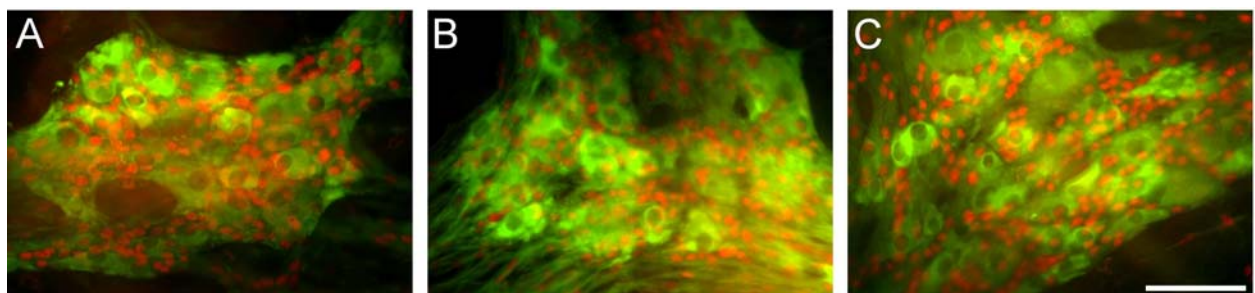
Figure 17. Expression of Sox8/9/10 and neuron specific enolase (NSE) in the ENS of patients with Crohn's disease. Double-labeled whole-mount preparations of the myenteric plexus from unaffected ileum (A), from an inflamed area of the ileum (B) and uninvolved region of the colon (C) showing ganglia with enteric glial cell nuclei displayed as red dots. Neuronal structures are green colored. Original magnification 20X, scale bar = 50 µm.

Quantitative assessment of tissues from CD patients showed that, glial density was 2940 – 4840 cells per mm^2 ganglionic area versus 2920 - 5240 in controls (Figure 18 A). These numbers were not significantly different. In contrast, statistically significant differences were observed for neuronal density (p≤0.001): The number of neurons per

ganglionic area was increased in affected areas of CD patient tissues compared to proximal and distal sampling sites, whereas there was no difference compared to proximal and distal control tissues (Table 6; Figure 18 B). Dilatation of tissues sampled proximal and distal to affected gut segments of CD patient was not observed. The proximal resection margin of CD samples exhibited the lowest neuronal density. These differences were independent of the glia index from the same region, because they were not big enough to influence the glia index (Figure 18 C). Although the glia index was 5.1 ± 0.8 (mean $\pm$ SD; n=5) for the affected area of CD, the difference was not significant compared to all other areas ranging from 5.9 ± 0.9 (CD dist.; n=7) to 6.2 ± 0.6 (CD prox.; n=8) (; p=0.364; Table 6; Figure 18C). Most likely this was due to the small sampling number available for analysis.

No differences were detected between ileum and ascending colon from control patients for all variables assessed (glial and neuronal density, glia index, glial and neuronal cell numbers and the ganglionic area). Therefore, data from ileal and colonic specimens of affected CD areas were pooled for analysis.

Regarding absolute cell numbers, glial cells per ganglion and neurons per ganglion from colon (control) were higher than those numbers from CD areas (p=0.001 and p=0.004, respectively), but not ileum (control) (Figure 18 D,E). Also the control ileum did not differ from CD areas. Ganglionic area was significantly smaller in affected CD regions (p=0.005) and those distal to them (p=0.006) compared to ascending colon (Figure 18 F).

There was no significant correlation detected between age and any of the variables analyzed. Also, gender did not influence any of the parameters measured in the ENS of CD patients.

Table 6.   EGC and neurons in the ENS of CD patients and controls.

	n	Glial cells per ganglion	Neurons per ganglion	Glia index	Glial cells/mm^2 ganglionic area	Neurons/mm^2 ganglionic area	Ganglionic area mm^2 (x1000)
control ileum	6	315±160	53±25	5.9±0.8	3882±308	668±83	80±35
CD ileum unaffected	8	263±50	43±11	6.2±0.6	3442±336	539±48	80±17
CD affected	5	218±44*	44±10*	5.1±0.8	3953±573	782±72	55±8
CD colon unaffected	7	208±62	38±9	5.9±0.9	3587±382	617±77	60±12
control ascending colon	6	419±62	70±10	6.0±1.6	4079±925	687±95	100±13

Data are presented as mean ± standard deviation. *Not normally distributed data.
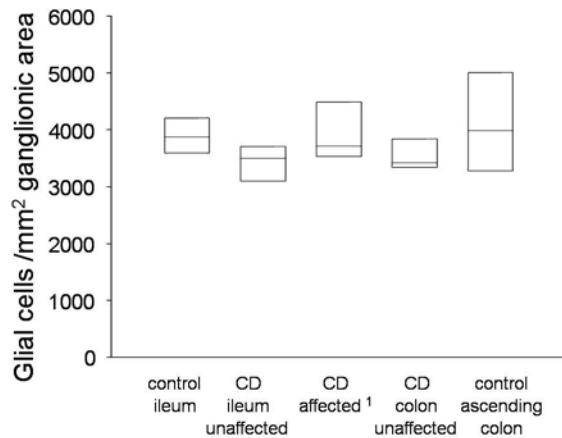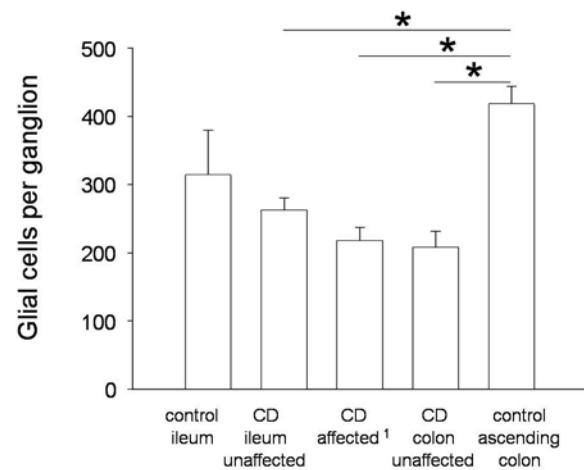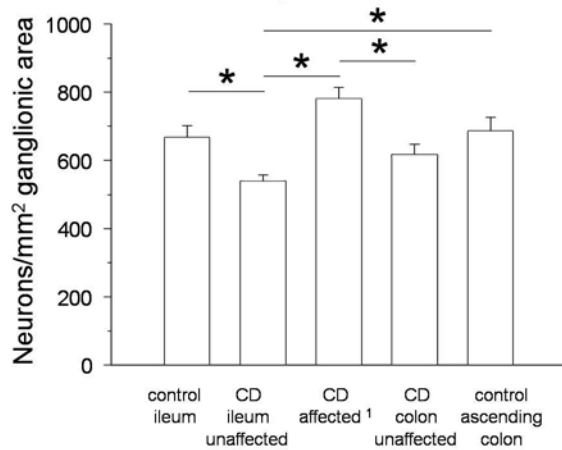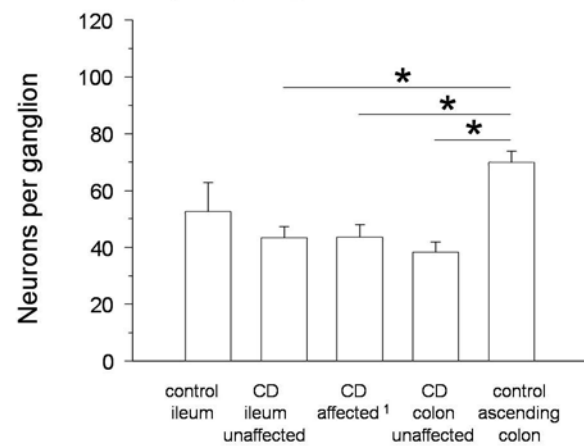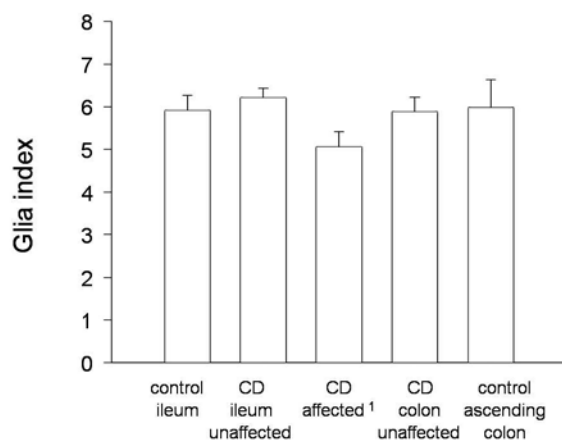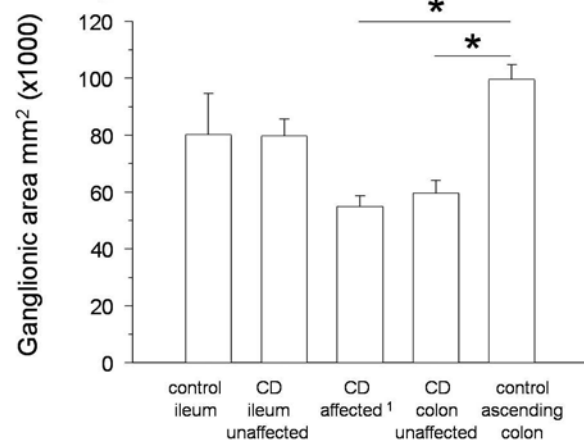
Figure 18. Quantitative assessment of the ENS in Crohn's disease (CD). Whole-mount preparations of the myenteric plexus of ileum from controls (n=6), unaffected ileum from CD patients (CD prox.; n=8), inflamed area (CD affected; n=5) from CD patients, uninvolved colon from CD patients (CD dist.; n=7) and ascending colon of controls (n=6) were double labeled with anti-Sox8/9/10 and anti-NSE. EGC and neuronal cell density per ganglionic area (A, B) and the glia index (i.e. glia:neuron ratio) (C) were computed for each tissue. EGC and neurons were counted and expressed per ganglion (D, E); the analyzed ganglionic area was multiplied by a factor of x1000 and is given as area per mm^2 (F). * Significant difference between groups; one-way ANOVA with the Holm-Sidak method. Bars represent the mean ± SD and boxes the median and interquartile ranges.

3.2.   Functional analyses (*in vitro* studies)

3.2.1. Isolation and characterization of EGC cultures

Enzymatic dissociation of human or rat longitudinal muscle-myenteric plexus preparations or human submucous plexus preparations yielded primary tissue cultures consisting of many different cell types amongst which fibroblasts, smooth muscle cells and EGCs were most frequently seen. In these primary cultures, EGC were morphologically characterized as small, bipolar or star shaped cells with a dense cytoplasm extending two or more processes of variable length that are irregularly branched, and a distinct centrally placed nucleus with one or several poorly defined nucleoli. EGC were growing in an island-like manner but closely intermingled with other cell populations. A minimum percentage of EGC had to be present in the mixed cell culture to ensure appropriate glial proliferation which competed with fibroblasts on growth area. Application of complement-mediated cell lysis using an antibody against human CD90 (Thy-1.1), a cell surface marker exhibited by fibroblasts, hematopoietic stem cells, neurons and some CD34+ cells could enrich the percentage of EGC in the primary cultures by eliminating mainly fibroblasts. Up to ten complement-mediated cell lyses were performed in order to obtain purified human EGC cultures from MP preparations. After about 2-3 month in culture, the cells exhibited signs of degeneration. Proliferation rates declined, vacuoles were seen in the cytoplasm and small granula near the cell nuclei. Cell debris was present as dark particles by phase contrast microscopy and cells began to detach from the bottom of the culture vessels. Primary cultures from human SMP were challenged by bacterial overgrowth due to their exposure to the microbiotia of the gut lumen at the time of the dissection process. This could not be controlled by even the highest concentrations of antibiotic and antimycotic agents. Further, due to the low percentage of EGC in the SMP, human SMP cultures were regularly overgrown by fibroblasts. In contrast to these mixed primary cultures, purified rat cultures consisted of homogeneous cell populations as evidenced by phase contrast microscopy and immunohistochemistry. Rat EGC also grow in islands and, thereafter, form honeycomb-like macro structures before becoming subconfluent. At subconfluence, EGC typically showed a spindleshaped or stellate morphology. Proliferation continued until stable flat monolayers were formed. At confluency the cells were polygonal with indistinct or invisible intercellular borders (Ruhl et al 2001c). Immunohistochemically, purified rat EGC cultures could be selectively labeled with anti-Sox8/9/10, anti-GFAP and anti-S-100 (Figure 19 A-H). Immunostaining confirmed that

purified rat cultures consisted of a homogeneous cell population which was free from any contaminating cell types. All EGC exhibited strong immunoreactivity for Sox8/9/10 and GFAP and somewhat weaker staining for S100b (Figure 19). To confirm the specificity of the monoclonal anti-Sox8/9/10 and the polyclonal anti-GFAP antibodies, these were used in mixed cultures consisting of primary EGC and the intestinal epithelial cell (IEC) line Caco-2 (Figure 19 I-L). The nuclear stain Hoechst 33258 was used to identify all cells present in the cultures. Strong immunoreactivity (IR) for Sox8/9/10 and GFAP was present in EGC exhibiting an exclusive nuclear and exclusive cytoplasmic staining pattern, respectively. Caco-2 cells were not immunoreactive for Sox8/9/10 and GFAP. Nuclei of both cell types were stained with Hoechst 33258, but only EGC showed colabeling with Sox8/9/10 and Hoechst 33258, evidencing the nuclear localization of Sox8/9/10-IR (Figure 19 L).
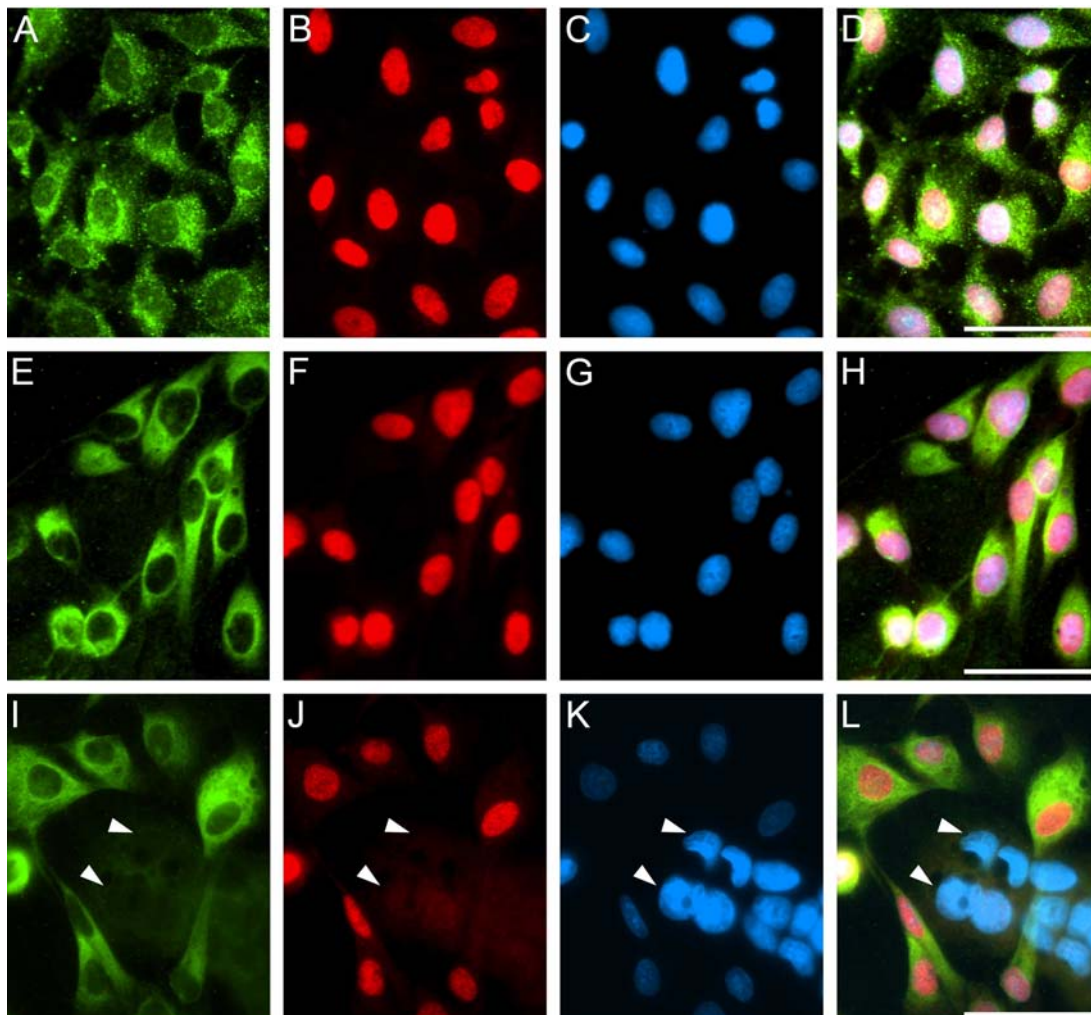
Figure 19. Verification of enteric glial cell (EGC) culture purity. Enzymatically dissociated preparations from rat MP were purified by complement mediated cell lysis. EGC (A-H) or EGC and Caco-2 cells (I-L) were seeded on cover slips and stained for S100b (A) or GFAP (E,I), Sox8/9/10 (B,F,J) and Hoechst 33258 (C,G,K). Purified EGC cultures were triple labeled with either S100b (A) or GFAP (B), Sox8/9/10 (B,F) and Hoechst 33258 (C,G) as seen in the overlay pictures (D,H). Caco-2 cells are immunonegative for the glial markers GFAP (I) and Sox8/9/10 (J), but show nuclear Hoechst 33258 staining (K). (L) Overlay of the triple labeled coculture of Caco-2 and EGC. Arrowheads indicate GFAP immunonegative and Sox8/9/10 immunonegative Caco-2 cells. Scale bars = 50 µm.

In agreement with the immunohistochemical detection of the classical glia marker GFAP *in vitro* and *in situ*, mRNA of this glial intermediate filament protein was found to be constitutively expressed by EGC cultures (Figure 20). mRNA for the intermediate filament protein nestin (NES) was also detected, indicating a certain degree of de-differentiation of EGC in tissue culture.

Beside the glial marker GFAP, which is a glia-restricted intermediate filament protein, some nestin expression was demonstrated in purified EGC cultures. Nestin is primarily expressed in glial precursor cells that are not yet terminally differentiated (Chalazonitis et al 1998a, Chalazonitis et al 1998b). The expression of this intermediate filament species in cultured EGC thus indicates that cultured glial cells de-differentiate from a terminally differentiated state to a somewhat de-differentiated state (Eaker & Sallustio 1998, Jaeger 1995).
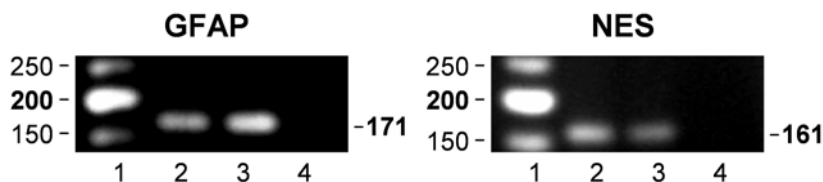
Figure 20. Detection of glial fibrillary acidic protein (GFAP) and nestin (NES) mRNA in enteric glial cell (EGC) cultures. mRNA expression was assessed by RT-PCR with specific primers. PCR products were analyzed on an ethidium bromide-stained 2 %-agarose gel. Lane 1: Low molecular weight DNA ladder (New England Biolabs, Frankfurt); lane 2: EGC; lane 3: rat brain total RNA (Ambion, Austin, TX, USA); lane 4: no template. Results shown for each reaction are from a single representative experiment. Predicted size of RT-PCR products are given on the right hand of each gel image.

Metaphase spreads

Metaphase spreads for karyotyping of rat EGC cultures were prepared to verify species specificity and to exclude cross contamination. Under a phase contrast microscope, the chromosomes could clearly be identified as fine blue filaments. Centromers are typically located in the middle or near to one end of the chromosomes. A fluorescence image of a metaphase spread is in shown in Figure 21.
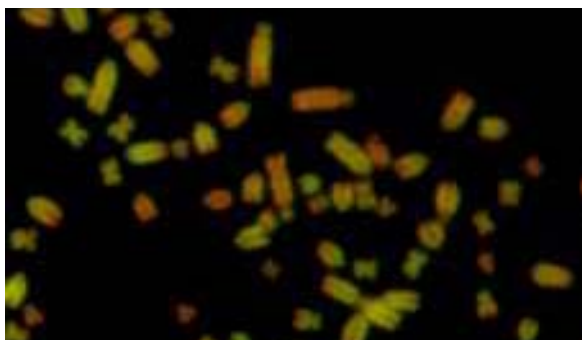
Figure 21. Metaphase spread of enteric glial cell chromosomes. Rat EGC were treated with colcemid to freeze highly condensed chromosomes in the metaphase. After isolation of metaphase nuclei, the chromosomes were stained and spread on microscopy slides and subsequently evaluated by a geneticist.

3.2.2. Coculture experiments – characterization of transepithelial resistance in different cell lines with and without EGC

The influence of EGC on transepithelial electrical resistance (TER) of intestinal epithelial cells (IEC) as represented by the cell lines T84, Caco-2, HT-29 and IEC-6 was investigated at different stages of differentiation of the respective IECs. Epithelial cells were cocultured at different time points after seeding with EGC that had been pre-grown for 2 days. TER values were measured regularly and additionally, morphology and growth characteristics were assessed with an inverted phase contrast microscope.

The Caco-2 cells showed good proliferation and formed a confluent monolayer after about 1 week (Figure 22). TER values of control cultures increased continuously to a maximum of 2570 ± 63 $\Omega \times cm^2$ (mean $\pm$ SEM). On Day 2, TER values of the coculture group (i.e. CaCo-2 plus EGC) were significantly higher compared to control (196 ± 8 $\Omega \times cm^2$ vs. 155 ± 10 $\Omega \times cm^2$; p=0.002). No difference was seen on Day 3. On Day 4 cocultured CaCo-2 cells had significantly lower TER values than the control. Caco-2 cells that had been cultured without EGC reached the highest TER values. On Day 9, a second group of IEC was combined with EGC and also exhibited significantly lower TER values two days later (coculture Day 9: 1512 ± 36 $\Omega \times cm^2$; control: 1801 ± 67 $\Omega \times cm^2$; p<0.05). TER values of the coculture group Day 9 subsequently declined to the level of the coculture group "Day 1" at the end to the assessment period (Day 23).

T84 cells showed a slower proliferation rate compared to Caco-2 cells, whereas TER values increased more quickly than those of Caco-2 monolayers. T84 cells reached their maximum TER values after 10 days in culture (control: 2360 $\Omega \times cm^2$; T84 cells cocultured with EGC from Day 8 on: 2900 $\Omega \times cm^2$) which constantly decreased thereafter (Figure 24). T84 cells that had been in coculture since Day 1 showed higher TER values between Day 5 and 9 compared to control. T84 cells that had been cocultured since Day 8 exhibited higher TER values on Days 11 to 18. T84 cells combined with EGC on Day 22 showed an increased TER value from Day 24 on.

Each time (Day 1, Day 8, and Day 22) when EGC were combined with T84 cells, an increase in TER values was observed. Additionally, coculturing T84 cells with EGC augmented the maximum TER values when compared to T84 cells without EGC in the basolateral compartment of the coculture system.

The primary rat intestinal epithelial cell line IEC-6 showed a different morphology than all other intestinal epithelial cell lines: After seeding, the cells displayed a cobblestone pattern which changed after a couple of days when a three-dimensional structure was formed. Contrary to Caco-2 and T84 cells which reached TER values of 2500 $\Omega \times cm^2$

and more, TER values of IEC-6 cells did not exceed 30 Ω x cm^2 (Figure 23). No differences were detected between groups, and EGC showed no effect on IEC-6 TER values.

HT-29 cells were also slower proliferating than Caco-2 cells. They did not reach TER values above 30 Ω x cm^2 as seen before for the IEC-6 cells (Figure 23). Again, EGC did not affect TER values of this cell line. No significant differences were seen between groups.
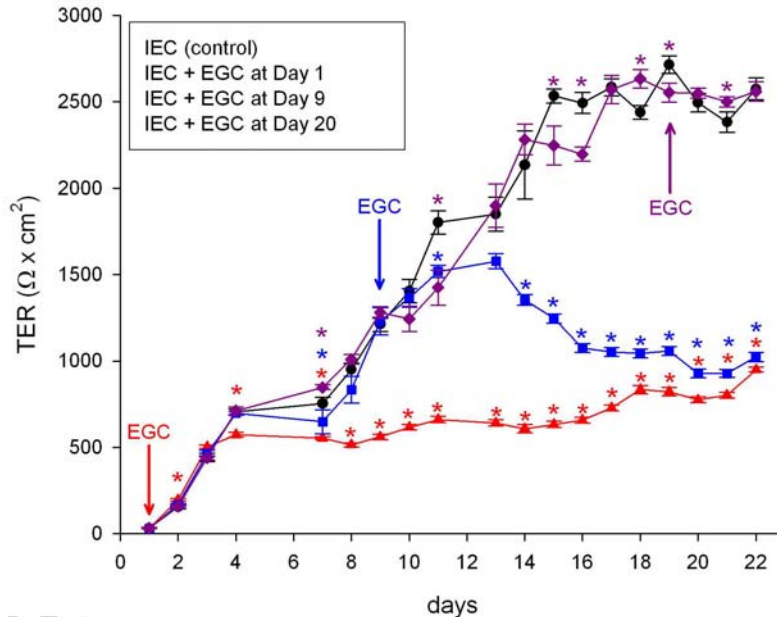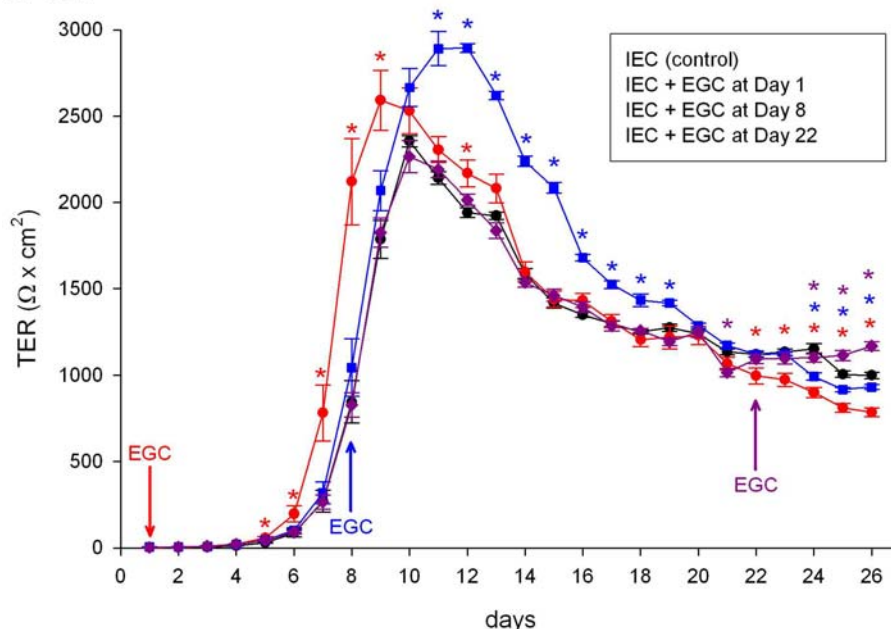
Figure 22. Measurement of transepithelial electrical resistance (TER) of the intestinal epithelial cell (IEC) lines Caco-2 and T84 cells. The Caco-2 (A) or T84 cells (B) were cultured in the apical compartment of the Transwell® system at a density of 50,000 cells/well. At various time points enteric glial cells (EGC; 20,000 cells/well) precultured for 2 days were added to the basolateral compartment of the coculture system. Each data point represents the mean ± SEM of 6 wells.* Significant difference between control and coculture group Day 1 (red), Day 8 (blue) and Day 22 (dark pink); one-way ANOVA or ANOVA on ranks, p≤0.05.

A. HT-29

B. IEC-6
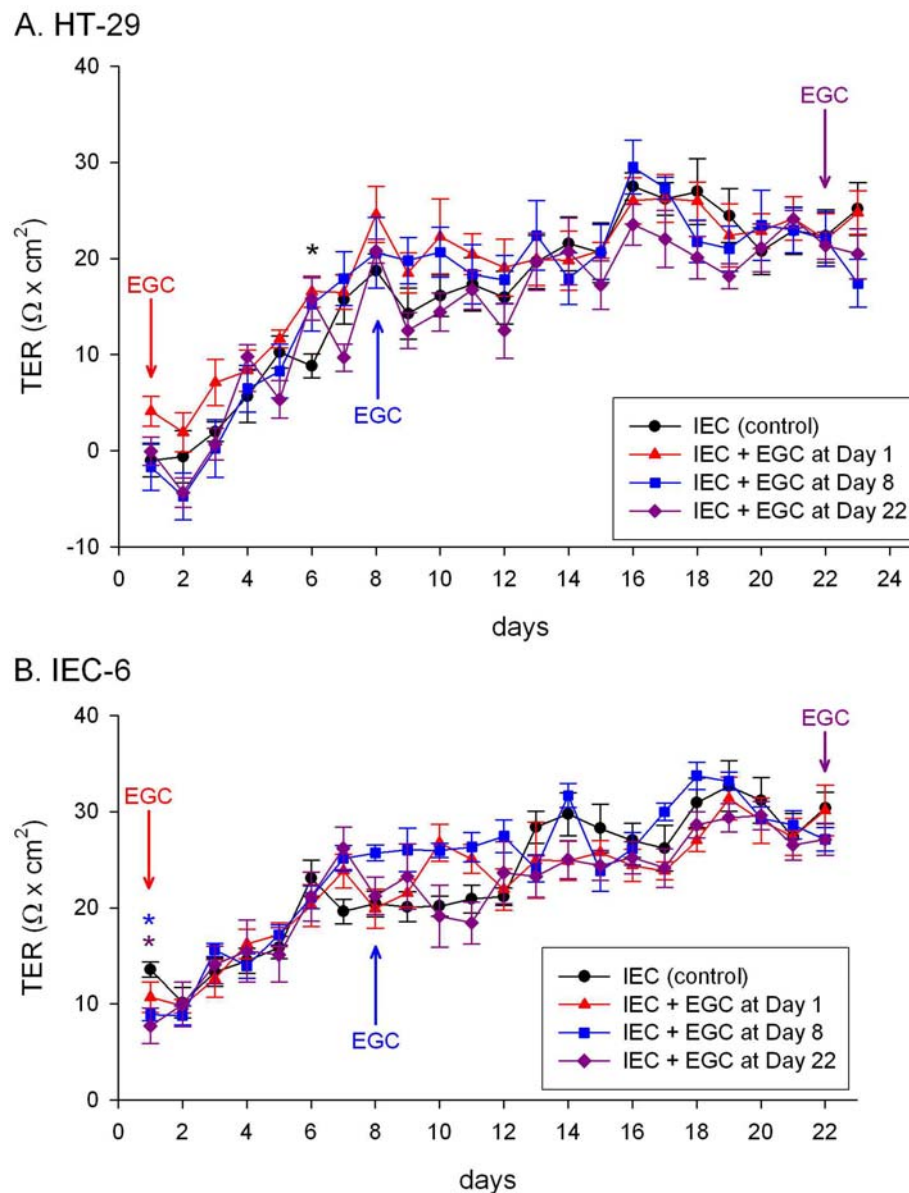
Figure 23. Measurement of transepithelial electrical resistance (TER) of the intestinal epithelial cell (IEC) line HT-29 and IEC-6 cells. The IEC cell lines HT-29 (A) or IEC-6 (B) were cultured in the apical compartment of the Transwell® system at a density of 50,000 cells/well. At Day 1, 8 or 22 enteric glial cells (EGC; 20,000 cells/well) precultured for 2 days were put into coculture with IEC. Each data point represents the mean ± SEM of 6 wells. (A) * Significant difference between control and all other groups; ANOVA on ranks. (B) * Significant difference between control and coculture group Day 8 (blue) and Day 22 (dark pink); one-way ANOVA with Holm-Sidak method, $p \leq 0.05$.

Coculture experiments – Flux

Macromolecular flux did not differ from baseline at any time point with all used TNFα concentrations. Relative fluorescence unit (RFU) was 6.2 ± 1.2 for FSA and 0.7 ± 0.1 for FD (mean ± SEM).

3.2.3. Coculture experiments – cytokine effects and EGC

A prerequisite to study the effects of cytokine treatment on IEC cocultured in the presence or absence of EGC was expression of cytokine receptors on EGC. RT-PCR revealed mRNA expression for receptors of all cytokines used in the coculture experiments (Figure 24). Expression of the alpha subunit of the interleukin-1 receptor, named IL-1 receptor type I (IL-1R1) was found. It binds IL-1 and transduces the signal in cooperation with the IL-1 receptor accessory protein (IL-1RAP) that is also expressed by EGC. IL-1 receptor type 2 (IL-1R2) is not expressed in EGC. That receptor is a putative decoy for IL-1 to prevent it from binding to IL-1 receptor.

Receptor mRNA for the interferon-γ receptor (IFNGR) as well as for the alpha chain of the interleukin-13 receptor (IL13RA1) and for the TNF receptor 1 (TNFR1) was detected in EGC (Figure 24).
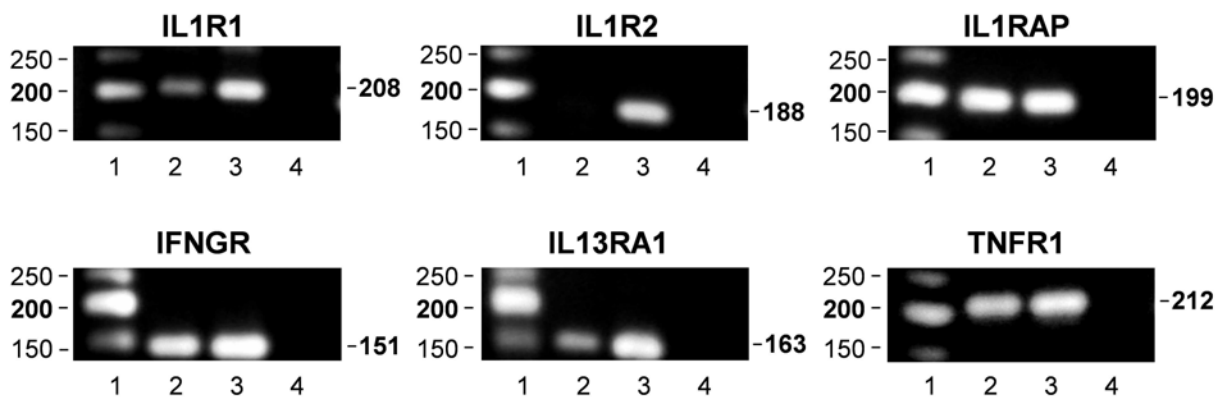
Figure 24. Detection of cytokine receptor mRNA in cultured rat enteric glia cell (EGC). mRNA expression was assessed by RT-PCR with specific primers for IL1R1, IL2R2, IL1RAP (top row), and IFNGR, IL13RA1 and TNFR1 (bottom row). PCR products were analyzed on an ethidium bromide-stained 2 %-agarose gel. Lane 1: Low molecular weight DNA ladder (New England Biolabs, Frankfurt); lane 2: EGC; lane 3: rat spleen total RNA (Ambion, Austin, TX, USA); lane 4: no template. Results shown for each reaction are from a single representative experiment. Predicted size of RT-PCR products are given on the right hand of each gel image. IFNGR1, interferon gamma receptor 1; IL13RA1, interleukin 13 receptor, alpha 1; IL1R1, interleukin 1 receptor, type I; IL1R2, interleukin 1 receptor, type II; IL1RAP, interleukin 1 receptor accessory protein; TNFR1, tumor necrosis factor receptor superfamily, member 1A.

Cytokine effects on transepithelial electrical resistance of T84 cells cocultured with and without EGC

The impact of different cytokines on TER values of T84 cells cocultured with EGC in the Transwell® system or T84 cells alone was explored in this experimental series. Both cell types were treated with or without various cytokines and different combinations of coculture schedules were employed. On the basis of previous reports suggesting that GDNF is involved in the protective effects EGC exert on the epithelium in health and

disease (Bar et al 1997, Steinkamp et al 2003, von Boyen et al 2006a), influences of GDNF blocking on cytokine treatment of cocultures was also examined.

In each experiment, basal TER values were recorded before cytokine treatment was introduced (baseline t=0 h). To exclude variation between experiments, relative TER values (percental changes) were computed from these basal values for analyzes. Absolute TER values of all experiments at baseline are given in Table 7.

Table 7.   TER values of T84 cells measured at baseline in cytokine experiments.

Cytokine treatment	TER (Ω x cm$^{2)*}$
TNFα (1 ng/ml)	1757 – 2092
TNFα (10 ng/ml)	1243 – 1416
TNFα (100 ng/ml)	1930 – 2148
TNFα (10 ng/ml) + anti-GDNF	1039 – 1099
TNFα (10 ng/ml) control	902 – 1099
IL-1β (1 ng/ml)	1390 – 1627
IL-1β (10 ng/ml)	1779 – 1913
IL-1β (100 ng/ml)	1767 – 1896
IL-13 (10 ng/ml)	1063 – 1183
IFNγ (100 ng/ml)	1083 – 1151

* Normalized TER values (mean of 6 wells).

Percent changes of the basal TER values of T84 cells alone or in coculture with EGC after treatment with TNFα are given in Figure 25. Eight different groups were included in this series with TNFα concentrations of 1 and 100 ng/ml, whereas in the series with 10 ng/ml of TNFα only 6 groups were assessed. Significant differences between groups are given on the right hand of each panel for the respective time points (24 h, 48h, 72 h) comprising the results of multiple comparison procedures using ANOVA and ANOVA on ranks.

In the series with 1 ng/ml of TNFα (Figure 25 A), at t=24 h TER values of the untreated coculture that has been grown together for 2 days prior the experiment (grey line) differed from the rest. 24 h later, at t=48 h, all groups with EGC in the basolateral compartment of the Transwell® system exhibited higher TER values than both untreated and treated controls. This effect was also seen at t=72 h, when all groups were significantly different from untreated control. At this time point (t=72 h), all groups also were significantly different from treated control (green line) except from the treated coculture grown together for 2 days prior to the experiment (orange line).

In the experimental series using 10 ng/ml of TNFα (Figure 25 B), the most prominent effect was the increase of TER values in the coculture group in which both, EGC and T84 cells, were independently expose to TNFα (orange graph). This effect became more pronounced over time. At the end of the experiment (t=72 h), all T84 cells cocultured with EGC had increased TER values compared to baseline (t=0 h). TER values of the treated control (treated T84 cells; green line) recovered till the end of the experiment after a cytokine dependent decline (t=24 h and t=48 h).

In the experimental series using 100 ng/ml of TNFα (Figure 25 C), the cytokine concentration had a significant effect. All groups that had been exposed to TNFα showed decreased TER values after the treatment period (t=24 h). The untreated group cocultured 2 days prior to the experiment (T84 cells + EGC; grey graph) had increased TER values at this time point (t=2 h). For this group (grey graph), the same effect was also observed in the series with 1 ng/ml of TNFα . Within the next 24 hours (t=48 h), all groups cocultured with EGC that had also been exposed to TNFα showed a positive change of TER, whereas those without TNFα (blue graph) and control (black line) did not. In the end, all groups cocultured with EGC exhibited a positive percentage change in TER values compared to those without EGC independently of prior cytokine treatment.
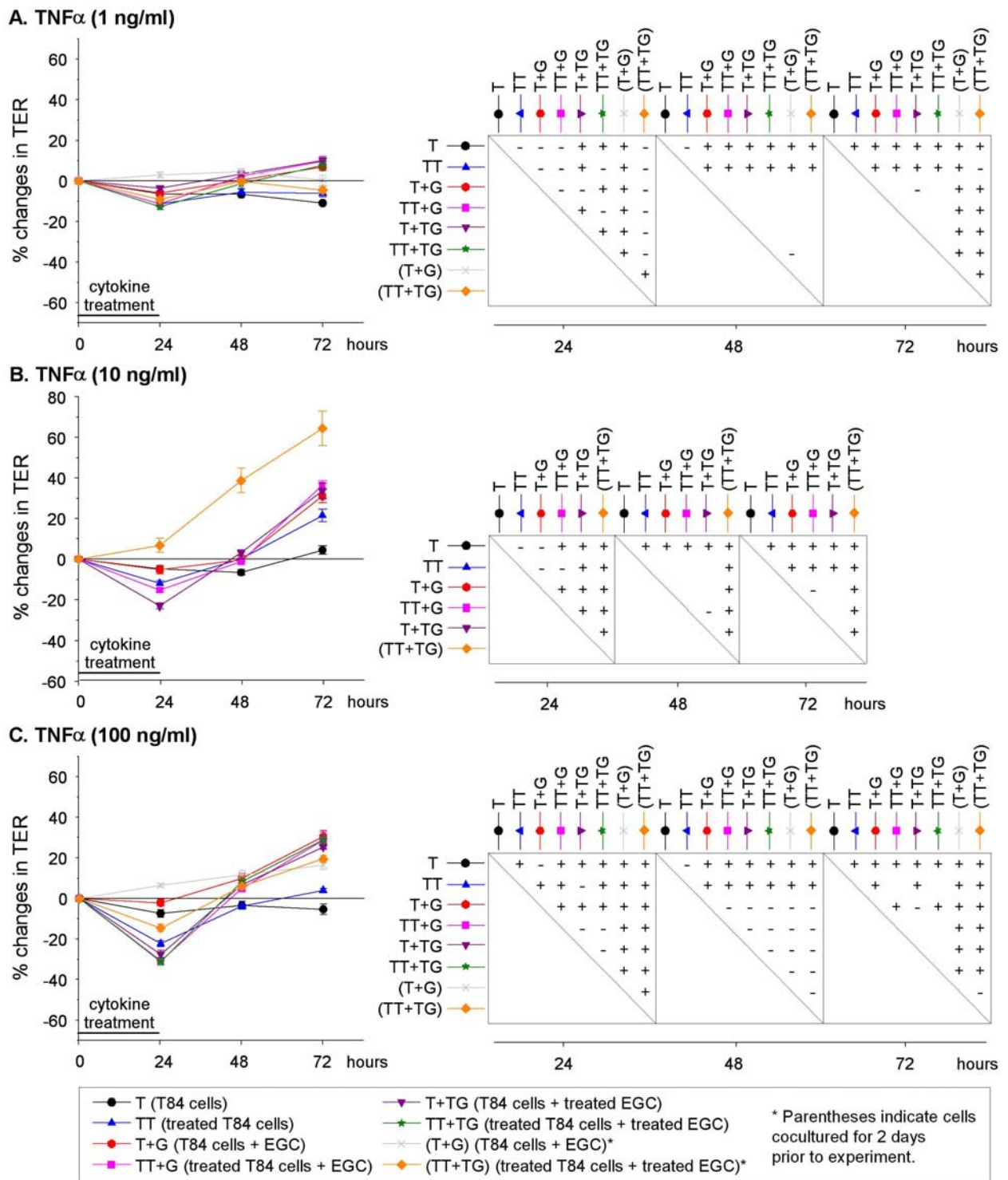
Figure 25. Effects of tumor necrosis factor alpha (TNFα) treatment on intestinal epithelial cells (EGC) cultured with or without enteric glial cells (EGC). Mature IEC monolayers and EGC were grown in the Transwell® system and incubated for 24 h with different concentrations of TNFα. Transepithelial electrical resistance (TER) was assessed before and after (24 h, 48 h, 72 h) the treatment period and is given as % changes in TER. + and - indicate significant difference and no difference between groups, respectively; one-way ANOVA. Blank fields in an upper triangle indicate that ANOVA on ranks was used.

Exposure of T84 cells and EGC to IL-1β showed less clear effects than TNFα (Figure 26). At the lowest concentration of (1 ng/ml), IL-1β decreased TER values in all treated groups (blue, pink, dark pink, green, orange) within 24 hours (Figure 26 A). While

treated T84 cells further decreased with time, the other groups showed less pronounced effect.

At the 10x fold concentration (10 ng/ml), IL-1β produced a decrease in TER values which was most pronounced for the coculture group that had been separately treated before being combined (t=24 h; green graph) (Figure 26 B). Both groups that had been cocultured prior to the experiment (grey and orange line) showed TER values that were above those of the control group (t=48 h and t=72 h.

In the experimental series using a concentration of 100 ng/ml of IL-1β, 6 different groups were included (Figure 26 C): Both groups in which T84 cells and EGC had been simultaneously exposed to IL-1β differed from control (black line) and one another (t=24 h). Over time, all groups cocultured with EGC showed increased TER values. Lack of significance at t=72 h is due to a statistical problem because only 5 wells for the treated IEC group (blue line) were compared to n=6 for all other groups.

IL-13 disrupted the epithelial barrier of T84 cells at a concentration of 10 ng/ml (Figure 27 A) (Sanders et al 1995). A huge decrease in TER was seen 24 hours after beginning of the treatment. The groups with treated IEC (blue, pink, orange) slowly recovered thereafter (t=48 h and t=72 h), but did not regain the basal value within 48 hours after IL-13 treatment. IEC without IL-13 exposure that had been in coculture with EGC - either treated (dark pink) or not (red) - showed significantly higher TER values than IEC that had been treated (blue, pink, orange).

IFNγ (100 ng/ml) showed similar effects as IL-13 (Figure 27 B). Concentration of IFNγ was chosen according to previous reports (Fish et al 1999, Sanders et al 1995). TER values of treated T84 cells alone (blue) or in coculture with treated (orange) or untreated (pink) EGC decreased significantly compared to the other groups and did not regenerate to the basal value within the recording period. The group already grown together prior to the experiment showed less pronounced effects of IFNγ exposure, which was particularly pronounced at t=48 h and t=72 h. Coculturing of untreated T84 cells in the presence of EGC that had or had not been exposed to IFNγ also increased TER values at t=72 h.

Application of an anti-GDNF antibody was used to investigate whether this soluble factor is in part responsible for the effects that EGC exert on T84 cells under normal and inflammatory conditions as mimicked by the treatment of TNFα *in vitro*. Eight groups were compared with each other and with the corresponding group of the control experiment using a two-way ANOVA (Figure 28).
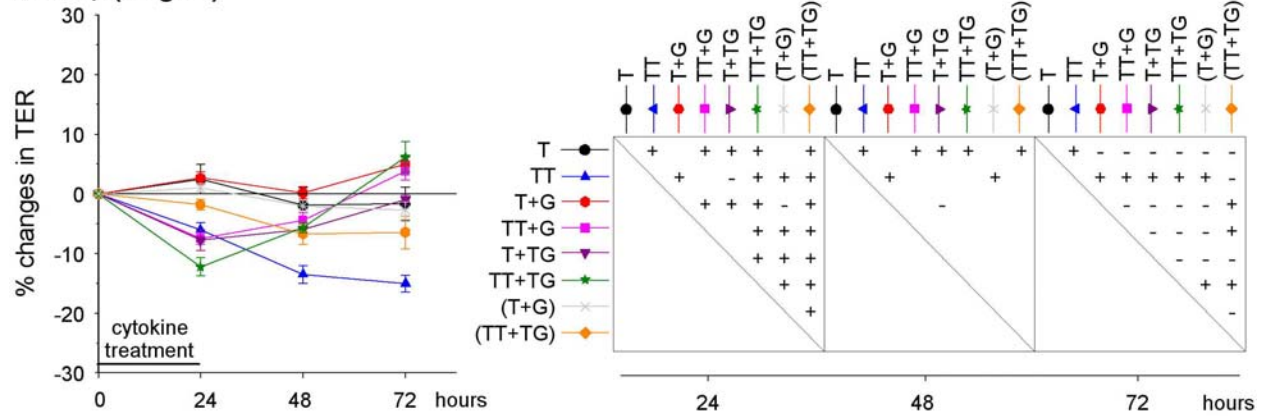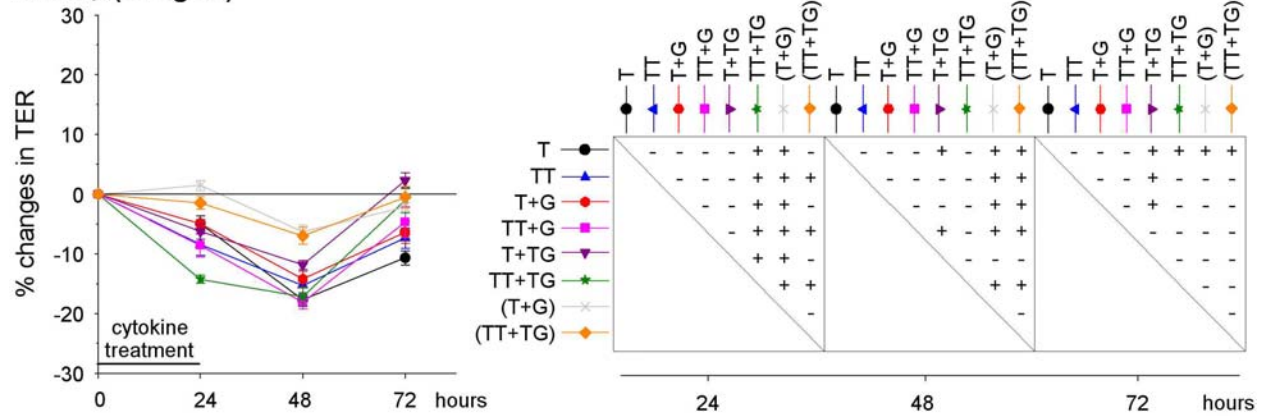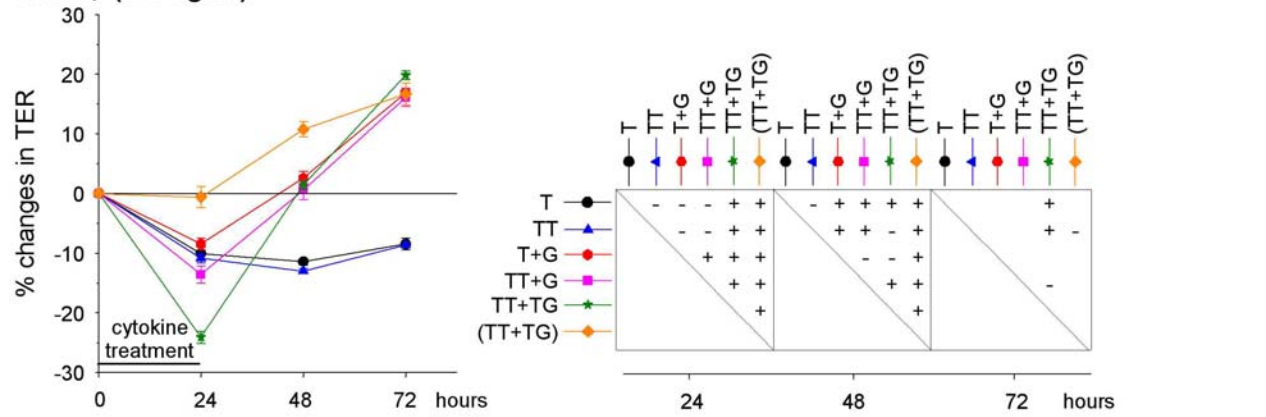
Figure 26. Effect of interleukin-1β (IL-1β) treatment on intestinal epithelial cells (EGC) cultured in the presence or absence enteric glial cells (EGC). Mature IEC monolayers and EGC were grown in the Transwell® system and incubated for 24 h with different concentrations of IL-1β. Transepithelial electrical resistance (TER) was assessed before and after (24 h, 48 h, 72 h) the treatment period and is given as % changes in TER. + and - indicate significant difference and no difference between groups, respectively; one-way ANOVA. Blank fields in an upper triangle indicate that ANOVA on ranks was used.
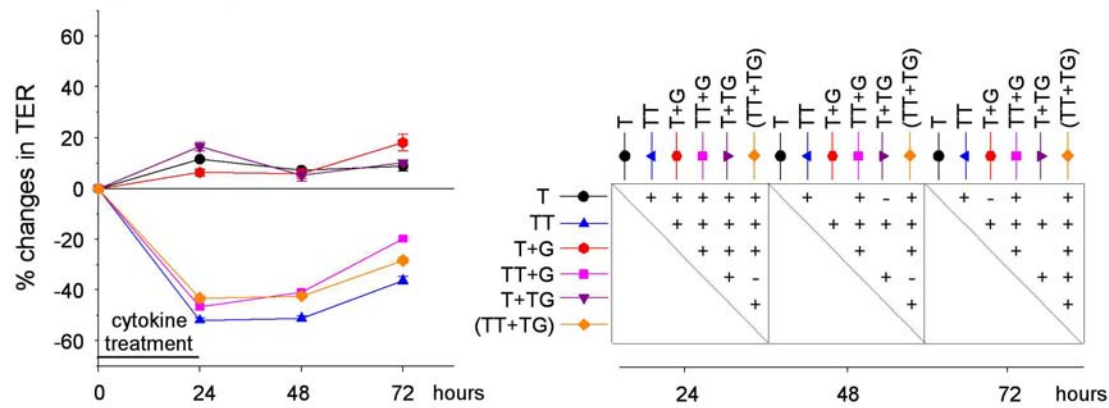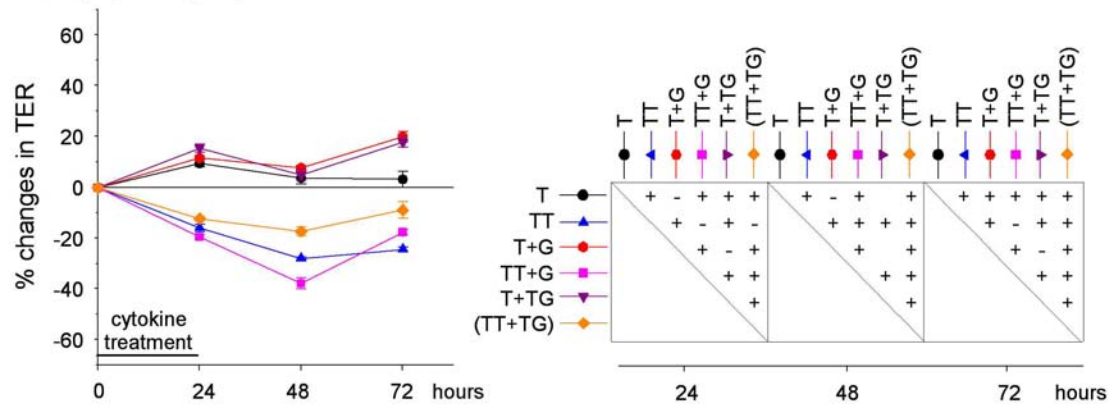
Figure 27. Effect of interleukin-13 (IL-13) and interferon-γ (IFNγ) treatment on intestinal epithelial cells (T84 cells) cocultured with or without enteric glial cells (EGC). Mature IEC monolayers and EGC were grown in the Transwell® system and incubated for 24 h with IL-13 (A) or IFNγ (B). Transepithelial electrical resistance (TER) was assessed before and after (24 h, 48 h, 72 h) the treatment period and is displayed as % changes in TER. + and - indicate significant difference and no difference between groups, respectively; one-way ANOVA. Blank fields in an upper triangle indicate that ANOVA on ranks was used.

At t=24 h, significant differences existed between the anti-GDNF application groups and those without anti-GDNF in the parallel control experiment. T84 cells that had been combined with EGC exposed to anti-GDNF and TNFα (dark pink) showed decreased TER values compared to the corresponding group of the control experiment. This group (dark pink) also differed significantly within the anti-GDNF experiment to T84 cells (control; black line) and T84 cells cocultured with EGC (red line), but not within the control experiment. Another effect of anti-GDNF application was detected comparing the TNFα treated group cocultured prior to the experiment (orange graphs). Although there was an increase in TER values in both groups, the one where anti-GDNF was added was less pronounced. Cells that had been cocultured prior to the experiment and were never exposed to TNFα (grey line) exhibited the highest positive changes in TER

values compared to all other groups. Anti-GDNF exposure did not affect the control group (Figure 28 A). No differences for anti-GDNF application were tested at the two following measurements (t=48 h and t=72 h) due to lack of statistical significance.

At the subsequent time point (t=48 h), the coculture groups grown for 2 days before the experiment (grey and orange graphs) had the highest percentage change in TER compared to all other groups. In the control experiment at t=72 hours, all groups cocultured with EGC had an increased TER value compared to those grown without EGC in the system (Figure 28 B). Similar effects could also be observed in the anti-GDNF experiment (Figure 28 A).
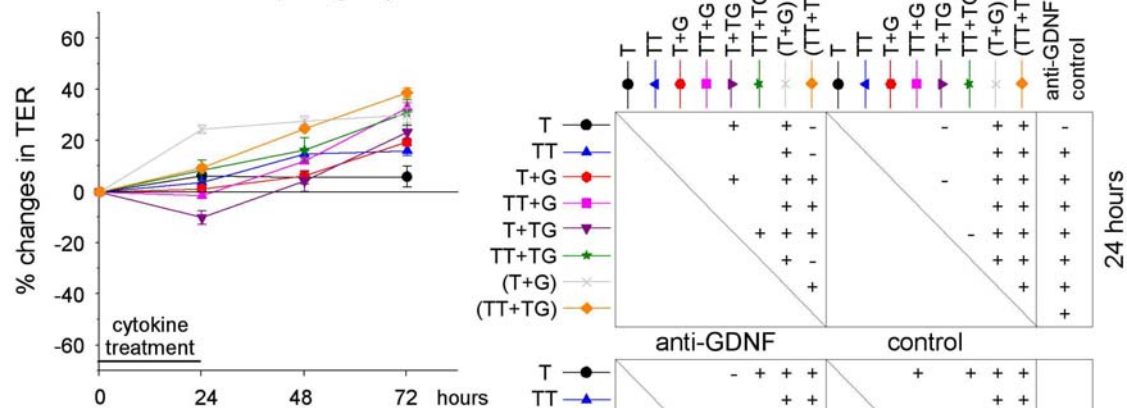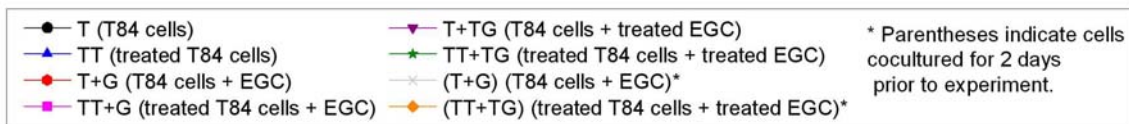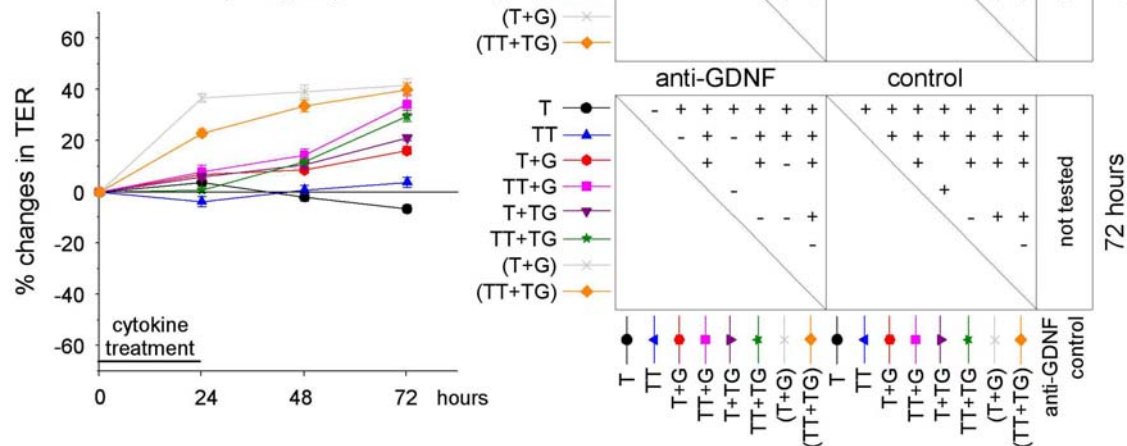
Figure 28. Application of an anti-glial cell line-derived neurotrophic factor (anti-GDNF) antibody affects intestinal integrity assessed by transepithelial electrical resistance (TER). Mature IEC monolayers in the presence or absence of EGC were grown in the Transwell® system and incubated for 24 h with TNFα (10 ng/ml) and anti-GDNF (0.05 µg/ml) or medium as the control. TER was assessed before and after (24 h, 48 h, 72 h) the treatment period and is given as % changes in TER. + and - indicate significant difference and no difference between groups, respectively; one-way ANOVA. Blank fields in an upper triangle indicate that ANOVA on ranks was used. Note: Anti-GDNF was added to the medium when IEC were combined with EGC. This was at t=0 for all groups except those two that where cocultured for 2 days prior to the experiment, i.e. (T+G) and (TT+TG).

Cultured EGC express neurotrophins and neurotrophin receptors

Nerve growth factor (NGF) mRNA and neurotrophin-3 (NT-3) mRNA expression was found in EGC cultures (Figure 15). The specific primers and the used real-time RT-PCR protocol yielded DNA amplification products with bands of predicted size on agarose gels. Both NGF and NT-3 belong to the family of neurotrophins and signal through binding to neurotrophin receptors. A receptor that all neurotrophins share is the low-affinity nerve growth factor receptor p75 (p75NGFR or NGFR). NGFR mRNA expression was clearly detected in EGC as bright bands visualized by ethidium bromide on a DNA gel (Figure 15). mRNA for neurotrophic tyrosine kinase receptor type 1 (NTRK1 or TrkA) and type 2 (NTRK2 or TrkB) was not expressed by EGC, whereas NTRK3 (or TrkC) was expressed (Figure 15). Total RNA from rat brain served as positive control and mRNA for all studied molecules was easily detected in cerebral RNA. Of note, gel electrophoresis and image editing was for qualitative analysis and band intensity merely reflects gel loading.
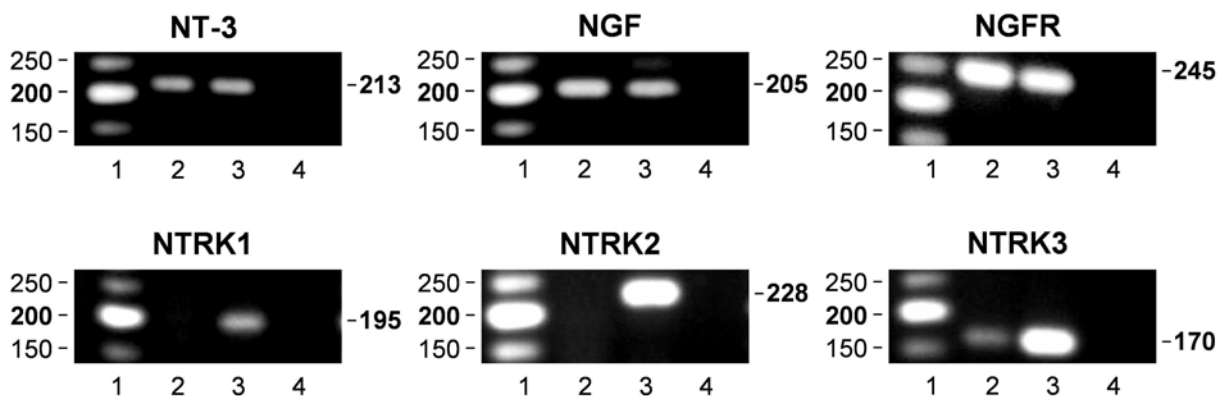
Figure 29. Detection of neurotrophin-3 (NT-3), nerve growth factor (NGF) and their receptor mRNA in cultured enteric glial cells (EGC). mRNA expression was assessed by RT-PCR and PCR products were resolved on 2 % agarose gels using primers specific for NT-3, NGF, NGF receptor (NGFR) (top row), and neurotrophic tyrosine kinase receptor, type 1 (NTRK1), type 2 (NTRK2) and type 3 (NTRK3) (bottom row). Lane 1: Low molecular weight DNA ladder (New England Biolabs, Frankfurt); lane 2: EGC; lane 3: rat brain total RNA (Ambion, Austin, TX, USA); lane 4: no template. Results shown for each reaction are from a single representative experiment. Predicted size of RT-PCR products are given on the right hand of each gel image.

Cultured EGC express GDNF and receptors for neurotrophic factors

Glial cell line-derived neurotrophic factor (GDNF) mRNA was found to be expressed in EGC cultures. The commonly used reference genes, actin beta (ACTB) and histone 3 H3 (HIST3H3) were reliably detected in all experiments (Figure 31 B).

To address the issue of cytokine mediated regulation of GDNF expression by EGC cultured alone or in combination with IEC, mRNA expression of GDNF was quantitatively assessed by real time RT-PCR (Figure 30). Application of TNFα (Figure 30 *A,B*) or IL-1β (Figure 30 *C,D*) in concentrations ranging from 1 – 100 ng/ml for 24 h

to EGC cultured alone (Figure 30 *A,C*) or in combination with IEC (T84 cells) (Figure 30 *B,D*) did not significantly change GDNF expression levels. In more detail, EGC cocultured with T84 cells treated with TNFα at a concentration of 100 ng/ml was not significantly different from the other concentrations due to relatively high SEM values (Figure 30 B; p=0.227). RT-PCR amplification efficiencies (mean ± SD) of experiments with TNFα treatment were 1.72 ± 0.03, 1.75 ± 0.03 and 1.71 ± 0.04, for ACTB, HIST3H3 and GDNF, respectively. In the experimental series with IL-1β treatment, PCR efficiencies of ACTB, HIST3H3 and GDNF were 1.72 ± 0.03, 1.65 ± 0.07 and 1.60 ± 0.10, respectively. In both series, the reference genes ACTB and HIST3H3 were not regulated as validated by linear regression analyses and, thus, were qualified for quantitative analysis of GDNF gene expression (data not shown).

GDNF family receptor 1 (GFRA1) and GFRA2 mRNA were detected in EGC, whereas RET tyrosine kinase mRNA was not expressed by cultured EGC (Figure 31 A). mRNA for fibroblast growth factor 2 (FGF2) was also detected (Figure 31 C).
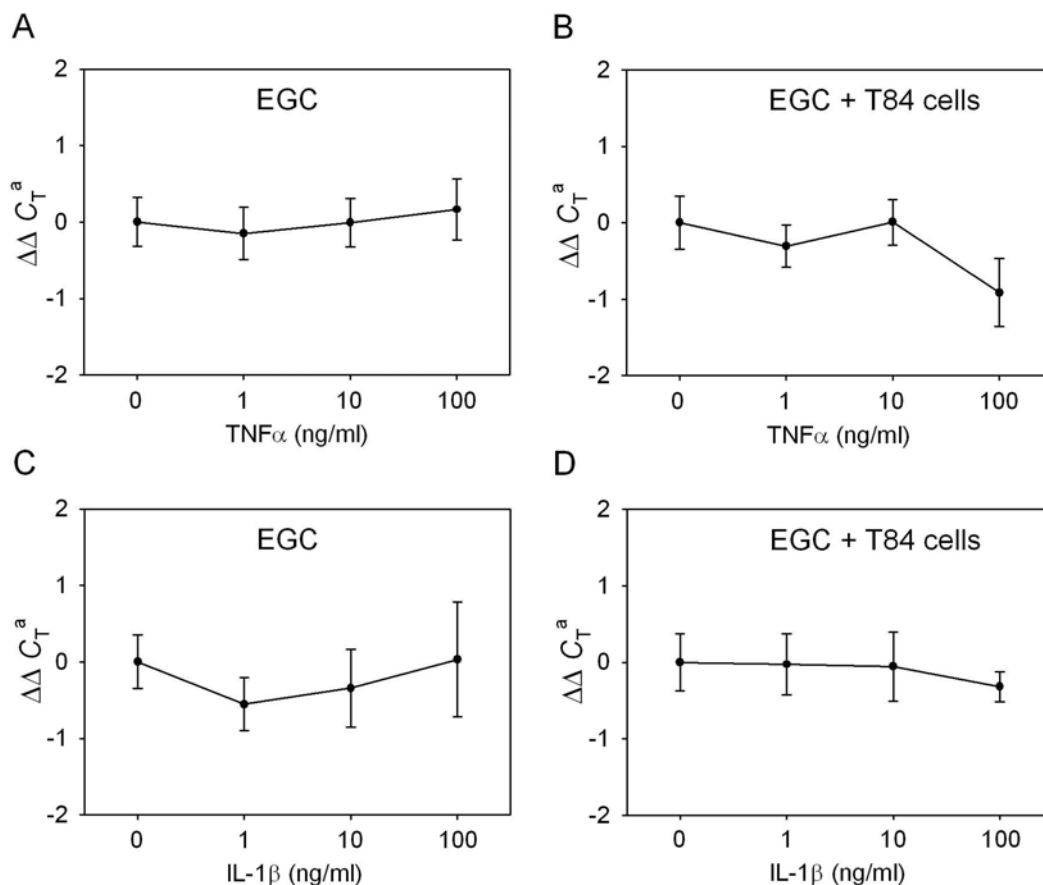
Figure 30. Effects of cytokine treatment (TNFα or IL-1β) on glial cell line-derived neurotrophic factor (GDNF) mRNA expression of cultured enteric glial cells (EGC). EGC alone (A,C) or in coculture with T84 cells (B,D) were incubated for 24 h with 0, 1, 10 and 100 ng of TNFα or IL-1β per ml of medium. mRNA expression was quantified with RT-PCR and standardized with the reference genes ACTB and HIST3H3 and with the mean of the group without TNFα or IL-1β (n = 6-7; mean ± SEM). [a]Positive values indicate a down-regulation and negative values an up-regulation. One-way ANOVA or ANOVA on ranks. No significant difference between treatment and control for all data points. The x-axis is log-scaled.
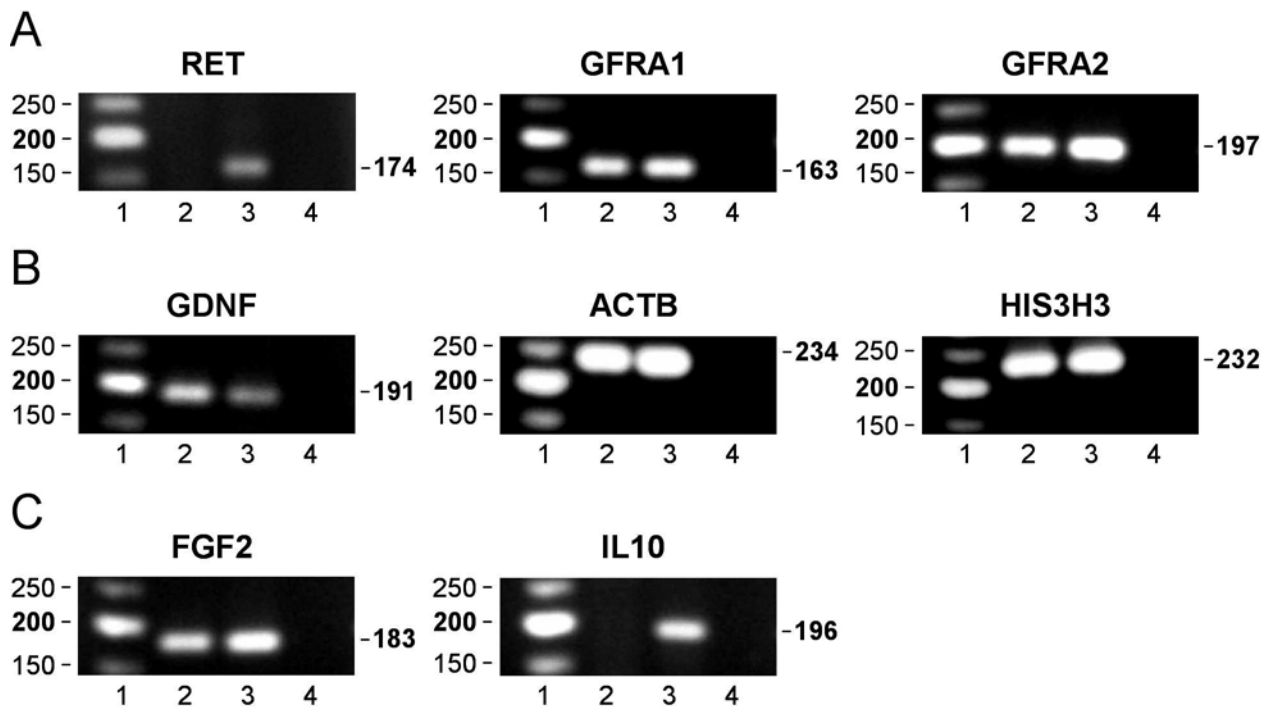
Figure 31. Detection of mRNA expression of growth factors, growth factor receptors and reference genes by cultured enteric glial cells (EGC). mRNA expression was assessed by RT-PCR using specific primers and PCR products were resolved on 2 % agarose gels. Panel A includes RET tyrosine kinase, GDNF family receptor 1 (GFRA1) and GDNF family receptor 2 (GFRA2). Panel B includes GDNF, actin beta (ACTB) and histone 3, H3 (HIST3H3). Panel C includes Fibroblast growth factor 2 (FGF2) and IL-10. Lane 1: Low molecular weight DNA ladder (New England Biolabs, Frankfurt); lane 2: EGC; lane 3: rat brain total RNA or rat spleen total RNA (only for ACTB) (Ambion, Austin, TX, USA); lane 4: no template. Results shown for each reaction are from a single representative experiment. Predicted size of RT-PCR products are given on the right hand of each gel image.

4.   Discussion

Morphological analysis (*ex vivo* studies)

This study aimed to provide a comprehensive set of quantitative data on enteric glia in the normal human and guinea pig ENS. To achieve this, the available glial markers were reassessed in the human and guinea pig ENS, and concurrently, an antibody against the transcription factors Sox8/9/10 that selectively and completely labels glial nuclei was employed. Based on the findings reported here, the anti-Sox8/9/10 antibody is proposed as a novel staining tool that allows for accurate quantification of EGC in the mature human and guinea pig ENS.

Sox8, Sox9 and Sox10 are closely related to each other and, together, constitute group E of the transcription factor family of Sox proteins which are characterized by a highly conserved SRY-related high-mobility-group DNA-binding domain (Wegner 1999). Sox8 expression has been demonstrated in neural crest cells and early glial cells of the developing mouse ENS, but not in the adult mouse gut (Maka et al 2005, Sock et al 2001). Sox9 expression precedes that of Sox8 and Sox10 in neural crest cells and the embryonic spinal cord (Cheung & Briscoe 2003, Stolt et al 2005, Stolt et al 2003) and has been detected in immature glial cells of the central nervous system (Stolt et al 2003). In the ENS, Sox9 is not expressed, neither during development nor in adults (M.W., unpublished data). In contrast, Sox10 has been shown to be present in undifferentiated enteric neural crest cells and to be down-regulated in cells acquiring a neuronal fate while it persists in cells which differentiate into EGC, indicating that Sox10 plays a crucial role in the differentiation of peripheral glia (Britsch et al 2001). Northern blot analysis revealed significant expression of Sox10 in human adult small intestine and colon (Bondurand et al 1998, Pusch et al 1998). Consequently, Sox10 expression appears to be restricted to EGC in the mature ENS (Britsch et al 2001, Paratore et al 2001, Young et al 2003). This was also corroborated by the fact that Sox8/9/10-IR in glial cells could specifically be abolished by pre-incubation of the Sox8/9/10 anti-serum with a Sox10 fusion protein. Based on this evidence, it can be proposed that the positive immunolabeling obtained with the polyvalent monoclonal anti-Sox8/9/10 antibody used in this study represents Sox10 expression in structures of the mature ENS.

In the systematic evaluation of established immunohistochemical glial markers, it was confirmed that antibodies against the calcium binding protein S100b (Ferri et al 1982), GFAP (Jessen & Mirsky 1980) and p75NGFR (Young et al 2003) cannot be used to reliably identify and quantify enteric glia in human whole-mount preparations, because

(a) their cytoplasmatic staining pattern does not allow to distinguish individual cells, and (b) the irregular and patchy nature of S100b and GFAP immunoreactivity in human intestinal tissues does not permit consistent quantitative immunohistochemical studies. In contrast, the presented data evidence that robust quantification of EGC can be achieved with an anti-Sox8/9/10 antibody, both in man and in guinea pig: In this study, S100b and GFAP were fully co-localized with Sox8/9/10, and the cellular localization of the reporter peptide Ala-Lys-AMCA that has previously been established as a pan-glial marker in vital gut tissue (Ruhl et al 2005) displayed a total overlap with Sox8/9/10 immunolabeling in all glial cell bodies of the ENS. In addition, the fact that Sox8/9/10 immunopositivity is entirely restricted to glial cell nuclei allows to clearly and unequivocally discern individual cells which can consequently be easily and reliably quantified.

Earlier reports have claimed that EGC can be indirectly quantified with hematoxylin counterstained PGP 9.5 labeled tissue sections (Wedel et al 2002). However, this method cannot be readily used in whole-mount preparations due to the mass of nuclei from multitudinous other cell types residing in the tissue layers adjacent to the enteric plexuses. Particularly, this holds true in inflamed tissues in which accumulation of mononuclear cells infiltrating the ENS may occur and thus interfere with a hematoxylin-based indirect glial cell quantification method.

There were several pan-neuronal markers available to label enteric neurons when the study was set up, such as NADH (Gabella 1987), PGP (Krammer et al 1993, Wilkinson et al 1992), HuC/D (Lin et al 2002) and NSE (Bishop et al 1982). Although HuC/D seems to label a little more neurons in the ENS than NSE does (Murphy et al 2007), the last one was chosen out of the pool of neuron markers, because (a) it does stain cell bodies and nerve fibers and, thus, allows for the quantification of the ganglionic area and (b) the antiserum was not raised in the same species as the Sox8/9/10 antibody. Furthermore, NSE has previously been used in human (Neunlist et al 2003a, Schneider et al 2001) and guinea pig (Parr & Sharkey 1994) whole mount preparations to label enteric neurons.

A laminar preparation technique was used in this study because laminar whole-mount preparations are best suited to provide a comprehensive view of the entire two-dimensional architecture of the ENS network so that differences in topography, architecture and morphology are clearly better discernible than in tissue sections (Wedel et al 1999). On the other hand, preparing laminar whole-mounts is tedious and time-consuming, as well as technically limited in thick (e.g. fibrotic) human tissues.

Further, whole-mount preparations may sometimes be too thick to allow antibodies to penetrate the tissues and quantitatively reach their epitopes.

To facilitate glial quantification in clinical routine histopathology studies it will, therefore, be necessary to advance the current methodology: Anti-Sox10 immunostaining can be useful to directly depict EGC in tissue sections of human intestinal tissues which are much easier to obtain, but, by definition, reveal only a limited portion of the ENS and not its entire meshwork. Hence, a novel read-out is desirable to allow for glial quantification even if only small tissue sections are accessible.

In this study, glial and neuronal cells per ganglion were counted, and ganglionic areas for each plexus in all studied regions and species were measured. In this set of analyses it was found that, overall, there are substantially more EGC in the MP than in the SMP, both in man and guinea pig. In addition, it became evident that EGC are significantly more numerous in the human than the guinea pig ENS. It may be argued that these observations merely reflect the well-known fact that ganglia are larger in the MP than in the SMP, and, likewise, larger in bigger than in smaller mammals (Gabella & Trigg 1984). However, neuronal cell counts were identical between human and guinea pig tissues, and at least in human ileum and sigmoid colon, all SMP ganglia were *smaller* than in the corresponding guinea pig regions.

Strikingly, the neuronal numbers per ganglion were quite similar between man and guinea pig, varying by a factor of 0.3-1.1, whereas the glial cell number per ganglion differed by a factor of 1.5-3.8. This resulted in a significant difference in the glia index which describes the ratio of glial cells to neurons: The glia index was about 3.5-4 times higher in human MP and twice as high in the guinea pig MP compared to the SMP. Between species, the glia index was approximately 2 times higher in the SMP and 3.5 times in the MP of the human as compared to the guinea pig ENS. The glia index would have risen substantially if glial cells from nerve fiber strands (extraganglionic area) had been included in the quantitation, but the present analysis comprised only primary and secondary nerve strands and ignored all small fibers. Since there were just some single nerve cells located in nerve fiber strands, all other cells are glia (Gabella 1981), so that the glia index is huge in the extraganglionic compartments of the ENS. These data illustrate that the majority of glial cells are associated with nerve fiber strands, thus extending the knowledge about the localization of glial cells in the human ENS (Ruhl 2005).

The human gastrointestinal tract contains the largest number of nerve cells outside the CNS with an estimated number of 100 million neurons (Furness & Costa 1987). Based on the glia index, it can be calculated that the ENS contains several hundred million glial cells. This is reminiscent of the human brain which also contains much more glial cells than neurons.

It has been previously demonstrated that the glia index of various mammals is positively correlated with body size (Gabella & Trigg 1984, Komuro et al 1982, Phillips et al 2004b, Wedel et al 2002), and the observation that the glia index is higher in man than in guinea pig, and in the MP – which exhibits a more complex neurochemical code than the SMP (Schemann & Neunlist 2004) – supports the notion that the glia index may indeed reflect the functional complexity of the associated neuronal structures as previously suggested for different CNS regions (Reichenbach 1989).

In addition, the finding that myenteric glial nuclei are consistently twice as large as their submucous counterparts points to differences in the complexity of the various ENS compartments and confirm earlier reports on differences in glial nuclear size between the SMP and MP (Gabella & Trigg 1984).

As a read-out for glial quantification, the glia index appears to be very consistent across gut regions in the human ENS, particularly when compared to much more variable parameters like cell numbers and cell densities. In addition, neuronal cell numbers in tissue sections from a control group in a previously published study on idiopathic slow-transit constipation showed substantial variation from the presented results, whereas the glia index was well comparable with what was presently reported from whole-mount preparations (Wedel et al 2002). Based on these findings, the assessment of the glia index as a well suited investigative and clinical tool would be suggested. It can be applied to sections of diseased tissues from which whole-mounts cannot be obtained e.g. due to tissue hypertrophy or sample size, as well as whole-mount preparations.

Further, glial density from cell counts and planimetric data were calculated which revealed that not only absolute numbers, but also glial density was higher in all plexus layers and gut regions of the human as compared to the guinea pig ENS. Interestingly, glial density was significantly higher in the ganglionic *vs.* extraganglionic areas in the guinea pig, but not in the human ENS. This finding reflects a major architectural difference between the human and guinea pig ENS, namely the apparent difference in size between human and guinea pig interganglionic nerve strands that primarily constitute the extraganglionic areas of the ENS.

Morphological (Hanani & Reichenbach 1994, Komuro et al 1982) and functional data (von Boyen et al 2004, Tjwa et al 2003) and data from developmental studies (Rothman et al 1986) indicate that EGC are not a homogenous cell population, but different glial cell types exist like in the CNS also in the ENS. Nevertheless, this topic will remain controversial until a marker is available to precisely discern glial subpopulations in the gut (Ruhl 2005).

The neuronal counts that were obtained are largely in accordance with previously published data (Ruhl et al 2005, Schneider et al 2001), whereas a comparable EGC data set has not yet been available. With respect to neuronal cell counts, there are some disparities in the MP for which higher numbers in human, and lower numbers in guinea pig preparations were counted in this study than previously published (Neunlist et al 2003a, Ruhl et al 2005, Young et al 1993), which may be explained by variable definitions of ganglia and ganglionic borders. In the present study, rigid definitions for ganglionic borders were used based on the presence of neuronal cell bodies. This is particularly crucial in the human ENS because regions that appear to belong to a ganglion may lack neuronal cell bodies (cf. Fig.8A and Fig.15B), whereas in the guinea-pig ENS, neuronal cell bodies are densely packed within a ganglion.

Another well established aspect that has an important impact on the ENS is ageing, as gastrointestinal motility dysfunctions are increased in the elderly. A decrease in neuronal density with age has been consistently reported (for review see (Saffrey 2004)), and there is evidence for a selective neurodegeneration occurring in the ageing ENS (Cowen et al 2000, Phillips et al 2003). In contrast, evidence for glial loss in the ageing gut is scarce (Phillips et al 2004b). It is not known if neurons and glia disappear synchronously or rather, which occurs first. In contrast to data reported from animal models, no age-related effects on glial cell numbers in the ENS were observed, which may be due to the limited age range that was studied.

Also, gender was no confounding parameter of the ENS data. Since just one single out of a huge number of comparisons showed a difference, this result may be due to chance, although this issue has to be further observed in future studies. Further, this result may be explained by the limited number of tissues per group that were assessed and the consequential low statistical power.

Doubts could be raised about quantification bias due to difficulties in tissue preparation and limited penetration of the antibodies and subsequently a subjective tendency to select smaller ganglia which showed better immunoreactivity in affected CD tissues. This argument can be countered with the observation of also lower cell numbers (glia

and neurons) per ganglia in the proximal and distal resection margins of CD were observed which showed homogeneity in immunoreactivity.

The importance of enteric glia for normal gastrointestinal function is becoming increasingly clear (Ruhl 2005), and the concept that abnormalities in glial numbers may reflect certain, still to be defined, disturbances in gastrointestinal physiology opens an extremely exciting area of research which may ultimately lead to novel approaches in the treatment of both functional and inflammatory bowel diseases (Ferrante et al 2006, Bassotti et al 2006a, Bassotti et al 2005).

To gain further insights into glial roles in human gastrointestinal disorders, any histopathological investigation of intestinal full thickness biopsies should not only assess enteric neurons but start searching for abnormalities of the glial network. In the recent past, histopathological studies on glial changes in slow transit constipation and diverticulitis have been published (Bassotti et al 2005, Bassotti et al 2006a). Further, a highly exciting recent publication has suggested that in Crohn's disease resectates, inflammatory infiltrates at the level of the MP may predict endoscopic disease recurrence (Ferrante et al 2006).

In conclusion, an antibody against the transcription factors Sox8/9/10 was established as a reliable and specific marker to label all EGC, with whole-mount preparations being the method of choice. By this, marked differences between EGC and neuron numbers, plexus layers and species and the glia index, which reflects the glia:neuron ratio, were revealed. Since there are hundred million neurons in the ENS, the glia index leads to the conclusion that there must be several hundred million EGC in the human ENS (Furness and Costa, 1980). This data constitutes the first comprehensive data set on human EGC numbers and density, providing a basis for pathological assessment of glial proliferation or degeneration in the diseased human gut.

Subsequently, the nuclear staining pattern of the Sox8/9/10 antibody in EGC and the ability to quantify them in whole-mount preparations was used as a novel tool to investigate EGC numbers in the diseased gut of patients with Crohn's disease (CD). Uninvolved distal and proximal margins of the resected specimen of CD patients were compared to the affected areas sampled as well as to ileal and colonic tissue specimens from patients undergoing surgery for colorectal cancers which served as controls. MP was used in this experimental series, while SMP could not be assessed due to the following technical reasons: hyperplastic and fibrotic tissue areas or damaged tissue structure and integrity due to inflammation. Tissues from CD patients

used in this study were classified as B2 and B3 according to Vienna classification (please see below), thus having the MP being potentially affected (Table 2). Second variable used for grouping of tissues for statistical analyses was based on anatomical location of CD. Inflammation was not graded microscopically and an inflammation score such as Crohn's disease activity index (CDAI) could not be completed, because all patients underwent acute surgery.

Overall, a major finding of the present study was that there is a difference between cell counts per ganglion (neurons and glia) and ganglionic area obtained from colonic CD tissues and affected CD tissues when compared to colonic samples from controls, whereas no differences were observed between ileal CD and control tissues. Also, no difference between both control regions was observed.

The concomitantly reduced glial cell numbers and ganglionic area of the distal resection margin and the affected region from CD patients compared to colonic tissues from controls may most likely account for the lack of difference seen in the glial density in myenteric ganglia of these groups. If this would have been an effect of tissue fibrosis and, therefore, the tissue could not be adequately stretched, the neuron number would rise when ganglia size decreases, but this is not the case. For a stretch effect both parameters (neuron number and ganglion size) would have to be inversely.

The glia index as the most robust parameter was not altered in unaffected or affected CD tissues and controls, but there was a tendency observed towards a decrease of the glia index in tissues from the affected gut regions of CD patients. This was not significant due to the small number of samples used. Alternative statistical approaches were rejected, because splitting of dataset into 3 groups (prox. control, prox. unaffected and affected) vs. 2 groups (dist. unaffected, distal control) would lead to a limitation of the results' scientific significance. In order to compare all regions sampled in one test and to validate conclusions to be drawn, ANOVA with Holm-Sidak post hoc testing was chosen, instead of comparing only two groups using e.g. Student's *t*-test. The last would have revealed more significant differences, but lacking the ability to compare all groups. Further studies with higher sample numbers are needed to elucidate alterations of the glia index in inflammation states of the gut.

It has been suggested that EGC are altered in intestinal inflammation, with the inflammatory environment potentially inducing either glial proliferation or degeneration. Several reports are providing evidence for glial proliferation in IBD, at least in various animal models (Bradley, Jr. et al 1997, Bush et al 1998, Ho et al 2003), and mostly

assessed in whole-mount preparations of the enteric plexuses. Enteric glial cell proliferation *in vitro* displays a bimodal behaviour with IL-1β dose-dependently suppressing EGC proliferation, whereas IL-10 at low concentrations also suppresses proliferation, but at higher concentrations enhances EGC growth (Ruhl et al 2001b). In humans, mucosal upregulation of GFAP expression – which the authors are proposing as a surrogate marker of EGC proliferation – has been observed in the colon of CD patients (von Boyen et al 2006a). Histopathological observations describing structural ENS abnormalities in CD have also added to the evidence that enteric glia proliferate in an inflamed intestine (Geboes & Collins 1998).

Recently the presence of myenteric plexitis in the proximal margins of ileocolonic resection specimen was described as a predictor of endoscopic recurrence of CD (Ferrante et al 2006). In the absence of surrounding inflammation only about half of the patients showed myenteric plexitis, which is defined as the presence of inflammatory cells appositioned to or within enteric neuronal structures. One might suggest that an increased EGC number may also be included in the higher cell density observed by the authors, but this is tentative and could not confirmed with the herein presented approach, although inflammatory cells were not assessed. Compared to the cited reference (Ferrante et al 2006), it has to be distinguished between patients undergoing surgery for the first time due to CD complications or those resected due to reoccurring disease.

In contrast to this vast body of evidence, a recent study has asserted that CD is indeed associated with a diminished glial network (Cornet et al 2001): The authors of this study described a reduction in glial cell density in both non-involved and involved mucosal and submucosal tissues specimens from CD patients which were immunohistochemically assessed using anti-GFAP and anti-S100b antibodies. The immunohistochemical findings were subsequently confirmed with western blotting and ELISA (Enzyme-Linked ImmunoSorbent Assay).

Such a loss of glial cell numbers in CD – if confirmed – could actually point to a pathogenetic role of enteric glia in CD, although there is currently no data support for the contention that glial loss actually precedes intestinal inflammation, rather than being secondary to pre-existing intestinal inflammation.

A possible explanation for the discrepancy between the cited reports could be the different methods used. Further, CD is not a single disease entity, but rather comprises a genetic heterogeneous group of disorders which share some clinical characteristics. Efforts have been made to overcome this problem and to better define phenotypes.

Since CD displays a broad spectrum of anatomic and disease behavior characteristics, the Vienna classification, has recently been introduced. This classification solely relies on disease phenotype, using three different variables – namely age at diagnosis (A1 <40y; A2 ≥40y), location (L1 terminal ileum; L2 colon; L3 ileocolon; L4 upper GI) and disease behavior (B1 non-stricturing non-penetrating; B2 stricturing; B3 penetrating) – to define a total of 24 subcategories (Gasche et al 2000). The Vienna classification is becoming more widely accepted over the last years, although some criticism has been also been voiced (Gasche & Grundtner 2005).

Unfortunately, no age matched controls were available for the present study. This is a common problem because of the early onset of CD (Loftus 2004), whereas unaffected control specimens often originate from healthy segments of patients undergoing surgery for gastrointestinal cancer diseases which mainly occur in an older age group (see Material and methods). In subgroup analyses, age could not be identified as an independent factor influencing any variable assessed in CD or control tissues, but due to the small sample size of the current study, age-related results should be interpreted with care. A direct comparison of age-matched tissues would be desirable to support this interpretation.

Location is the second criterion used to classify CD based on the Vienna classification. Location has been shown to be useful because it is relatively stable over time (Louis et al 2001). The first described genetic defect linked to CD was NOD2/CARD15, which provided some insight into disease pathogenesis. NOD2/CARD15 appears to be related to ileal disease location which may be mechanistically explained because NOD2/CARD15 is selectively expressed in ileal Paneth cells and regulates antibacterial host defense (Gasche & Grundtner 2005). Reduced Paneth cell α-defensins were observed in ileal CD, whereas there was no change in colonic CD (Wehkamp et al 2005b). In contrast, attenuated induction of β-defensins has been described in colonic CD (Wehkamp et al 2005a). Location of disease and potentially different pathogenetic mechanisms for disease should be kept in mind when assessing EGC in CD. Thus, elevated levels of GFAP positive EGC were observed in colonic mucosa (von Boyen et al 2006a), whereas the tissue samples used by Cornet and co-workers who apparently came to an opposing conclusion where not grouped based on ileal *versus* colonic origin of the tissue samples (Cornet et al 2001).

Disease behavior is also an important factor. For example, a penetrating behavior will affect the neuro-muscular compartment of the gastrointestinal wall and thus the MP, whereas a more superficial disease phenotype may primarily involve mucosal and

submucosal ENS structures. In addition, behavior is correlated with age, with a penetrating behavior being more prominent with duration of disease (Louis et al 2001). Larger numbers of samples from well-defined disease phenotypes according to the Vienna classification will have to be selected and studied in order to assess whether EGC alterations are linked to a specific CD phenotype. In addition, inflammatory cell accumulation in the ENS – particularly the MP (Ferrante et al 2006) – should also be assessed to grade inflammation and to better characterize the role of EGC in CD.

Functional analysis (*in vitro* studies)

EGC have been shown to play a pivotal role in gut homeostasis (Bush et al 1998, Cornet et al 2001). Disturbance of the epithelial lining is an initial event in CD pathogenesis (Podolsky 2002). Invasion of intestinal bacterial antigens trigger an (atypical) stimulation of the mucosal immune system which may lead into a self-sustaining cycle of immune activation (Podolsky 2002). EGC can influence epithelial barrier function (Bush et al 1998, Cornet et al 2001), but the underlying mechanisms yet have to be elucidated (Neunlist et al 2007, Savidge et al 2007). Recently, it has been shown that TGF-b1 secretion by EGC exerts anti-proliferative effects upon intestinal epithelial cells (Neunlist et al 2007). Therefore, alterations of EGC functions may modify mucosal barrier functions and be involved in disease pathogenesis. Glial-derived *s*-nitrosoglutathione was also identified as an potent agent to modify intestinal barrier function (Savidge et al 2007). *In vitro* and *in vivo* experiments showed an increase of mucosal barrier function by glial-derived *s*-nitrosoglutathione, which also attenuated tissue inflammation after ablation of EGC in a transgenic mouse model (Savidge et al 2007). Functional studies may serve as tools to study mechanisms and mediators by which EGC regulate epithelial barrier function.

A prerequisite basis for (1) the molecular assessment of EGC *in vitro* and (2) the analysis of interactions between EGC and IEC in a novel coculture system was the availability of isolated purified EGC cultures. For the current experiments, EGC from rat intestine have been generated according to a previously published protocol (Ruhl et al 2001c). This method is an adaptation from protocols used for the establishment of purified Schwann cell cultures (Assouline et al 1983, Brockes et al 1979, Raff et al 1978) and allows to generate pure cultures of EGC. Apart from several descriptions regarding the establishment of mixed neuronal-glial ganglia cultures (Baluk et al 1983, Bannerman et al 1988, Hanani 1993, Jessen et al 1983, Schafer & Mestres 1997), only two other reports in the literature describe an isolation culture of purified EGC (Schafer et al 1997, Bernstein & Vidrich 1994). In one of those, EGC were isolated from the

mucosa of murine colon (Bernstein & Vidrich 1994). The other uses enzymatic digestion and mechanical agitation to isolate EGC from rat myenteric plexus (Schafer et al 1997) and has been recently utilized to analyze enteric glial cell functions (von Boyen et al 2006b, von Boyen et al 2006a, von Boyen et al 2004).

The method established by Rühl (Ruhl et al 2001c) was used and adapted to human EGC in pursuit of and continued a previously started attempt of this approach (Boguth et al 2003). In the human gut wall EGC are tightly intermingled with several other cell types. This network is more complex and also more difficult to dissect, because it has less tissue homogeneity as compared to those of small animal species (e.g. mouse, rat, guinea pig). Enzyme digestion was used to isolate EGC from human MP and some SMP preparations, and it was planned to purify primary cultures by complement-mediated cytolysis of contaminating fibroblasts similar to the rat cultures. Several consecutive complement lyses were used, but no pure human EGC cultures were obtained, because, overall, human fibroblasts divide much more quickly than the glial cells which ultimately showed first signs of degenerations after multiple passages. Addition of forskolin to elevate cellular cAMP levels – what is a mitotic signal in glial cells - as well as the mitogenic activity of pituitary extracts (BPE) (Jessen & Mirsky 1991, Raff et al 1978) was not sufficient to change the balance between EGC and fibroblast growth in favor of the EGC. A further attempt was addition of the cytostatic agent cytosine β-D-arabinofuranoside to hamper fibroblast growth and subsequently accelerate glial growth with forskolin and BPE, but unfortunately this was also not successful.

Another novel approach, which has been successfully employed for Schwann cell purification, is the isolation of glial cells by cell sorting (Vroemen & Weidner 2003). It was tried to use the glial cell surface marker p75NGFR to retain cells from the mixture of different cell types which constitute the primary MP/SMP cultures, but it was not feasible to identify an appropriate antibody to p75NGFR in a series of preliminary experiments. Nevertheless, this method could be a potential tool for future EGC purification once a proper cell surface marker for human EGC becomes available.

Due to the unavailability of purified human EGC, primary rat EGC cultures were used to analyze glial-epithelial interactions and to conduct gene expression analyses.

The established glial markers GFAP (Jessen & Mirsky 1980) and the calcium binding protein S100b (Ferri et al 1982) were used to confirm purity of EGC cultures by immunohistochemical and gene expression analyses. Further, Sox8/9/10 was also shown to be expressed in EGC *in vitro*. The anti-Sox8/9/10 was restricted to the cell

nuclei of cultured rat EGC, showing the same staining pattern as *in situ* which was evidenced by immunohistochemistry and discussed above.

It is important to note that the Sox8/9/10 antibody stained human, guinea pig and rat EGC in whole-mount preparations and human and rat EGCs *in vitro*. EGC from murine whole-mounts could not be labeled with this Sox antibody because it was raised in the species mouse.

A striking finding in the purified rat EGC cultures was the simultaneous expression of GFAP and nestin. The name of the intermediate filament nestin is derived from <u>ne</u>uroepithelial <u>st</u>em cell specific prote<u>in</u> (Lendahl et al 1990). Nestin is a marker of the common neuronal and glial precursor cells and is predominantly expressed in stem cells of the central nervous system in the neural tube during early development and is downregulated and replaced by glial specific or neuron specific intermediate filaments upon terminal neuronal differentiation. In accordance with observations in this study, earlier reports have demonstrated that EGC express immunocyotchemical reactivity for nestin in culture (Eaker & Sallustio 1998, Jaeger 1995). Reactive gliosis may in part be responsible for modification of intermediate filaments with an upregulation of GFAP being is the most prominent feature observed in reactive astrocytes as well as in EGC (Eddleston & Mucke 1993, Laping et al 1994, von Boyen et al 2004). In the CNS, astrocytes re-express nestin in response to a variety of CNS lesions (Lin et al 1995) and may play a major role in the healing process, which is inevitably associated with glial proliferation. These findings suggest that nestin expression inevitably occurs in proliferating glial cells, EGC included. This result could be a hint towards EGC that revert to a more immature phenotype in culture. Reactive astrocytes have also been shown to simultaneously coexpress neuronal and glial markers (Geisert, Jr. et al 1990, Lin & Matesic 1994, Vinores & Rubinstein 1985) which may be an explanation for the small amount of EGC see in some studies simultaneously expressing glial and neuronal markers (Phillips et al 2004b, Phillips et al 2004a). It can be speculated that EGC constitute a reservoir or include a portion of potential progenitors that can differentiate upon stimulation or that mature EGC can be activated and may be involved in inflammation and regeneration, which opens a wide and novel field of research (Estrada-Mondaca et al 2007, Steindler & Laywell 2003).

Coculturing EGC with intestinal epithelial cells alters transepithelial electrical resistance

Recently, it has been reported that coculturing EGC and Caco-2 cells enhances TER values (Neunlist et al 2007). This effect was described to be sustained for at least 6

days of coculture. Such a sustained effect could not be replicated, but more acute glia-induced changes were seen in TER kinetics in Caco-2 cells with a shortening of the time period to reach maximal TER values to 3 days. After 3 days, EGC appeared to inhibit rather than augment Caco-2 TER.

EGC have been shown to exert profound anti-proliferative effects upon IEC proliferation, which may contribute to glial modification of intestinal barrier function (Neunlist et al 2007). In parallel to reducing Caco-2 proliferation, EGC induced cytoskeletal changes in the IEC which resulted in enhanced IEC surface areas and which may also have directly affected high junction formation since tight junctions are intimately connected to the cytoskeleton (Fanning et al 1998, Furuse et al 1994).

Such a glia-induced increase in cell surface area could explain the acute effects of EGC on Caco-2 TER values of glial-epithelial cocultures in the first 3 days, irrespective of the time when coculturing was started: similar effects did occur both in the 1st and 3rd week of Caco-2 cultures. The reversal of the EGC effects on Caco-2 TER could also be due the decreased IEC proliferation, which could affect a net loss of cultured IEC over time with consecutive loss of the monolayer tightness that was observed in the presented experiments.

Caco-2 cells reach their maximum in TER and tight junction tightness, about three weeks after seeding, which is an argument against the use of Caco-2 in the experimental design of the present study. Possibility of contaminating the cultures increases with time after seeding. Additional methodological issues concerning coculture experiments and TER relate to the support on which cells are grown, the passage number, cell density, conditions at the time of measurement (Delie & Rubas 1997). TER is usually higher for older passage numbers in Caco-2 cells, which have been related to the fact that cells may grow as multilayers instead of monolayers. Thus, IEC within a narrow range of passage numbers were used. A low cell density means fewer paracellular spaces and therefore a higher TER. Bias was excluded by using always the same cell density. Furthermore, at the time of TER measurement if temperature decreases TER increases. Conditions were kept constant by using a thermal plate to eliminate this factor.

T84 were chosen for the coculture experiments because they are fully differentiated, polarized cells after two weeks in culture and show higher TER values than any other cell line tested. This made it easier to reliably detect cytokine induced effects on TER. In contrast to Caco-2 cells, T84 cells reach (1) higher TER values and (2) maximum TER values within a shorter time-frame. The present studies showed, that each time EGC

were added to T84 cells an increase in TER values was observed. This increase in epithelial resistance by addition of EGC to intestinal epithelial cells has been previously reported (Neunlist et al 2007). Very low TER values were observed for the primary IEC line IEC-6 and HT-29 as well as no effect of coculturing with EGC and, thus, they were not useful for the intended experiments. HT-29 cells are undifferentiated in standard culture conditions and the mucin-secreting subclone HT29-Cl.19A or HT29-Cl.16E (Augeron & Laboisse 1984) was not available in this study, but the latter can be used as a model system to study the interactions between the ENS and the epithelium as demonstrated by another group (Neunlist et al 2003b, Neunlist et al 2007).

Cytokine treatment of intestinal epithelial cells and enteric glial cells

Luminal substances can cross the epithelium via two routes: the transcellular or the paracellular pathway. Tight junctions are the rate limiting factor that regulate paracellular permeability by forming a circumferential seal at the luminal pole of adjacent epithelial cells (Anderson & Van Itallie 1995). There is accumulating evidence that such junctions express a high degree of plasticity and may be impaired in disease states (Madara et al 1992).

Intestinal permeability is a clinically useful term to describe the integrity of the epithelial barrier *in vivo* which has been repeatedly shown to be compromised in pathological conditions such as IBD (Buhner et al 2006, Fries et al 2005, Suenaert et al 2005). Transepithelial electrical resistance (TER) is determined by the Ohmic relation and has been used as an index of barrier permeability (McKay & Baird 1999). Permeability to macromolecules can also be determined quantitatively in vitro to study modulation of permeability of the intestinal lining by extracellular macromolecules including cytokines (Sanders et al 1995). However, there is not always a direct correlation between both methods (TER and permeability to marker molecules) (Balda et al 1996).

The human colonic cancer cell line T84 was chosen as model epithelium to examine direct actions of cytokines on IEC and on IEC in coculture with EGC as well as their mutual effects. Exogenous addition of various cytokines has been shown to influence TER. Most studies implicated proinflammatory cytokines such as TNFα, IFNγ, IL-1β, IL-6, and IL-13 as agents which decreases barrier integrity, whereas some anti-inflammatory substances like IL-10 and TGFβ appear to play a protective role in maintaining the intestinal tight junctional barrier function

Since the first report in 1989 (Madara & Stafford 1989), findings from numerous laboratories have demonstrated that addition of IFNγ substantially diminishes transepithelial resistance of monolayer using model intestinal epithelial cell lines such

as T84 (Adams et al 1993, Bruewer et al 2003, Madara & Stafford 1989) and Caco-2 (Wang et al 2005). It has been shown that an initial decrease of TER by addition of IFNγ to T84 cell monolayers returned to nearly baseline after 8 days (Adams et al 1993). In the present experiments similar effects were demonstrated, however also different which can be explained by the time-course (only 3 days monitoring) that was chosen for the experiments and, therefore, full reversibility could not be shown. Moreover, the disruption comes along with a prolonged alteration in TER, even after limited time (24 h) of IFNγ exposure as demonstrated before (Adams et al 1993). Interaction of IFNγ with a cell surface receptor linked to the basolateral side of intestinal epithelial cells has been identified as one mechanism of action (Adams et al 1993). This receptor-ligand mediated effect was attenuated if treated or non-treated EGC were cocultured with T84. In contrast, there was no difference of the effect that EGC exhibited on T84 cells, if they had been exposed to IFNγ before or not. Expression of the IFNγ receptor was found at the RNA level, but protein expression was not assessed. The question if IFNγ could influence EGC directly and thereby interfere in the glia-mediated attenuation of epithelial disruption or not needs to be further investigated. Alterations in tight junction function seems to responsible for the IFNγ-induced monolayer dysfunction rather than cell death (Adams et al 1993, Bruewer et al 2003, Fish et al 1999) or a paracellular pathway (Adams et al 1993).

TNFα plays a central role in Crohn's disease and other inflammatory conditions. Elevated levels of TNFα have been measured in a intestinal inflammatory disorders, and the use of neutralizing antibodies to TNFα has been found to be an effective therapeutic strategy in patients suffering from Crohn's disease (Stack et al 1997, Targan et al 1997). TNFα induced increase in intestinal TJ permeability has been proposed as an important proinflammatory mechanism (Hollander 2002, Ma et al 2004, Sands 2000, Suenaert et al 2002). In the present study, the effects of TNFα on T84 permeability were less consistent than those for IFNγ. Observations from several independent research groups have shown that low dose TNFα (<10 ng/ml) has no effect on T84 permeability assessed with a transwell system (Taylor et al 1997) and Ussing chambers (Madara & Stafford 1989, McKay et al 1996, Zareie et al 1998), whereas other reports using the renal cell line LLC-PK1 (Mullin & Snock 1990) or Caco-2 cells (Ma et al 2004) suggest that epithelial barrier function is reduced by TNFα. Moreover, the effect induced by IFNγ is potentiated by TNFα in T84 cell monolayers (Bruewer et al 2003).

In the present study TNFα could not decrease TER at concentrations up to 10 ng/ml, but at a concentration of 100 ng/ml of TNFα a significant drop in TER was observed compared to control. Nevertheless, the effects of coculturing EGC with T84 and how TER was influenced in the context of an inflammatory environment created by TNFα were much more interesting and novel. While there were little effects seen at the lowest TNFα concentration used, 10 ng/ml showed more prominent effects as well as 100 ng/ml of TNF did. After an initial drop in TER the monolayer integrity recovered and, moreover, increased thereafter. This biphasic response of epithelial monolayers to TNF has also been reported in a porcine renal epithelial cell line (LLC-PK1) (Marano et al 1993). The authors suggest a compensatory mechanism of the epithelial cells to re-establish its effectiveness as a physiological barrier following acute inflammatory insults by TNFα. Results from the present study showed that treatment of T84 cells with TNFα decreased barrier function as assessed by TER, and EGC can modulate this effect.

Another cytokine investigated was IL-1β which has also been shown to be elevated in patients with IBD (Podolsky 2002). In these experiments, IL-1β affected TER of T84 cells alone or in coculture with EGC, and this effect was seen most clearly in concentrations as high as 100 ng/ml. A uniform effect was observed for the group with both T84 cells and EGC separately treated with IL-1β before cocultured, which had the lowest TER values after 24 h of cytokine exposure, but recovered to baseline over time. IL-1β can stimulate IL-6 expression by EGC (Ruhl et al 2001a) and IEC (McGee et al 1995) and receptors for IL-1β are readily detectable on IEC (Panja et al 1998). Thereby, EGC might indirectly affect IEC and this might be a reasonable explanation for this observed high decrease in TER compared to the other groups.

IL-13 has also been reported to disrupt epithelial barrier *in vitro* (Ceponis et al 2000, Heller et al 2005, Sanders et al 1995). This was also the case in this study, where IL-13 significantly disrupted the epithelial barrier of T84 cells. IL-13 had a profound effect and TER did not reach pre-treatment values within the monitoring period of 72 h. Whether this effect is reversible or the slow increase in TER after treatment constitutes a normal healing process is not known. Nevertheless, addition of EGC reduced the harmful action of IL-13. Receptors for IL-13 have been demonstrated in a human colonic epithelial cell line (Blanchard et al 2004) and on colonic enterocytes (Heller et al 2005). RT-PCR revealed mRNA expression of the IL-13 receptor alpha 1 also in EGC. It needs to be further investigated, if the positive actions of EGC on IEC may be activated by IL-13. IL-

13 induced decrease in TER was not due to cell necrosis as shown in another IEC line (Heller et al 2005).

In summary, the present observation with all tested cytokines indicate that coculturing of EGC attenuates detrimental effects of cytokines as inflammatory mediators on epithelial tightness, suggesting that EGC play an important role to maintain intestinal epithelial tightness and hence gut homeostasis. Despite all cytokines used having the ability to disrupt the epithelial barrier, it has to be distinguished between the type of cytokine such as IFNγ, TNFα, IL-1β and IL-13, and the concentration of cytokine, which also did influenced the effects.

This adds further evidence to the hypothesis, that soluble factors released from EGC into the culture medium are responsible for the effects of EGC on IEC and that those modulate the tight junctional barrier. GDNF is a key candidate to be responsible for those kind of interactions (von Boyen et al 2006a, Steinkamp et al 2003).

The idea of application of an antibody against GDNF was to block the positive effects EGC exert on epithelial barrier function suggesting GDNF to being of special importance. Especially in those groups, in which the cells had been cocultured prior to the experiment anti-GDNF treatment alleviated positive EGC effects on IEC. The effects could not be fully reversed, but this would fit with the observation of a constitutive expression of GDNF in EGC. In contrast to previous findings (von Boyen et al 2006a), GDNF expression levels was not modulated by TNFα in this study.

A newly published paper (Savidge et al 2007) demonstrated that another glial derived factor (s-nitrosoglutathione) was identified as a potent protective agent who could attenuate tissue inflammation and induce epithelial barrier function *in vitro* and *in vivo*. In a coculture model consisting of EGC and Caco-2 cells, EGC increased Caco-2 cell surface area while reducing cell density (Neunlist et al 2007). This effect could be partly reproduced by addition of TGF-β1 which has been identified to be also produced by EGC (Neunlist et al 2007). Both studies underline that EGC are a source of a variety of soluble factors interacting with epithelial cells. This leads to the conclusion that a number of substances released by EGC may contribute to epithelial barrier homeostasis and GDNF being one of them.

EGC express NGF, NT-3, GDNF and related receptors

Neuronal growth factors generally belong to one of 2 major families: the neurotrophins and the neurotrophic factors.

Neurotrophins are target-derived soluble growth factors essential for the development, maintenance and survival of central and peripheral neurons (Thoenen 2000). Besides these well-known functions, neurotrophins influence neurotransmitter and neuropeptide synthesis and release (Thoenen 2000). In mammals, the neurotrophin family includes the four growth factors nerve growth factor (NGF), which was the first neurotrophin to be discovered (Levi-Montalcini 1987), brain-derived neurotrophic factor (BDNF), neurotrophin-3 (NT-3) and neurotrophin-4/5 (NT-4/5). Two other members of this protein family, neurotrophin-6 (Gotz et al 1994) and neurotrophin-7(Lai et al 1998) have been identified in different fish species, but not yet in humans.

Neurotrophins bind to two classes of cell surface receptors, p75NGFR and the neurotrophic tyrosine kinase receptor or "Trk" family. Nerve growth factor receptor p75 (p75NGFR or NTRK) is a low-affinity receptor that all neurotrophins can bind to. The Trk family comprises the high-affinity receptors TrkA (or NTRK1), TrkB (or NTRK2) and TrkC (or NTRK3) all of which will specifically bind a single neurotrophin ligand: TrkA is the high-affinity receptor for NGF, TrkB transduces signals after binding with BDNF or NT-4/5 and TrkC is the specific high-affinity receptor for NT-3, but it can also activate each of the other Trk receptors with less efficiency (Bothwell 1995).

Neurotrophins have been implicated in the development of neurons and glia in the ENS (Chalazonitis et al 1994, Chalazonitis 2004), which are derived from neural crest progenitor cells (Gershon & Rothman 1991).

In the adult human ENS, NT-3 immunoreactivity, as well as TrkA and TrkB receptor immunoreactivity has been localized to EGC, neurons and neuronal fiber bundles in the MP and SMP, whereas TrkC appears to be exclusively localized to enteric neurons (Hoehner et al 1996). Another study has demonstrated TrkA and TrkC immunoreactivity to be confined to human enteric neurons of the SMP and MP in oesophagus, stomach, duodenum, jejunum, ileum, colon, sigmoideum and rectum, and to the SMP and MP in the jejunum and ileum of several other species including rat (Esteban et al 1998).

In contrast, TrkB immunoreactivity is restricted to EGC, with the exception of humans where mainly EGC and also a small percentage of neurons have been demonstrated to be immunopositive for TrkB (Esteban et al 1998). *In situ* hybridization has revealed TrkC mRNA only in enteric neurons of the adult rat gut, but not TrkA or TrkB mRNA (Sternini et al 1996). The TrkC ligand NT-3 appears to also be localized to rat enteric neurons (De Giorgio et al 2000). The pan-neurotrophin receptor p75NGFR has been found in EGC, enteric neurons and nerve fiber bundles of man (Esteban et al 1998) and

rat (Baetge et al 1990, Esteban et al 1998). An overview of immunoreactivity of neurotrophins and their receptors in the ENS is given below:

Table 8.   Immunoreactivity of neurotrophins and their receptors in the ENS

	EGC	Neurons	Nerve bundles
TrkA	+ [1,5]	+ [1,4]/- [2,5]	+ [1]/- [5]
TrkB	+ [1,4]	+ [1]/- [2,4]	+ [1,4]
TrkC	- [1]	+ [1,2,4]	- [1]
NT-3	+ [1]	+ [1,3]	+ [1,3]
p75NGFR	+ [4]	+ [4]	+ [4]
NGF	- [5]	+ [5]	+ [5]

[1](Hoehner et al 1996); [2](Sternini et al 1996); [3](De Giorgio et al 2000); [4](Esteban et al 1998); [5](Di Mola et al 2000).

Functional effects of neurotrophins in the gut

In the ENS prokinetic functions of the neurotrophins BDNF and NT-3 have been demonstrated. Administration of recombinant human BDNF and NT-3 in healthy subjects and patients with constipation stimulates gut motility (Coulie et al 2000). This was corroborated in a phase II trial in patients with functional constipation (Parkman et al 2003). Injections of NT-3 enhanced colon transit, and improved symptoms of chronic constipation (Parkman et al 2003).

Besides involvement of neurotrophins in functional disease, NGF and TrkA have been shown to be elevated in tissue sample from patients with Crohn's disease (Di Mola et al 2000). Using *in situ* hybridization, NGF expression was found in SMP and MP neurons, lamina propria cells (polymorphonuclear-like cells) and mast cells. Immunohistochemistry revealed intense NGF and TrkA immunoreactivity polymorphonuclear-like cell in lamina propria cells and many mast cells. NGF was also found in SMP and MP neurons and additionally TrkA was found in EGC (Di Mola et al 2000).

The presence of NGF and its high affinity receptor TrkA in both neuronal and non-neuronal cells suggests neuroimmune interactions in chronic inflammation: Mast cells are closely apposed to nerves in the mucosa of the human gut, which demonstrates the anatomical connection between enteric nerves and inflammatory cells and lead to this hypothesis of neuroimmune interactions (Stead et al 1989). There are more studies showing NGF and NT-3 involvement in inflammatory processes and visceral sensitivity. Immunoneutralization of both NGF and NT-3 worsens TNBS-induced experimental

colitis in rat, which suggests a regulatory and protective role of these neurotrophic factors in inflammation and gut integrity (Reinshagen et al 2000). NGF is also involved in the maintenance of colonic sensitivity and mucosal integrity of the gut (Barreau et al 2004).

The results obtained in the present study show NGF and NT-3 expression in EGC cultures, which is consistent with immunohistochemical data from an earlier study. (Hoehner et al 1996) and a recently published paper also demonstrating NGF expression in EGC cultures from rat MP (von Boyen et al 2006b). Proinflammatory cytokines like IL-1, TNFα and lipopolysaccharides, found in the bacterial wall increased NGF secretion, while the anti-inflammatory cytokine IL-4 had no effect. IL-1 and TNFα effects could be blocked with receptor agonists, although presence of receptors was not tested (von Boyen et al 2006b); NGF and TrkA mRNA were also found to be increased after cytokine treatment (von Boyen et al 2006b). In the CNS, there is extensive evidence that proinflammatory cytokines, like IL-1β, IL-6, TGFβ1, TNFα and IFNγ as well as the anti-inflammatory cytokine IL-10 are capable of regulating NGF secretion in astrocytes (Brodie 1996, Juric & Carman-Krzan 2000, Kuno et al 2006).

In contrast to some other studies (Di Mola et al 2000, Esteban et al 1998, Hoehner et al 1996, Sternini et al 1996, von Boyen et al 2006b), TrkC expression was detected in EGC, but TrkA and TrkB mRNA was not found to be present in EGC cultures used. This is consistent with an immunohistochemical study which showed TrkA immunoreactivity was restricted to neurons and did not label rat EGC (Lin et al 2005).

One could speculate that different results obtained in this study are due to contamination of EGC cultures with other cell types, a cause which could be excluded because of verification of EGC culture purity (see above); another cause of discrepancy could be due to different methods for EGC isolation and purification used to obtain EGC *in vitro* (Ruhl et al 2001c, Schafer et al 1997). There were also different antibodies used and different species investigated. Despite this facts, there is agreement of neurotrophins and neurotrophin receptors to be involved in the regulation of gut inflammation (Di Mola et al 1999, Reinshagen et al 2000).

Expression of the pan-neurotrophin receptor p75NGFR was easily detected in EGC *in vitro* by RT-PCR and by immunohistochemistry. The same p75NGFR antibody used in EGC cultures also stained EGC in whole-mount preparations from the human ENS. This has been shown before (Lin et al 2005).

The expression of NGF, NT-3, the NT-3 high affinity receptor TrkC and the low-affinity receptor p75NGFR suggest EGC to be a source of these substances and a central role

in inflammation of the intestines. EGC are closely apposed to the epithelium in the intestinal mucosa (Neunlist et al 2007) and, thus, secretion of neurotrophic factors during inflammation of the gut could be one of the important functions of EGCs to maintain gut integrity.

It is believed that the intestinal mucosa is in homeostatic state of controlled inflammation, although the responsible processes are poorly understood (Fiocchi 2005). NGF is secreted by epithelial cells, fibroblasts, a number of immune cells, such as activated T cells, mast cells, and dendritic cells and glial cells (Levi-Montalcini et al 1996). This is supported by the herein presented data that NGF was also expressed by EGC. NGF causes dose-depended upregulation of IL-10 secretion in the epithelium, and, reciprocally, IL-10 causes an increase of NGF in intestinal epithelial cells (IEC) (Ma et al 2003). IL-10 receptors are expressed on IEC from the murine small and large intestine (Denning et al 2000). Binding of IL-10 to its receptor could block the effects of IFNγ on interruption of epithelial barrier integrity (Madsen et al 1997). IL-10 is a potent anti-inflammatory agent that inhibits the expression of genes encoding proinflammatory cytokines (Stordeur & Goldman 1998). An induction of IL-10 expression by NGF secreted from EGC could therefore be one possible way to indirectly downregulate immune function in the epithelium and maintain gut integrity. Additionally, the fact that EGC do not express IL-10 itself does confirm this argument.

Neurotrophic factors have been implicated in gut homeostasis

The second family of proteins, which have been implicated in the mediation of gut inflammation and integrity, are the neurotrophic factors. The glial cell line-derived neurotrophic factor (GDNF) family in a member of the superfamily of transforming growth factors and comprises four molecules to date, which are GDNF, neurturin, artemin and persephin (Sariola & Saarma 2003). GDNF was the first of this group to be discovered in 1993 as a growth factor promoting the survival of midbrain dopaminergic neurons (Lin et al 1993). The GDNF ligands bind to a multicomponent receptor complex, with the receptor tyrosine kinase RET as the central receptor and glycosyl-phosphatidyl inositol (GPI)-anchored ligand-binding coreceptor protein named GDNF family receptor α (GFRα) (Sariola & Saarma 2003). GDNF, neurturin, artemin and persephin specifically bind to GFRα1, GRFα2, GFRα3 and GFRα4, respectively. New findings also suggest the GNDF family members also signal independently of RET (Sariola & Saarma 2003).

During development GNDF and neurturin are expressed in many areas of the central and peripheral nervous system. By this they have neurotrophic functions on

dopaminergic and noradrenergic CNS neurons and spinal motorneurons and are crucial for ENS development. Artemin and persephin seem not to be important for development of the ENS (Durbec et al 1996, Heuckeroth et al 1999, Moore et al 1996, Nishino et al 1999, Sanchez et al 1996, Schuchardt et al 1994, Tomac et al 2000). GDNF and neurturin have been shown to be important factors for the survival and proliferation of enteric neurons (Heuckeroth et al 1998).

In the inflamed gastrointestinal tract, expression of GDNF, RET, GFRα1 and GFRα2 could be induced in a model of experimental colitis in rat; but cellular localization of these molecules was not determined (Reinshagen et al 1999). An earlier study which was the first to investigate GDNF in the gastrointestinal tract, detected GDNF in EGC of the adult and the developing human gut (Bar et al 1997). Immunoreactivity for the receptor component RET was only found in neuronal cell bodies of the SMP and MP (Bar et al 1997). GDNF expression to be confined to EGC structures was confirmed by another study (Steinkamp et al 2003).

Results obtained from gene expression analysis using RT-PCR showed GDNF in EGC cultures which confirm EGC as one source of this neurotrophic factor in the gut. Also, the investigated cultures did not express RET tyrosine kinase, which is consistent with the results cited above. Additionally GFRα1 and GFRα2 expression was found in EGC.

In IBD and experimental rat colitis, GDNF was specifically upregulated, whereas GFRα1 was expressed at a constant level in human and rat colonic epithelium (Steinkamp et al 2003). GDNF was restricted to the SMP and MP, whereas there was strong immunoreactivity seen at the top of the crypts in Crohn's disease. GFRα1 and RET receptor expression was also shown in epithelial cells *in vitro* (Steinkamp et al 2003). The data showed strong anti-apoptotic effects of GDNF on colonic epithelial cells through activation of mitogen-activated protein kinase (MAPK) and phosphatidylinositol 3-kinase/Akt (PKB) pathways (Steinkamp et al 2003). Since subepithelial myofibroblasts were excluded as a possible source of GDNF (Steinkamp et al 2003) and EGC are capable of providing neurotrophins and neurotrophic factors in the gut, EGC might regulate IEC apoptosis and tissue integrity by secretion of GDNF (Steinkamp et al 2003, von Boyen et al 2006a). It sounds conceivable that GDNF secretion by EGC might act in a protective way, because GDNF upregulation took place after initiation of experimental inflammation and therefore it may play a role in limiting epithelial impairment and promoting epithelial restitution (Steinkamp et al 2003). Evidence for EGC to be a major source of GDNF in CD was added by confirming GDNF expression in EGC and not in subepithelial myofibroblasts (von Boyen et al 2006a). Synthesis and

secretion of this neurotrophic factor could be stimulated by IL-1, TNFα and lipopolysaccharides (LPS) *in vitro*. An interesting fact is the speculation on how LPS might directly activate EGC. Toll-like receptor 2 (TLR2) which recognizes the bacterial cell wall product peptidoglycan and TRL4 which is a specific receptor for LPS recently have been demonstrated in astrocytes (Bowman et al 2003, Esen et al 2004) and it can be speculated that mucosal EGC act in a similar way.

Expression of the neurotrophic factor fibroblast growth factor 2 (FGF2; also known as basic FGF or bFGF) in EGC has been detected by gene expression analysis. Just recently, this finding has been reported using immunohistochemistry showing for the first time FGF2 localized to enteric neurons and EGC nuclei (Chadi et al 2004). Paracrine actions of EGC on enteric neurons and an autocrine effect of FGF2 on neurons are discussed (Chadi et al 2004), but FGF2 may also act on other cell types and, thus, is additional promising target of further research into EGC effects mediating IEC permeability.

Based on these observations, it can be concluded that enteric glia have the potential to interact with the gut epithelium and are the source of mucosa-protective factors. Protective mucosal factors belonging to the GDNF family and the family of neurotrophins and other growth factors seem to be involved. This contention is supported by previous reports which have demonstrated that neuroglia is capable of synthesizing neurotrophins and members of the GDNF family which in turn have been shown to be capable of down-regulating inflammatory processes of the central nervous system and be cyto-protective (Appel et al 1997, Bar et al 1997, Stanisz & Stanisz 2000). Evidence that a similar mechanism may be effective in the gut was provided by earlier reports of an involvement of neurotrophins and neurotrophic factors in the regulation of intestinal inflammation (Bar et al 1997, Reinshagen et al 1999, Reinshagen et al 2002). Furthermore, evidence was published indicating that members of the GDNF-family may be directly involved in the preservation of the intestinal mucosal barrier (Steinkamp et al 2003). Together with the findings that ablation of the enteric glia results in fulminant intestinal inflammation (Marano et al 1993, Bush et al 1998, Cornet et al 2001, Savidge et al 2007), these data strongly support the conjecture that enteric glia may release and control a complex network of neurotrophins, neurotrophic factors and additional growth factors to maintain mucosal integrity.

Summary

The Sox8/9/10 antibody is an excellent investigative tool to assess the glial cells in the enteric nervous system. In this study, conspicuous structural differences were described between various ENS plexus layers and species, and the glia index as the most robust quantitative descriptor within a species was identified.

Using the Sox8/9/10 antibody, this work provides a comprehensive set of quantitative EGC data which can be used as a basis for pathological assessments of glial proliferation and/or degeneration in the diseased gut. Data from this study was employed to compare EGC numbers in the healthy and chronically inflamed human intestine. The observed differences in Crohn's disease are promising and underline the involvement of the ENS in chronic inflammation. The great potential of the presented methodology should be further used to assess gastrointestinal diseases which may affect the ENS.

The presented functional studies support the thesis that EGC have the potential to maintain epithelial barrier function and protect the gut epithelium from inflammatory insults. These effects were dependent on the involved cytokine, suggesting that glial responses vary in different inflammatory settings (e.g. Th1 vs. Th2 etc.). Although the regulatory mechanisms underlying these processes were not identified, the expression of GDNF, NGF, NT-3 and their receptors are promising targets of further research to elucidate the exact nature of glial-derived mucosa-protective factors.

Overall, more attention should be paid to enteric glial cells in order to elucidate the multiple functions of this fascinating cell type in the ENS in health and disease, since this could identify new pharmacological targets and in turn open new avenues for the treatment of gastrointestinal diseases in the future.

5.   Abstract – Kurzfassung

Abstract

Plasticity of glial cells in the enteric nervous system during intestinal inflammation

Quantitative changes of enteric glia (EGC) have been implicated in gastrointestinal disorders. To facilitate future studies of EGC in human pathology, glial markers in the human enteric nervous system (ENS) were thoroughly characterized and glial cell numbers were compared in man and guinea pig: Whole-mount preparations of the enteric nerve plexuses from human and guinea pig ileum and colon were labeled with antibodies against S100b, GFAP, p75NGFR, and the transcription factors Sox8/9/10 and neuronally counterstained. As a result, the Sox8/9/10 antibody was shown to be an excellent investigative tool to assess the glial cells in the enteric nervous system. Conspicuous structural differences were described between various ENS plexus layers and species, and the glia index was identified as the most robust quantitative descriptor within a species.

Overall, a comprehensive set of quantitative EGC measures in man and guinea pig is provided which may serve as a basis for future pathological assessment of glial proliferation and/or degeneration in the diseased gut. Subsequently, this Sox8/9/10 was used in Crohn´s disease (CD) specimens to quantify enteric glia, because CD has been previously shown to affect the neuromuscular compartment of the gastrointestinal wall. CD resectates from a highly inflamed area and 1 or 2 specimens from the resection margins were studied in order to compare affected and non-affected areas. This assessment was restricted to myenteric plexus (MP) samples only, because dissection of submucous plexus (SMP) was technically not feasible in CD tissues. As in controls, Sox8/9/10 labeled all EGC nuclei within ganglia as well as glial nuclei associated with large nerve fiber tracts and neuronal fibers ramifying into the muscle coat. Marked differences were detected in absolute cell numbers (glial cells and neurons) per ganglion between colonic control tissues and affected and unaffected CD regions. In CD, the glia index tends to be reduced in affected tissues compared to all other regions, which should be confirmed in a larger study.

The observed differences in glial cell numbers in CD underscore the involvement of the ENS in chronic intestinal inflammation. The potential of the presented methodology should be further used to assess gastrointestinal diseases which may affect the ENS.

In a parallel approach the potential contribution of enteric glia to intestinal inflammation was investigated as loss of EGC is accompanied by a breakdown of epithelial integrity and subsequent intestinal inflammation. Interactions between EGC and the intestinal epithelial barrier were analyzed in experimental conditions mimicking in un-inflamed and inflamed conditions: For these experiments, the intestinal epithelial cell (IEC) line T84 was selected as the most appropriate cell line from a range of different cell lines (Caco-2, HT-29, IEC-6) and T84 cells were grown on filter supports in the apical compartment of a transwell co-culture system in the presence or absence of EGC in the basolateral compartment. Mature T84 cells were stimulated with human recombinant tumor necrosis factor (TNF)α, interleukin (IL)-1β, IL-13 or interferon (IFN)γ for 24hrs. Subsequently, the integrity of T84 monolayers was determined by assessing the transepithelial electrical resistance (TER) over a period of 48hrs. To detect cytokine-induced defects in the epithelial monolayers, macromolecular permeability was measured. While inflammatory mediators like TNFα, IL-1β, IFNγ, and IL-13 diminish the tightness of IEC, most likely via alterations of epithelial tight junctions, these effects were abolished or reduced in the presence of EGC. This observation indicates a protective effect of EGCs on the intestinal epithelial barrier in intestinal inflammation which seems to be determined by the immunological profile of the inflammatory response.

Overall, the presented functional studies support the thesis that EGC have the potential to maintain epithelial barrier function and protect the gut epithelium from inflammatory insults. The oberserved effects were dependent on the involved cytokines, suggesting that glial responses may vary in different inflammatory settings (e.g. Th1 vs. Th2 etc.). Although the underlying regulatory mechanisms were not identified in this work, the observed expression of GDNF, NGF, NT-3 and their receptors by EGC points to promising targets for further research to elucidate the exact nature of glial-derived mucosa-protective factors.

In summary, more scientific attention should be paid to EGC in order to elucidate the multiple functions of this fascinating cell type in the ENS in health and disease, which could lead to the identification of new pharmacological targets and in turn open new avenues for the treatment of gastrointestinal diseases in the future.

Kurzfassung

Plasticity of glial cells in the enteric nervous system during intestinal inflammation

Strukturelle Veränderungen enterischer Gliazellen (EGZ) wurden mit gastrointestinalen Erkrankungen in Zusammenhang gebracht. Um enterische Gliazellen im Bereich der Humanpathologie besser untersuchen zu können, wurden Gliamarker im human enterischen Nervensystem (ENS) umfassend charakterisiert und die Zellzahlen enterischer Gliazellen von Mensch und Meerschweinchen verglichen. Dazu wurden Häutchenpräparate der enterischen Nervengeflechte aus Ileum und Kolon von Mensch und Meerschweinchen angefertigt und mit Antikörpern gegen S100b, GFAP, p75NGFR sowie die Transkriptionsfaktoren Sox8/9/10 markiert und mit neuronalen Antikörpern gegengefärbt.

Es stellte sich heraus, dass der Sox8/9/10 Antikörper ein hervorragend innovatives Arbeitsmittel ist, um EGZ im ENS zu quantifizieren. Deutliche strukturelle Unterschiede zeigten sich sowohl zwischen den verschiedenen Plexusschichten des ENS als auch zwischen den Spezies. Dabei stellte sich der Gliaindex als widerstandsfähigsten Parameter innerhalb einer Spezies dar.

Insgesamt wurde ein umfassender Datensatz quantitativer EGZ Messwerte bei Mensch und Meerscheinchen erstellt, der als Basis zukünftiger pathologischer Bewertungsmerkmale von Proliferation und/oder Degeneration enterischer Gliazellen im erkrankten Darm dienen könnte. Folglich wurde der Sox8/9/10-Antikörper bei Gewebeproben von Morbus Crohn (MC) Patienten verwendet, um EGZ zu quantifizieren, da vorhergehende Arbeiten zeigten, dass bei MC der neuromuskuläre Bereich der Darmwand betroffen ist.

Es wurden Darmresektate von MC Patienten aus einem stark entzündeten Bereich sowie 1 bis 2 Proben der Resektionsrändern untersucht, um betroffene mit nicht betroffene Bereichen vergleichen zu können. Diese Untersuchungen beschränkten sich auf Proben des myenterischen Plexus (MP), da eine Präparation des submukösen Plexus von MC Geweben technisch nicht möglich war. Wie in den Kontrollgeweben, färbte Sox8/9/10 alle EGZ Zellkerne in Ganglien als auch die mit großen Nervensträngen assoziierten und mit in die Muskelschicht verlaufenden neuronalen Fasern assoziierte Gliazellkerne. Die gezeigten Unterschiede waren in den absoluten Zellzahlen (Gliazellen und Neurone) pro Ganglion zwischen Kontrollgeweben und entzündeten und nicht entzündeten MC Geweben messbar. Bei MC scheint der

Gliaindex in stark entzündeten Geweben geringer zu sein als in allen anderen Regionen, was jedoch durch eine umfangreichere Studie bestätigt werden sollte. Die gemessenen Unterschiede der Gliazellzahlen bei MC bekräftigen eine Beteiligung des ENS bei chronischen intestinalen Entzündungsprozessen. Das Potential der dargestellten Methode sollte weiter genutzt werden, um gastrointestinale Erkrankungen zu erforschen, die das ENS beeinträchtigen können.

In einem parallelen Ansatz wurde die potentielle Beteiligung enterischer Gliazellen an intestinalen Entzündungsprozessen untersucht, da ein Verlust von EGZ mit einer Beschädigung der epithelialen Integrität und einer darauffolgenden intestinalen Entzündung einhergeht. Wechselwirkungen zwischen EGZ und der intestinalen epithelialen Grenzschicht wurden unter experimentellen Bedingungen analysiert, welche nicht entzündete und entzündete Gegebenheiten imitierten. Für diese Versuchsreihe, wurde die intestinale epitheliale Zelllinie (IEZ) T84 aus einer Reihe verschiedener Zelllinien (Caco-2, HT-29, IEC-6) als die adäquateste Zelllinie ausgewählt. T84 Zellen wurden auf Filtereinsätzen im apikalen Bereich eines Transwell Kokultursystems in Gegenwart oder Abwesenheit von EGZ im basolateralen Teil des Systems kultiviert. Voll differenzierte T84 Zellen wurden mit humanen rekombinantem Tumornekrosefator (TNF)α, Interleukin (IL)-1β, IL-13 oder Interferon (IFN)γ über einen Zeitraum von 24 Stunden stimuliert. Anschließend wurde die Integrität der T84 Zellmonolayer durch die Aufzeichnung des transepithelialen Widerstands über 48 Stunden bestimmt. Um Defekte der epithelialen Monolayer durch Zytokineinfluss zu detektieren, wurde die makromolekulare Permeabilität gemessen. Während Entzündungsmediatoren wie TNFα, IL-1β, IFNγ, und IL-13 die Durchlässigkeit von IEZ sehr wahrscheinlich über Veränderungen der epithelialen Tight Junctions verringerten, wurden diese Effekte in Gegenwart von EGZ aufgehoben oder reduziert. Diese Beobachtung deutet auf einen protektiven Effekt von EGZ auf die epitheliale Grenzschicht im Darm bei intestinalen Entzündungsprozessen hin, welche aber durch das immunologische Profil des Entzündungsverlaufs bestimmt zu sein scheint.

Insgesamt unterstützen die vorliegenden funktionalen Studien die These, dass EGZ das Potential besitzen die epitheliale Grenzschicht aufrechtzuerhalten und das Darmepithel vor inflammatorischen Angriffen zu schützen. Die beobachteten Effekte waren von den beteiligten Zytokinen abhängig, was die Vermutung nahe legt, dass die EGZ Antwort unter verschiedenen Entzündungsbedingungen (z.B. Th1 vs. Th2 etc.) variieren kann. Obgleich die zugrunde liegenden regulatorischen Mechanismen in der vorliegenden

Arbeit nicht identifiziert wurden, deutet die beobachtete Expression von GDNF, NGF, NT-3 und deren Rezeptoren in EGZ auf ein vielversprechendes nachfolgendes Forschungsziel hin, um die genaue Quelle der von EGZ ausgeschütteten mukosaprotektiven Faktoren zu identifizieren.

Zusammenfassend lässt sich sagen, dass EGZ mehr wissenschaftliche Aufmerksamkeit beigemessen werden sollte, um die vielfältigen Funktionen dieses faszinierenden Zelltyps im ENS von gesundem wie auch von erkranktem Darm zu erforschen. Dieses könnte zur Identifizierung neuer pharmakologischer Ansatzpunkte führen und schließlich neue Möglichkeiten zur Behandlung gastrointestinaler Erkrankungen aufzeigen.

6.   References

Adams RB, Planchon SM, Roche JK. 1993. IFN-gamma modulation of epithelial barrier function. Time course, reversibility, and site of cytokine binding. *J Immunol* 150(6):2356-63

Anderson JM, Van Itallie CM. 1995. Tight junctions and the molecular basis for regulation of paracellular permeability. *Am J Physiol Gastrointest Liver Physiol* 269(4):G467-G475

Annese V, Latiano A, Andriulli A. 2003. Genetics of inflammatory bowel disease: The beginning of the end or the end of the beginning? *Digestive and Liver Disease* 35(6):442-9

Appel E, Kolman O, Kazimirsky G, Blumberg PM, Brodie C. 1997. Regulation of GDNF expression in cultured astrocytes by inflammatory stimuli. *Neuroreport* 8(15):3309-12

Assouline JG, Bosch EP, Lim R. 1983. Purification of rat Schwann cells from cultures of peripheral nerve: an immunoselective method using surfaces coated with anti-immunoglobulin antibodies. *Brain Res.* 277(2):389-92

Aube AC, Cabarrocas J, Bauer J, Philippe D, Aubert P, Doulay F, Liblau R, Galmiche JP, Neunlist M. 2006. Changes in enteric neurone phenotype and intestinal functions in a transgenic mouse model of enteric glia disruption. *Gut* 55(5):630-7

Augeron C, Laboisse CL. 1984. Emergence of Permanently Differentiated Cell Clones in a Human Colonic Cancer Cell Line in Culture after Treatment with Sodium Butyrate. *Cancer Res* 44(9):3961-9

Baetge G, Pintar JE, Gershon MD. 1990. Transiently catecholaminergic (TC) cells in the bowel of the fetal rat: precursors of noncatecholaminergic enteric neurons. *Dev. Biol.* 141(2):353-80

Balda MS, Whitney JA, Flores C, Gonzalez S, Cereijido M, Matter K. 1996. Functional dissociation of paracellular permeability and transepithelial electrical resistance and disruption of the apical-basolateral intramembrane diffusion barrier by expression of a mutant tight junction membrane protein. *J Cell Biol.* 134(4):1031-49

Baluk P, Jessen KR, Saffrey MJ, Burnstock G. 1983. The enteric nervous system in tissue culture. II. Ultrastructural studies of cell types and their relationships. *Brain Res.* 262(1):37-47

Bannerman PG, Mirsky R, Jessen KR. 1988. Establishment and properties of separate cultures of enteric neurons and enteric glia. *Brain Res.* 440(1):99-108

Bar KJ, Facer P, Williams NS, Tam PK, Anand P. 1997. Glial-derived neurotrophic factor in human adult and fetal intestine and in Hirschsprung's disease. *Gastroenterology* 112(4):1381-5

Barreau F, Cartier C, Ferrier L, Fioramonti J, Bueno L. 2004. Nerve growth factor mediates alterations of colonic sensitivity and mucosal barrier induced by neonatal stress in rats. *Gastroenterology* 127(2):524-34

Bassotti G, Battaglia E, Bellone G, Dughera L, Fisogni S, Zambelli C, Morelli A, Mioli P, Emanuelli G, Villanacci V. 2005. Interstitial cells of Cajal, enteric nerves, and glial cells in colonic diverticular disease. *J Clin Pathol* 58(9):973-7

Bassotti G, Villanacci V, Maurer CA, Fisogni S, Di Fabio F, Cadei M, Morelli A, Panagiotis T, Cathomas G, Salerni B. 2006a. The role of glial cells and apoptosis of enteric neurones in the neuropathology of intractable slow transit constipation. *Gut* 55(1):41-6

Bassotti G, Villanacci V, Cathomas G, Maurer CA, Fisogni S, Cadei M, Baron L, Morelli A, Valloncini E, Salerni B. 2006b. Enteric neuropathology of the terminal ileum in patients with intractable slow-transit constipation. *Human Pathology* 37(10):1252-8

Bernstein CN, Vidrich A. 1994. Isolation, identification, and culture of normal mouse colonic glia. *Glia* 12(2):108-16

Bishop AE, Polak JM, Facer P, Ferri GL, Marangos PJ, Pearse AG. 1982. Neuron specific enolase: a common marker for the endocrine cells and innervation of the gut and pancreas. *Gastroenterology* 83(4):902-15

Bjorklund H, Dahl D, Seiger A. 1984. Neurofilament and glial fibrillary acid protein-related immunoreactivity in rodent enteric nervous system. *Neuroscience* 12(1):277-87

Blanchard C, Durual S, Estienne M, Bouzakri K, Heim MH, Blin N, Cuber JC. 2004. IL-4 and IL-13 up-regulate intestinal trefoil factor expression: requirement for STAT6 and de novo protein synthesis. *J Immunol* 172(6):3775-83

Boguth N, Stremmel W, Ruhl A. 2003. Human enteric glia have the potential to modulate inflammatory processes. *Gastroenterology* 124(4) (Abstr.)

Bondurand N, Kobetz A, Pingault V, Lemort N, Encha-Razavi F, Couly G, Goerich DE, Wegner M, Abitbol M, Goossens M. 1998. Expression of the SOX10 gene during human development. *FEBS Letters* 432(3):168-72

Bothwell M. 1995. Functional interactions of neurotrophins and neurotrophin receptors. *Annu. Rev. Neurosci.* 18:223-53

Bowman CC, Rasley A, Tranguch SL, Marriott I. 2003. Cultured astrocytes express toll-like receptors for bacterial products. *Glia* 43(3):281-91

Bradley JS, Jr., Parr EJ, Sharkey KA. 1997. Effects of inflammation on cell proliferation in the myenteric plexus of the guinea-pig ileum. *Cell Tissue Res.* 289(3):455-61

Britsch S, Goerich DE, Riethmacher D, Peirano RI, Rossner M, Nave KA, Birchmeier C, Wegner M. 2001. The transcription factor Sox10 is a key regulator of peripheral glial development. *Genes Dev.* 15(1):66-78

Brockes JP, Fields KL, Raff MC. 1979. Studies on cultured rat Schwann cells. I. Establishment of purified populations from cultures of peripheral nerve. *Brain Res.* 165(1):105-18

Brodie C. 1996. Differential effects of Th1 and Th2 derived cytokines on NGF synthesis by mouse astrocytes. *FEBS Lett.* 394(2):117-20

Brookes SJ. 2001. Classes of enteric nerve cells in the guinea-pig small intestine. *Anat Rec.* 262(1):58-70

Bruewer M, Luegering A, Kucharzik T, Parkos CA, Madara JL, Hopkins AM, Nusrat A. 2003. Proinflammatory Cytokines Disrupt Epithelial Barrier Function by Apoptosis-Independent Mechanisms. *J Immunol* 171(11):6164-72

Buhner S, Buning C, Genschel J, Kling K, Herrmann D, Dignass A, Kuechler I, Krueger S, Schmidt HH, Lochs H. 2006. Genetic basis for increased intestinal permeability in families with Crohn's disease: role of CARD15 3020insC mutation? *Gut* 55(3):342-7

Bush TG. 2002. Enteric glial cells. An upstream target for induction of necrotizing enterocolitis and Crohn's disease? *Bioessays* 24(2):130-40

Bush TG, Savidge TC, Freeman TC, Cox HJ, Campbell EA, Mucke L, Johnson MH, Sofroniew MV. 1998. Fulminant jejuno-ileitis following ablation of enteric glia in adult transgenic mice. *Cell* 93(2):189-201

Cabarrocas J, Savidge TC, Liblau RS. 2003. Role of enteric glial cells in inflammatory bowel disease. *Glia* 41(1):81-93

Cario E. 2005. Bacterial interactions with cells of the intestinal mucosa: Toll-like receptors and NOD2. *Gut* 54(8):1182-93

Ceponis PJM, Botelho F, Richards CD, McKay DM. 2000. Interleukins 4 and 13 Increase Intestinal Epithelial Permeability by a Phosphatidylinositol 3-Kinase Pathway. LACK OF EVIDENCE FOR STAT 6 INVOLVEMENT. *J. Biol. Chem.* 275(37):29132-7

Cereijido M, Gonzalez-Mariscal L, Borboa L. 1983. Occluding junctions and paracellular pathways studied in monolayers of MDCK cells. *J Exp Biol* 106(1):205-15

Chadi G, Gomide VC, Rodrigues dS, Scabello RT, Mauricio dS. 2004. Basic fibroblast growth factor, neurofilament, and glial fibrillary acidic protein immunoreactivities in the myenteric plexus of the rat esophagus and colon. *J Morphol.* 261(3):323-33

Chalazonitis A. 2004. Neurotrophin-3 in the development of the enteric nervous system. *Prog. Brain Res.* 146:243-63

Chalazonitis A, Rothman TP, Chen J, Gershon MD. 1998a. Age-dependent differences in the effects of GDNF and NT-3 on the development of neurons and glia from neural crest-derived precursors immunoselected from the fetal rat gut: expression of GFRalpha-1 in vitro and in vivo. *Dev. Biol.* 204(2):385-406

Chalazonitis A, Rothman TP, Chen J, Lamballe F, Barbacid M, Gershon MD. 1994. Neurotrophin-3 induces neural crest-derived cells from fetal rat gut to develop in vitro as neurons or glia. *J Neurosci.* 14(11 Pt 1):6571-84

Chalazonitis A, Rothman TP, Chen J, Vinson EN, MacLennan AJ, Gershon MD. 1998b. Promotion of the development of enteric neurons and glia by neuropoietic cytokines: interactions with neurotrophin-3. *Dev. Biol.* 198(2):343-65

Chambers TJ, Morson BC. 1979. The granuloma in Crohn's disease. *Gut* 20(4):269-74

Cheung M, Briscoe J. 2003. Neural crest development is regulated by the transcription factor Sox9. *Development* 130(23):5681-93

Collins SM. 1996. The immunomodulation of enteric neuromuscular function: implications for motility and inflammatory disorders. *Gastroenterology* 111(6):1683-99

Cook RD, Burnstock G. 1976. The ultrastructure of Auerbach's plexus in the guinea-pig. II. Non-neuronal elements. *J Neurocytol.* 5(2):195-206

Cornet A, Savidge TC, Cabarrocas J, Deng WL, Colombel JF, Lassmann H, Desreumaux P, Liblau RS. 2001. Enterocolitis induced by autoimmune targeting of enteric glial cells: a possible mechanism in Crohn's disease? *Proc. Natl. Acad. Sci U. S. A* 98(23):13306-11

Coulie B, Szarka LA, Camilleri M, Burton DD, McKinzie S, Stambler N, Cedarbaum JM. 2000. Recombinant human neurotrophic factors accelerate colonic transit and relieve constipation in humans. *Gastroenterology* 119(1):41-50

Cowen T, Johnson RJ, Soubeyre V, Santer RM. 2000. Restricted diet rescues rat enteric motor neurones from age related cell death. *Gut* 47(5):653-60

Crohn BB, Ginzburg L, Oppenheimer GD. 1932. Regional ileitis; a pathologic and clinical entity. *Am J Med.* 13(5):583-90

De Giorgio R, Arakawa J, Wetmore CJ, Sternini C. 2000. Neurotrophin-3 and neurotrophin receptor immunoreactivity in peptidergic enteric neurons. *Peptides* 21(9):1421-6

Delie F, Rubas W. 1997. A human colonic cell line sharing similarities with enterocytes as a model to examine oral absorption: advantages and limitations of the Caco-2 model. *Crit Rev. Ther. Drug Carrier Syst.* 14(3):221-86

Denning TL, Campbell NA, Song F, Garofalo RP, Klimpel GR, Reyes VE, Ernst PB. 2000. Expression of IL-10 receptors on epithelial cells from the murine small and large intestine. *Int. Immunol.* 12(2):133-9

Dharmsathaphorn K, McRoberts JA, Mandel KG, Tisdale LD, Masui H. 1984. A human colonic tumor cell line that maintains vectorial electrolyte transport. *Am J Physiol Gastrointest Liver Physiol* 246(2):G204-G208

Di Mola FF, Friess H, Scheuren A, Di Sebastiano P, Graber H, Egger B, Zimmermann A, Korc M, Buchler MW. 1999. Transforming growth factor-betas and their signaling receptors are coexpressed in Crohn's disease. *Ann. Surg.* 229(1):67-75

Di Mola FF, Friess H, Zhu ZW, Koliopanos A, Bley T, Di Sebastiano P, Innocenti P, Zimmermann A, Buchler MW. 2000. Nerve growth factor and Trk high affinity receptor (TrkA) gene expression in inflammatory bowel disease. *Gut* 46(5):670-9

Dogiel, A.S. 1899. Ueber den Bau der Ganglien in den Geflechten des Darmes und der Gallenblase des Menschen und der Säugethiere. *Arch Anat Physiol Anat Abt.*130-58

Durbec PL, Larsson-Blomberg LB, Schuchardt A, Costantini F, Pachnis V. 1996. Common origin and developmental dependence on c-ret of subsets of enteric and sympathetic neuroblasts. *Development* 122(1):349-58

Eaker EY, Sallustio JE. 1998. Myenteric plexus neurons in culture: developmental changes in neurofilament and related proteins. *Dig. Dis. Sci* 43(2):270-8

Eddleston M, Mucke L. 1993. Molecular profile of reactive astrocytes--Implications for their role in neurologic disease. *Neuroscience* 54(1):15-36

Esen N, Tanga FY, DeLeo JA, Kielian T. 2004. Toll-like receptor 2 (TLR2) mediates astrocyte activation in response to the Gram-positive bacterium Staphylococcus aureus. *J Neurochem.* 88(3):746-58

Esteban I, Levanti B, Garcia-Suarez O, Germana G, Ciriaco E, Naves FJ, Vega JA. 1998. A neuronal subpopulation in the mammalian enteric nervous system expresses TrkA and TrkC neurotrophin receptor-like proteins. *Anat Rec.* 251(3):360-70

Estrada-Mondaca S, Carreon-Rodriguez A, Belkind-Gerson J. 2007. Biology of the adult enteric neural stem cell. *Dev. Dyn.* 236(1):20-32

Fanning AS, Jameson BJ, Jesaitis LA, Anderson JM. 1998. The tight junction protein ZO-1 establishes a link between the transmembrane protein occludin and the actin cytoskeleton. *J Biol. Chem.* 273(45):29745-53

Ferrante M, de Hertogh G, Hlavaty T, D'Haens G, Penninckx F, D'Hoore A, Vermeire S, Rutgeerts P, Geboes K, Van Assche G. 2006. The value of myenteric plexitis to predict early postoperative Crohn's disease recurrence. *Gastroenterology* 130(6):1595-606

Ferri GL, Probert L, Cocchia D, Michetti F, Marangos PJ, Polak JM. 1982. Evidence for the presence of S-100 protein in the glial component of the human enteric nervous system. *Nature* 297(5865):409-10

Fiocchi C. 2005. The normal intestinal mucosa: a state of controlled inflammation.101-120 pp. 101-120 pp.

Fish SM, Proujansky R, Reenstra WW. 1999. Synergistic effects of interferon gamma and tumour necrosis factor alpha on T84 cell function. *Gut* 45(2):191-8

Fogh J. 1975. *Human tumor cells in vitro*. New York: Plenum Press. 115-159 pp.

Fries W, Renda MC, Lo Presti MA, Raso A, Orlando A, Oliva L, Giofre MR, Maggio A, Mattaliano A, Macaluso A, Cottone M. 2005. Intestinal permeability and genetic determinants in patients, first-degree relatives, and controls in a high-incidence area of Crohn's disease in Southern Italy. *Am J Gastroenterol.* 100(12):2730-6

Furness JB, Costa M. 1980. Types of nerves in the enteric nervous system. *Neuroscience* 5(1):1-20

Furness JB, Costa M. 1987. *The enteric nervous system*. New York: Churchill Livingstone.

Furuse M, Itoh M, Hirase T, Nagafuchi A, Yonemura S, Tsukita S, Tsukita S. 1994. Direct association of occludin with ZO-1 and its possible involvement in the localization of occludin at tight junctions. *J Cell Biol.* 127(6 Pt 1):1617-26

Gabella G. 1972. Fine structure of the myenteric plexus in the guinea-pig ileum. *J Anat.* 111(Pt 1):69-97

Gabella G. 1981. Ultrastructure of the nerve plexuses of the mammalian intestine: the enteric glial cells. *Neuroscience* 6(3):425-36

Gabella G. 1987. The number of neurons in the small intestine of mice, guinea-pigs and sheep. *Neuroscience* 22(2):737-52

Gabella G. 1989. Fall in the number of myenteric neurons in aging guinea pigs. *Gastroenterology* 96(6):1487-93

Gabella G, Trigg P. 1984. Size of neurons and glial cells in the enteric ganglia of mice, guinea-pigs, rabbits and sheep. *J Neurocytol.* 13(1):49-71

Gasche C, Grundtner P. 2005. Genotypes and phenotypes in Crohn's disease: do they help in clinical management? *Gut* 54(1):162-7

Gasche C, Scholmerich J, Brynskov J, D'Haens G, Hanauer SB, Irvine EJ, Jewell DP, Rachmilewitz D, Sachar DB, Sandborn WJ, Sutherland LR. 2000. A simple classification of Crohn's disease: report of the Working Party for the World Congresses of Gastroenterology, Vienna 1998. *Inflamm. Bowel. Dis.* 6(1):8-15

Geboes K, Collins S. 1998. Structural abnormalities of the nervous system in Crohn's disease and ulcerative colitis. *Neurogastroenterol. Motil.* 10(3):189-202

Geboes K, Rutgeerts P, Ectors N, Mebis J, Penninckx F, Vantrappen G, Desmet VJ. 1992. Major histocompatibility class II expression on the small intestinal nervous system in Crohn's disease. *Gastroenterology* 103(2):439-47

Geisert EE, Jr., Johnson HG, Binder LI. 1990. Expression of microtubule-associated protein 2 by reactive astrocytes. *Proc. Natl. Acad. Sci. U. S. A* 87(10):3967-71

Gershon MD, Rothman TP. 1991. Enteric glia. *Glia* 4(2):195-204

Gotz R, Koster R, Winkler C, Raulf F, Lottspeich F, Schartl M, Thoenen H. 1994. Neurotrophin-6 is a new member of the nerve growth factor family. *Nature* 372(6503):266-9

Goyal RK, Hirano I. 1996. The Enteric Nervous System. *N Engl J Med* 334(17):1106-15

Hanani M. 1993. Neurons and glial cells of the enteric nervous system: studies in tissue culture. *J Basic Clin. Physiol Pharmacol.* 4(3):157-79

Hanani M, Fellig Y, Udassin R, Freund HR. 2004. Age-related changes in the morphology of the myenteric plexus of the human colon. *Auton. Neurosci.* 113(1-2):71-8

Hanani M, Reichenbach A. 1994. Morphology of horseradish peroxidase (HRP)-injected glial cells in the myenteric plexus of the guinea-pig. *Cell Tissue Res.* 278(1):153-60

Hanani M, Zamir O, Baluk P. 1989. Glial cells in the guinea pig myenteric plexus are dye coupled. *Brain Res.* 497(2):245-9

Hansen MB. 2003. The enteric nervous system I: organisation and classification. *Pharmacol. Toxicol.* 92(3):105-13

Heller F, Florian P, Bojarski C, Richter J, Christ M, Hillenbrand B, Mankertz J, Gitter AH, Burgel N, Fromm M, Zeitz M, Fuss I, Strober W, Schulzke JD. 2005. Interleukin-13 is the key effector Th2 cytokine in ulcerative colitis that affects epithelial tight junctions, apoptosis, and cell restitution. *Gastroenterology* 129(2):550-64

Heuckeroth RO, Enomoto H, Grider JR, Golden JP, Hanke JA, Jackman A, Molliver DC, Bardgett ME, Snider WD, Johnson EM, Jr., Milbrandt J. 1999. Gene targeting reveals a critical role for neurturin in the development and maintenance of enteric, sensory, and parasympathetic neurons. *Neuron* 22(2):253-63

Heuckeroth RO, Lampe PA, Johnson EM, Milbrandt J. 1998. Neurturin and GDNF promote proliferation and survival of enteric neuron and glial progenitors in vitro. *Dev. Biol.* 200(1):116-29

Hidalgo IJ, Raub TJ, Borchardt RT. 1989. Characterization of the human colon carcinoma cell line (Caco-2) as a model system for intestinal epithelial permeability. *Gastroenterology* 96(3):736-49

Ho W, Keenan C, Wu H, Sharkey K. 2003. Enteric glia in a murine model of colitis. *Neurogastroenterol. Motil.*(15):228

Hoehner JC, Wester T, Pahlman S, Olsen L. 1996. Localization of neurotrophins and their high-affinity receptors during human enteric nervous system development. *Gastroenterology* 110(3):756-67

Hollander D. 2002. Crohn's disease, TNF-alpha, and the leaky gut. The chicken or the egg? *Am J Gastroenterol.* 97(8):1867-8

Hollenbach E, Rühl A, Zoller M, Stremmel W. 2000. T cell activation by enteric glia: a novel pathway for the amplification of inflammatory responses in the enteric nervous system. *Gastroenterology* 118

Hoyle CH, Burnstock G. 1989. Neuronal populations in the submucous plexus of the human colon. *J Anat.* 166:7-22

Huang WM, Gibson SJ, Facer P, Gu J, Polak JM. 1983. Improved section adhesion for immunocytochemistry using high molecular weight polymers of L-lysine as a slide coating. *Histochemistry* 77(2):275-9

Hugot JP, Chamaillard M, Zouali H, Lesage S, Cezard JP, Belaiche J, Almer S, Tysk C, O'Morain CA, Gassull M, Binder V, Finkel Y, Cortot A, Modigliani R, Laurent-Puig P, Gower-Rousseau C, Macry J, Colombel JF, Sahbatou M, Thomas G. 2001. Association of NOD2 leucine-rich repeat variants with susceptibility to Crohn's disease. Nature 411(6837):599-603

Ibba-Manneschi L, Martini M, Zecchi-Orlandini S, Faussone-Pellegrini MS. 1995. Structural organization of enteric nervous system in human colon. *Histol. Histopathol.* 10(1):17-25

Jaeger CB. 1995. Isolation of enteric ganglia from the myenteric plexus of adult rats. *J Neural Transplant. Plast.* 5(4):223-32

Jessen KR, Mirsky R. 1980. Glial cells in the enteric nervous system contain glial fibrillary acidic protein. *Nature* 286(5774):736-7

Jessen KR, Mirsky R. 1983. Astrocyte-like glia in the peripheral nervous system: an immunohistochemical study of enteric glia. *J. Neurosci.* 3(11):2206-18

Jessen KR, Mirsky R. 1991. Schwann cell precursors and their development. *Glia* 4(2):185-94

Jessen KR, Saffrey MJ, Burnstock G. 1983. The enteric nervous system in tissue culture. I. Cell types and their interactions in explants of the myenteric and submucous plexuses from guinea pig, rabbit and rat. *Brain Res.* 262(1):17-35

Johnson RJ, Schemann M, Santer RM, Cowen T. 1998. The effects of age on the overall population and on sub-populations of myenteric neurons in the rat small intestine. *J Anat.* 192 (Pt 4):479-88

Jumarie C, Malo C. 1991. Caco-2 cells cultured in serum-free medium as a model for the study of enterocytic differentiation in vitro. *J. Cell Physiol* 149(1):24-33

Juric DM, Carman-Krzan M. 2000. Cytokine-regulated secretion of nerve growth factor from cultured rat neonatal astrocytes. *Pflugers Arch* 440(5 Suppl):R96-R98

Karaosmanoglu T, Aygun B, Wade PR, Gershon MD. 1996. Regional differences in the number of neurons in the myenteric plexus of the guinea pig small intestine and colon: an evaluation of markers used to count neurons. *Anat. Rec.* 244(4):470-80

Kato H, Yamamoto T, Yamamoto H, Ohi R, So N, Iwasaki Y. 1990. Immunocytochemical characterization of supporting cells in the enteric nervous system in Hirschsprung's disease. *J Pediatr. Surg.* 25(5):514-9

Kirchgessner AL, Gershon MD. 1990. Innervation of the pancreas by neurons in the gut. *J Neurosci.* 10(5):1626-42

Komuro T, Baluk P, Burnstock G. 1982. An ultrastructural study of neurons and non-neuronal cells in the myenteric plexus of the rabbit colon. *Neuroscience* 7(7):1797-806

Kondyli M, Varakis J, Assimakopoulou M. 2005. Expression of p75NTR and Trk neurotrophin receptors in the enteric nervous system of human adults. *Anat. Sci Int.* 80(4):223-8

Krammer HJ, Karahan ST, Rumpel E, Klinger M, Kuhnel W. 1993. Immunohistochemical visualization of the enteric nervous system using antibodies against protein gene product (PGP) 9.5. *Ann. Anat.* 175(4):321-5

Krammer HJ, Karahan ST, Sigge W, Kuhnel W. 1994. Immunohistochemistry of markers of the enteric nervous system in whole-mount preparations of the human colon. *Eur. J Pediatr. Surg.* 4(5):274-8

Kuhlbrodt K, Herbarth B, Sock E, Hermans-Borgmeyer I, Wegner M. 1998. Sox10, a novel transcriptional modulator in glial cells. *J Neurosci.* 18(1):237-50

Kuno R, Yoshida Y, Nitta A, Nabeshima T, Wang J, Sonobe Y, Kawanokuchi J, Takeuchi H, Mizuno T, Suzumura A. 2006. The role of TNF-alpha and its receptors in the production of NGF and GDNF by astrocytes. *Brain Res.* 1116(1):12-8

Lai KO, Fu WY, Ip FC, Ip NY. 1998. Cloning and expression of a novel neurotrophin, NT-7, from carp. *Mol. Cell Neurosci.* 11(1-2):64-76

Laping NJ, Teter B, Nichols NR, Rozovsky I, Finch CE. 1994. Glial fibrillary acidic protein: regulation by hormones, cytokines, and growth factors. *Brain Pathol* 4(3):259-75

Laukoetter MG, Bruewer M, Nusrat A. 2006. Regulation of the intestinal epithelial barrier by the apical junctional complex. *Curr. Opin. Gastroenterol.* 22(2):85-9

Lee VM, Page CD, Wu HL, Schlaepfer WW. 1984. Monoclonal antibodies to gel-excised glial filament protein and their reactivities with other intermediate filament proteins. *J Neurochem.* 42(1):25-32

Lendahl U, Zimmerman LB, McKay RD. 1990. CNS stem cells express a new class of intermediate filament protein. *Cell* 60(4):585-95

Lesuffleur T, Barbat A, Dussaulx E, Zweibaum A. 1990. Growth adaptation to methotrexate of HT-29 human colon carcinoma cells is associated with their ability to differentiate into columnar absorptive and mucus-secreting cells. *Cancer Res* 50(19):6334-43

Levi-Montalcini R. 1987. The nerve growth factor 35 years later. *Science* 237(4819):1154-62

Levi-Montalcini R, Skaper SD, Dal Toso R, Petrelli L, Leon A. 1996. Nerve growth factor: from neurotrophin to neurokine. *Trends Neurosci.* 19(11):514-20

Lin A, Lourenssen S, Stanzel RD, Blennerhassett MG. 2005. Nerve growth factor sensitivity is broadly distributed among myenteric neurons of the rat colon. *J Comp Neurol.* 490(2):194-206

Lin LF, Doherty DH, Lile JD, Bektesh S, Collins F. 1993. GDNF: a glial cell line-derived neurotrophic factor for midbrain dopaminergic neurons. *Science* 260(5111):1130-2

Lin RC, Matesic DF. 1994. Immunohistochemical demonstration of neuron-specific enolase and microtubule-associated protein 2 in reactive astrocytes after injury in the adult forebrain. *Neuroscience* 60(1):11-6

Lin RC, Matesic DF, Marvin M, McKay RD, Brustle O. 1995. Re-expression of the intermediate filament nestin in reactive astrocytes. *Neurobiol. Dis.* 2(2):79-85

Lin T, Zhang W, Fan Y, Mulholland M. 2007. Interleukin-1[beta] and Interleukin-6 Stimulate Matrix Metalloproteinase-9 Secretion in Cultured Myenteric Glia. *Journal of Surgical Research* 137(1):38-45

Lin Z, Gao N, Hu HZ, Liu S, Gao C, Kim G, Ren J, Xia Y, Peck OC, Wood JD. 2002. Immunoreactivity of Hu proteins facilitates identification of myenteric neurones in guinea-pig small intestine. *Neurogastroenterol. Motil.* 14(2):197-204

Livak KJ, Schmittgen TD. 2001. Analysis of relative gene expression data using real-time quantitative PCR and the 2(-Delta Delta C(T)) Method. *Methods* 25(4):402-8

Loeffel SC, Gillespie GY, Mirmiran SA, Miller EW, Golden P, Askin FB, Siegal GP. 1985. Cellular immunolocalization of S100 protein within fixed tissue sections by monoclonal antibodies. *Arch Pathol Lab Med* 109(2):117-22

Loftus J. 2004. Clinical epidemiology of inflammatory bowel disease: incidence, prevalence, and environmental influences. *Gastroenterology* 126(6):1504-17

Lomax AE, Fernandez E, Sharkey KA. 2005. Plasticity of the enteric nervous system during intestinal inflammation. *Neurogastroenterol. Motil.* 17(1):4-15

Louis E, Collard A, Oger AF, Degroote E, Aboul Nasr El Yafi FA, Belaiche J. 2001. Behaviour of Crohn's disease according to the Vienna classification: changing pattern over the course of the disease. *Gut* 49(6):777-82

Ma D, Wolvers D, Stanisz AM, Bienenstock J. 2003. Interleukin-10 and nerve growth factor have reciprocal upregulatory effects on intestinal epithelial cells. *Am J Physiol Regul Integr Comp Physiol* 284(5):R1323-R1329

Ma TY, Anderson JM. 2006. Tight junctions and the intestinal barrier. In *Physiology of the Gastrointestinal Tract*, ed. Johnson LR, 61:1559-1594 pp. Academic Press. 1559-1594 pp.

Ma TY, Iwamoto GK, Hoa NT, Akotia V, Pedram A, Boivin MA, Said HM. 2004. TNF-alpha-induced increase in intestinal epithelial tight junction permeability requires NF-kappa B activation. *Am. J Physiol Gastrointest. Liver Physiol* 286(3):G367-G376

Madara J, Stafford J, Dharmsathaphorn K, Carlson S. 1987. Structural analysis of a human intestinal epithelial cell line. *Gastroenterology* 92(5):1133-45

Madara JL, Parkos C, Colgan S, Nusrat A, Atisook K, Kaoutzani P. 1992. The movement of solutes and cells across tight junctions. *Ann. N Y. Acad. Sci.* 664:47-60

Madara JL, Stafford J. 1989. Interferon-gamma directly affects barrier function of cultured intestinal epithelial monolayers. *J Clin. Invest* 83(2):724-7

Madsen KL, Lewis SA, Tavernini MM, Hibbard J, Fedorak RN. 1997. Interleukin 10 prevents cytokine-induced disruption of T84 monolayer barrier integrity and limits chloride secretion. *Gastroenterology* 113(1):151-9

Maka M, Claus Stolt C, Wegner M. 2005. Identification of Sox8 as a modifier gene in a mouse model of Hirschsprung disease reveals underlying molecular defect. *Developmental Biology* 277(1):155-69

Marangos PJ, Zomzely-Neurath C, Luk DC, York C. 1975. Isolation and characterization of the nervous system-specific protein 14-3-2 from rat brain. Purification, subunit composition, and comparison to the beef brain protein. *J Biol. Chem.* 250(5):1884-91

Marano CW, Laughlin KV, Russo LM, Peralta SA, Mullin JM. 1993. Long-term effects of tumor necrosis factor on LLC-PK1 transepithelial resistance. *J Cell Physiol* 157(3):519-27

Marusich MF, Furneaux HM, Henion PD, Weston JA. 1994. Hu neuronal proteins are expressed in proliferating neurogenic cells. *J Neurobiol.* 25(2):143-55

Matter K, Balda MS. 2003. Functional analysis of tight junctions. *Methods* 30(3):228-34

McGee DW, Bamberg T, Vitkus SJ, McGhee JR. 1995. A synergistic relationship between TNF-alpha, IL-1 beta, and TGF-beta 1 on IL-6 secretion by the IEC-6 intestinal epithelial cell line. *Immunology* 86(1):6-11

McKay DM, Baird AW. 1999. Cytokine regulation of epithelial permeability and ion transport. *Gut* 44(2):283-9

McKay DM, Croitoru K, Perdue MH. 1996. T cell-monocyte interactions regulate epithelial physiology in a coculture model of inflammation. *Am J Physiol Cell Physiol* 270(2):C418-C428

Moore MW, Klein RD, Farinas I, Sauer H, Armanini M, Phillips H, Reichardt LF, Ryan AM, Carver-Moore K, Rosenthal A. 1996. Renal and neuronal abnormalities in mice lacking GDNF. *Nature* 382(6586):76-9

Mullin JM, Snock KV. 1990. Effect of tumor necrosis factor on epithelial tight junctions and transepithelial permeability. *Cancer Res.* 50(7):2172-6

Murakami H, Masui H. 1980. Hormonal control of human colon carcinoma cell growth in serum-free medium. *Proc. Natl. Acad. Sci U. S. A* 77(6):3464-8

Murphy EM, defontgalland d, Costa M, Brookes SJ, Wattchow DA. 2007. Quantification of subclasses of human colonic myenteric neurons by immunoreactivity to Hu, choline acetyltransferase and nitric oxide synthase. *Neurogastroenterol. Motil.* 19(2):126-34

Nagahama M, Semba R, Tsuzuki M, Aoki E. 2001. L-arginine immunoreactive enteric glial cells in the enteric nervous system of rat ileum. *Biol. Signals Recept.* 10(5):336-40

Nasser Y, Fernandez E, Keenan CM, Ho W, Oland LD, Tibbles LA, Schemann M, MacNaughton WK, Ruhl A, Sharkey KA. 2006. Role of enteric glia in intestinal physiology: effects of the gliotoxin fluorocitrate on motor and secretory function. *Am J Physiol Gastrointest Liver Physiol* 291(5):G912-G927

Neunlist M, Aubert P, Bonnaud S, Van Landeghem L, Coron E, Wedel T, Naveilhan P, Ruhl A, Lardeux B, Savidge T, Paris F, Galmiche JP. 2007. Enteric glia inhibit intestinal epithelial cell proliferation partly through a TGF-beta1-dependent pathway. *Am J Physiol Gastrointest Liver Physiol* 292(1):G231-G241

Neunlist M, Aubert P, Toquet C, Oreshkova T, Barouk J, Lehur PA, Schemann M, Galmiche JP. 2003a. Changes in chemical coding of myenteric neurones in ulcerative colitis. *Gut* 52(1):84-90

Neunlist M, Toumi F, Oreschkova T, Denis M, Leborgne J, Laboisse CL, Galmiche JP, Jarry A. 2003b. Human ENS regulates the intestinal epithelial barrier permeability and a tight junction-associated protein ZO-1 via VIPergic pathways. *Am J Physiol Gastrointest Liver Physiol* 285(5):G1028-G1036

Nishino J, Mochida K, Ohfuji Y, Shimazaki T, Meno C, Ohishi S, Matsuda Y, Fujii H, Saijoh Y, Hamada H. 1999. GFR alpha3, a component of the artemin receptor, is required for migration and survival of the superior cervical ganglion. *Neuron* 23(4):725-36

Ogura Y, Bonen DK, Inohara N, Nicolae DL, Chen FF, Ramos R, Britton H, Moran T, Karaliuskas R, Duerr RH, Achkar JP, Brant SR, Bayless TM, Kirschner BS, Hanauer SB, Nunez G, Cho JH. 2001. A frameshift mutation in NOD2 associated with susceptibility to Crohn's disease. *Nature* 411(6837):603-6

Okada M, Maeda K, Yao T, Iwashita A, Nomiyama Y, Kitahara K. 1991. Minute lesions of the rectum and sigmoid colon in patients with Crohn's disease. *Gastrointest Endosc.* 37(3):319-24

Panja A, Goldberg S, Eckmann L, Krishen P, Mayer L. 1998. The Regulation and Functional Consequence of Proinflammatory Cytokine Binding on Human Intestinal Epithelial Cells. *J Immunol* 161(7):3675-84

Paratore C, Goerich DE, Suter U, Wegner M, Sommer L. 2001. Survival and glial fate acquisition of neural crest cells are regulated by an interplay between the transcription factor Sox10 and extrinsic combinatorial signaling. *Development* 128(20):3949-61

Parkman HP, Rao SSC, Reynolds JC, Schiller LR, Wald A, Miner PB, Lembo AJ, Gordon JM, Drossman DA, Waltzman L, Stambler N, Cedarbaum JM. 2003. Neurotrophin-3 improves functional constipation. *The American Journal of Gastroenterology* 98(6):1338-47

Parr EJ, Sharkey KA. 1994. The use of constitutive nuclear oncoproteins to count neurons in the enteric nervous system of the guinea pig. *Cell Tissue Res.* 277(2):325-31

Parr EJ, Sharkey KA. 1997. Multiple mechanisms contribute to myenteric plexus ablation induced by benzalkonium chloride in the guinea-pig ileum. *Cell Tissue Res.* 289(2):253-64

Phillips RJ, Hargrave SL, Rhodes BS, Zopf DA, Powley TL. 2004a. Quantification of neurons in the myenteric plexus: an evaluation of putative pan-neuronal markers. *J Neurosci. Methods* 133(1-2):99-107

Phillips RJ, Kieffer EJ, Powley TL. 2003. Aging of the myenteric plexus: neuronal loss is specific to cholinergic neurons. *Auton. Neurosci.* 106(2):69-83

Phillips RJ, Kieffer EJ, Powley TL. 2004b. Loss of glia and neurons in the myenteric plexus of the aged Fischer 344 rat. *Anat. Embryol. (Berl)* 209(1):19-30

Phillips RJ, Powley TL. 2001. As the gut ages: timetables for aging of innervation vary by organ in the Fischer 344 rat. *J Comp Neurol.* 434(3):358-77

Podolsky DK. 2002. Inflammatory Bowel Disease. *N Engl J Med* 347(6):417-29

Pusch C, Hustert E, Pfeifer D, Sudbeck P, Kist R, Roe B, Wang Z, Balling R, Blin N, Scherer G. 1998. The SOX10/Sox10 gene from human and mouse: sequence, expression, and transactivation by the encoded HMG domain transcription factor. *Hum. Genet.* 103(2):115-23

Quaroni A, Wands J, Trelstad RL, Isselbacher KJ. 1979. Epithelioid cell cultures from rat small intestine. Characterization by morphologic and immunologic criteria. *J. Cell Biol.* 80(2):248-65

Raddatz D, Bockemuhl M, Ramadori G. 2005. Quantitative measurement of cytokine mRNA in inflammatory bowel disease: relation to clinical and endoscopic activity and outcome. *Eur. J Gastroenterol. Hepatol.* 17(5):547-57

Raff MC, Abney E, Brockes JP, Hornby-Smith A. 1978. Schwann cell growth factors. *Cell* 15(3):813-22

Reichenbach A. 1989. Glia:neuron index: review and hypothesis to account for different values in various mammals. *Glia* 2(2):71-7

Reinshagen M, Engele J, Lakshmanan J, Geerling I, Eysselein V, Adler G. 1999. Expression of GDNF, Ret and GFR-alpha1/GFR-alpha2 during the timecourse of experimental colitis in the rat. *Gastroenterology*(116):A805

Reinshagen M, Rohm H, Steinkamp M, Lieb K, Geerling I, von Herbay A, Flamig G, Eysselein VE, Adler G. 2000. Protective role of neurotrophins in experimental inflammation of the rat gut. *Gastroenterology* 119(2):368-76

Reinshagen M, von Boyen G, Adler G, Steinkamp M. 2002. Role of neurotrophins in inflammation of the gut. *Curr. Opin. Investig. Drugs* 3(4):565-8

Rogler G. 2007. Pathophysiologie chronisch entzündlicher Darmerkrankungen. In *Lehrbuch der klinischen Pathophysiologie komplexer chronischer Erkrankungen. Band 2: Spezielle Pathophysiologie.*, ed. Straub RH, 30a:137-148 pp. Göttingen: Vandenhoeck & Ruprecht. 137-148 pp.

Rothman TP, Tennyson VM, Gershon MD. 1986. Colonization of the bowel by the precursors of enteric glia: studies of normal and congenitally aganglionic mutant mice. *J Comp Neurol.* 252(4):493-506

Ruhl A. 2005. Glial cells in the gut. *Neurogastroenterol. Motil.* 17(6):777-90

Ruhl A, Franzke S, Collins SM, Stremmel W. 2001a. Interleukin-6 expression and regulation in rat enteric glial cells. *Am J Physiol Gastrointest Liver Physiol* 280(6):G1163-G1171

Ruhl A, Franzke S, Stremmel W. 2001b. IL-1beta and IL-10 have dual effects on enteric glial cell proliferation. *Neurogastroenterology and Motility* 13(1):89-94

Ruhl A, Hoppe S, Frey I, Daniel H, Schemann M. 2005. Functional expression of the peptide transporter PEPT2 in the mammalian enteric nervous system. *J Comp Neurol.* 490(1):1-11

Ruhl A, Khan I, Blennerhassett MG, Collins SM. 1994. Enteroglial cells from rat myenteric plexus express interleukin-1b and interleukin-6 mRNA. *Gastroenterology* 106

Ruhl A, Trotter J, Stremmel W. 2001c. Isolation of enteric glia and establishment of transformed enteroglial cell lines from the myenteric plexus of adult rat. *Neurogastroenterol. Motil.* 13(1):95-106

Saffrey MJ. 2004. Ageing of the enteric nervous system. *Mech. Ageing Dev.* 125(12):899-906

Sambrook J, Fritsch EF, and Maniatis T. 1989. *Molecular Cloning: A Laboratory Manual.* New York: Cold Springs Harbor Laboratory Press.

Sanchez MP, Silos-Santiago I, Frisen J, He B, Lira SA, Barbacid M. 1996. Renal agenesis and the absence of enteric neurons in mice lacking GDNF. *Nature* 382(6586):70-3

Sanders SE, Madara JL, McGuirk DK, Gelman DS, Colgan SP. 1995. Assessment of inflammatory events in epithelial permeability: a rapid screening method using fluorescein dextrans. *Epithelial Cell Biol.* 4(1):25-34

Sands B. 2000. Therapy of inflammatory bowel disease. *Gastroenterology* 118(2):S68-S82

Sands BE. 2002. Crohn's disease. In *Sleisenger & Fordtran's gastrointestinal and liver disease: pathophysiology, diagnosis, management*, ed. Feldman M, Friedman LS, Sleisenger MH, 103:2005-2038 pp. Philadelphia: Saunders. 2005-2038 pp.

Sariola H, Saarma M. 2003. Novel functions and signalling pathways for GDNF. *J Cell Sci.* 116(Pt 19):3855-62

Sartor RB. 2004. Microbial influences in inflammatory bowel disease: role in pathogenesis and clinical implications. In Kirsner's Inflammatory Bowel Diseases, ed. Sartor RB, Sandborn WJ,138-162 pp. Philadelphia: Elsevier. 138-162 pp.

Sartor RB. 2006. Mechanisms of disease: pathogenesis of Crohn's disease and ulcerative colitis. *Nat. Clin. Pract. Gastroenterol. Hepatol.* 3(7):390-407

Savidge TC, Newman P, Pothoulakis C, Ruhl A, Neunlist M, Bourreille A, Hurst R, Sofroniew MV. 2007. Enteric glia regulate intestinal barrier function and inflammation via release of s-nitrosogluathione. *Gastroenterology*

Schafer KH, Mestres P. 1997. Human newborn and adult myenteric plexus grows in different patterns. *Cell Mol. Biol. (Noisy. -le-grand)* 43(8):1171-80

Schafer KH, Saffrey MJ, Burnstock G, Mestres-Ventura P. 1997. A new method for the isolation of myenteric plexus from the newborn rat gastrointestinal tract. *Brain Res. Brain Res. Protoc.* 1(2):109-13

Schemann M, Neunlist M. 2004. The human enteric nervous system. *Neurogastroenterol. Motil.* 16 Suppl 1:55-9

Schmidt K, Glaser G, Wernig A, Wegner M, Rosorius O. 2003. Sox8 is a specific marker for muscle satellite cells and inhibits myogenesis. *J Biol. Chem.* 278(32):29769-75

Schneider J, Jehle EC, Starlinger MJ, Neunlist M, Michel K, Hoppe S, Schemann M. 2001. Neurotransmitter coding of enteric neurones in the submucous plexus is changed in non-inflamed rectum of patients with Crohn's disease. *Neurogastroenterol. Motil.* 13(3):255-64

Schreiber S, Nikolaus S, Hampe J, Hamling J, Koop I, Groessner B, Lochs H, Raedler A. 1999. Tumour necrosis factor alpha and interleukin 1beta in relapse of Crohn's disease. *Lancet* 353(9151):459-61

Schuchardt A, D'Agati V, Larsson-Blomberg L, Costantini F, Pachnis V. 1994. Defects in the kidney and enteric nervous system of mice lacking the tyrosine kinase receptor Ret. *Nature* 367(6461):380-3

Sock E, Schmidt K, Hermanns-Borgmeyer I, Bosl MR, Wegner M. 2001. Idiopathic Weight Reduction in Mice Deficient in the High-Mobility-Group Transcription Factor Sox8. *Mol. Cell. Biol.* 21(20):6951-9

Stack WA, Mann SD, Roy AJ, Heath P, Sopwith M, Freeman J, Holmes G, Long R, Forbes A, Kamm MA. 1997. Randomised controlled trial of CDP571 antibody to tumour necrosis factor-alpha in Crohn's disease. *Lancet* 349(9051):521-4

Stanisz AM, Stanisz JA. 2000. Nerve growth factor and neuroimmune interactions in inflammatory diseases. *Ann. N. Y. Acad. Sci.* 917:268-72

Stead RH, Dixon MF, Bramwell NH, Riddell RH, Bienenstock J. 1989. Mast cells are closely apposed to nerves in the human gastrointestinal mucosa. *Gastroenterology* 97(3):575-85

Steindler DA, Laywell ED. 2003. Astrocytes as stem cells: nomenclature, phenotype, and translation. *Glia* 43(1):62-9

Steinkamp M, Geerling I, Seufferlein T, von Boyen G, Egger B, Grossmann J, Ludwig L, Adler G, Reinshagen M. 2003. Glial-derived neurotrophic factor regulates apoptosis in colonic epithelial cells. *Gastroenterology* 124(7):1748-57

Sternini C, Su D, Arakawa J, De Giorgio R, Rickman DW, Davis BM, Albers KM, Brecha NC. 1996. Cellular localization of Pan-trk immunoreactivity and trkC mRNA in the enteric nervous system. *J Comp Neurol.* 368(4):597-607

Stolt CC, Schmitt S, Lommes P, Sock E, Wegner M. 2005. Impact of transcription factor Sox8 on oligodendrocyte specification in the mouse embryonic spinal cord. *Dev. Biol.* 281(2):309-17

Stolt CC, Lommes P, Sock E, Chaboissier MC, Schedl A, Wegner M. 2003. The Sox9 transcription factor determines glial fate choice in the developing spinal cord. *Genes Dev.* 17(13):1677-89

Stordeur P, Goldman M. 1998. Interleukin-10 as a regulatory cytokine induced by cellular stress: molecular aspects. *Int. Rev. Immunol.* 16(5-6):501-22

Suenaert P, Bulteel V, Lemmens L, Noman M, Geypens B, Van Assche G, Geboes K, Ceuppens JL, Rutgeerts P. 2002. Anti-tumor necrosis factor treatment restores the gut barrier in Crohn's disease. *Am J Gastroenterol.* 97(8):2000-4

Suenaert P, Bulteel V, Vermeire S, Noman M, Van Assche G, Rutgeerts P. 2005. Hyperresponsiveness of the mucosal barrier in Crohn's disease is not tumor necrosis factor-dependent. *Inflamm. Bowel. Dis.* 11(7):667-73

Takahashi K, Okada TS. 1970. An analysis of the effect of "conditioned medium" upon the cell culture at low density. *Dev. Growth Differ.* 12(2):65-77

Targan SR, Hanauer SB, van Deventer SJH, Mayer L, Present DH, Braakman T, DeWoody KL, Schaible TF, Rutgeerts PJ, The Crohn's Dc. 1997. A Short-Term Study of Chimeric Monoclonal Antibody cA2 to Tumor Necrosis Factor {alpha} for Crohn's Disease. *N Engl J Med* 337(15):1029-36

Taylor CT, Murphy A, Kelleher D, BAIRD AW. 1997. Changes in barrier function of a model intestinal epithelium by intraepithelial lymphocytes require new protein synthesis by epithelial cells. *Gut* 40(5):634-40

Thoenen H. 2000. Neurotrophins and activity-dependent plasticity. *Prog. Brain Res.* 128:183-91

Tjwa ET, Bradley JM, Keenan CM, Kroese AB, Sharkey KA. 2003. Interleukin-1beta activates specific populations of enteric neurons and enteric glia in the guinea pig ileum and colon. *Am J Physiol Gastrointest Liver Physiol* 285(6):G1268-G1276

Tomac AC, Grinberg A, Huang SP, Nosrat C, Wang Y, Borlongan C, Lin SZ, Chiang YH, Olson L, Westphal H, Hoffer BJ. 2000. Glial cell line-derived neurotrophic factor receptor alpha1 availability regulates glial cell line-derived neurotrophic factor signaling: evidence from mice carrying one or two mutated alleles. *Neuroscience* 95(4):1011-23

Vinores SA, Rubinstein LJ. 1985. Simultaneous expression of glial fibrillary acidic (GFA) protein and neuron-specific enolase (NSE) by the same reactive or neoplastic astrocytes. *Neuropathol. Appl. Neurobiol.* 11(5):349-59

Virchow R. 1856. *Gesammelte Abhandlungen zur wissenschaftlichen Medicin.* Frankfurt a. M: Hamm.

von Boyen GB, Steinkamp M, Geerling I, Reinshagen M, Schafer KH, Adler G, Kirsch J. 2006a. Proinflammatory cytokines induce neurotrophic factor expression in enteric glia: a key to the regulation of epithelial apoptosis in Crohn's disease. *Inflamm. Bowel. Dis.* 12(5):346-54

von Boyen GB, Steinkamp M, Reinshagen M, Schafer KH, Adler G, Kirsch J. 2006b. Nerve growth factor secretion in cultured enteric glia cells is modulated by proinflammatory cytokines. *J Neuroendocrinol.* 18(11):820-5

von Boyen GBT, Steinkamp M, Reinshagen M, Schafer KH, Adler G, Kirsch J. 2004. Proinflammatory cytokines increase glial fibrillary acidic protein expression in enteric glia. *Gut* 53(2):222-8

Vroemen M, Weidner N. 2003. Purification of Schwann cells by selection of p75 low affinity nerve growth factor receptor expressing cells from adult peripheral nerve. *J Neurosci. Methods* 124(2):135-43

Wang F, Graham WV, Wang Y, Witkowski ED, Schwarz BT, Turner JR. 2005. Interferon-gamma and tumor necrosis factor-alpha synergize to induce intestinal epithelial barrier dysfunction by up-regulating myosin light chain kinase expression. *Am J Pathol* 166(2):409-19

Wedel T, Roblick U, Gleiss J, Schiedeck T, Bruch HP, Kuhnel W, Krammer HJ. 1999. Organization of the enteric nervous system in the human colon demonstrated by wholemount immunohistochemistry with special reference to the submucous plexus. *Ann. Anat.* 181(4):327-37

Wedel T, Roblick UJ, Ott V, Eggers R, Schiedeck TH, Krammer HJ, Bruch HP. 2002. Oligoneuronal hypoganglionosis in patients with idiopathic slow-transit constipation. *Dis. Colon Rectum* 45(1):54-62

Wegner M. 1999. From head to toes: the multiple facets of Sox proteins. *Nucleic Acids Res.* 27(6):1409-20

Wehkamp J, Fellermann K, Herrlinger KR, Bevins CL, Stange EF. 2005a. Mechanisms of disease: defensins in gastrointestinal diseases. *Nat. Clin. Pract. Gastroenterol. Hepatol.* 2(9):406-15

Wehkamp J, Salzman NH, Porter E, Nuding S, Weichenthal M, Petras RE, Shen B, Schaeffeler E, Schwab M, Linzmeier R, Feathers RW, Chu H, Lima H, Jr., Fellermann K, Ganz T, Stange EF, Bevins CL. 2005b. Reduced Paneth cell alpha-defensins in ileal Crohn's disease. *Proc. Natl. Acad. Sci. U. S. A* 102(50):18129-34

Wilkinson KD, Deshpande S, Larsen CN. 1992. Comparisons of neuronal (PGP 9.5) and non-neuronal ubiquitin C-terminal hydrolases. *Biochem. Soc. Trans.* 20(3):631-7

Woywodt A, Ludwig D, Neustock P, Kruse A, Schwarting K, Jantschek G, Kirchner H, Stange EF. 1999. Mucosal cytokine expression, cellular markers and adhesion molecules in inflammatory bowel disease. *Eur. J Gastroenterol. Hepatol.* 11(3):267-76

Yau WM, Dorsett JA, Parr EL. 1989. Characterization of acetylcholine release from enzyme-dissociated myenteric ganglia. *Am J Physiol* 256(1 Pt 1):G233-G239

Young HM, Bergner AJ, Muller T. 2003. Acquisition of neuronal and glial markers by neural crest-derived cells in the mouse intestine. *J Comp Neurol.* 456(1):1-11

Young HM, Furness JB, Sewell P, Burcher EF, Kandiah CJ. 1993. Total numbers of neurons in myenteric ganglia of the guinea-pig small intestine. *Cell Tissue Res.* 272(1):197-200

Zareie M, McKay DM, Kovarik GG, Perdue MH. 1998. Monocyte/macrophages evoke epithelial dysfunction: indirect role of tumor necrosis factor-alpha. *Am J Physiol Cell Physiol* 275(4):C932-C939

7.   Supplements

Tables Supplements

Table S 1. Laboratory equipment

Item	Supplier
Analytical balance (U6100S)	Sartorius, Göttingen
Cell disruptor (FastPrep® Instrument FP120)	Qbiogene, Heidelberg
Class II biological safety cabinet (Holten Lamin Air S 2010, type 1.2) equipped with a	Heto-Holten, Allerød, Denmark
Laboratory gas burner (gasprofi 2) and a	Wartewig Labor- und Dentaltechnik, Göttingen
Vacuum pump	KNF Neuberger, Freiburg
CO_2 incubator (CB150 and CB210)	Binder, Tuttlingen
Deep freezer (6485)	GFL - Gesellschaft für Labortechnik, Burgwedel
Dissection forceps with bent tip (HTC 091-10)	Hammacher, Solingen
Dissection forceps with fine tip (Dumont # 5; 11252-20)	Fine Science Tools, Heidelberg
Dissection scissors (Iris Scissors-ToughCut; 14058-11)	Fine Science Tools, Heidelberg
Dissection scissors (Scissors-ToughCut; 14054-13)	Fine Science Tools, Heidelberg
Dissection scissors with angled up blades (Moria Spring Scissors; 15396-02)	Fine Science Tools, Heidelberg
Dissection scissors with angled up blades (Noyes Spring Scissors; 15013-12)	Fine Science Tools, Heidelberg
Electrophoresis power supply (EPS 300)	Pharmacia Biotech, Freiburg
Electrophoresis unit (Mini D)	LTF Labortechnik, Wasserburg/Bodensee
Epifluorescence microscope (BX61 WI)	Olympus, Hamburg
Gas-dispersion tube with fritted disc (Z145475)	Sigma-Aldrich, Steinheim
Heating plate	Self made
Hemacytometer (Bright-Line™, Z359629)	Sigma-Aldrich, Steinheim
Horizontal shaker	Self made
Large volume centrifuge with cooling system (Z 513 K)	Hermle Labortechnik, Wehingen
Magnetic stirrer (RCT B) equipped with a Electronic contact thermometer (ETS-D4)	IKA Werke, Staufen IKA Werke, Staufen
Microliter centrifuge (5415 C)	Eppendorf, Hamburg
Microliter centrifuge (Z 233 M-2)	Hermle Labortechnik, Wehingen
Microliter pipettes (Transferpette®) 0.5-1.0 µl, 0.5-10 µl, 10-100 µl and 100-1000 µl	Brand, Wertheim
Microliter pipettes(eppendorf Research® adjustable) 0.1-2.5 µl, 0.5-10 µl, 2-20 µl and 20-200 µl	Eppendorf, Hamburg
Microplate reader (Varioskan)	Thermo Electron Corporation, Dreieich
Microwave oven (ER-654MD)	Goldstar

Table S 1. Laboratory *(Continued)*

Item	Supplier
Mini centrifuge (GMC-060)	Laboratory & Medical Supplies, Tokyo, Japan
MultiDoc-It Imaging System M20 equipped with a 5.1 megapixel color digicam, UV-Transilluminator M-20 and Doc-It 1D software for gel analysis	LTF Labortechnik, Wasserburg/Bodensee
pH meter (inoLab pH Level 1) equipped with a pH electrode (SenTix 81)	WTW – Wissenschaftlich Technische Werkstätten, Weilheim WTW – Wissenschaftlich Technische Werkstätten, Weilheim
Phase contrast microscope (DM IL)	Leica Microsystems, Wetzlar
Pipette controller (accu-jet®)	Brand, Wertheim
Plastic tubes (Tygon)	Saint-Gobain, Charny, France
Precision balance (440-47N)	Kern, Balingen
Precision balance (DeltaRange AT261)	Mettler-Toledo, Giessen
Real time thermal cycler (Rotor-Gene^{TM} 3000)	Corbett Research, Sidney, Australia
Shaking water bath (1083)	GFL - Gesellschaft für Labortechnik, Burgwedel
Spectrophotometer (GeneQuant pro)	Biochrom, Cambridge, UK
Stereo microscope (SZ51) equipped with a Cold light source (Highlight 2100)	Olympus, Hamburg Olympus, Hamburg
Thermomixer (Thermomixer compact)	Eppendorf, Hamburg
Ultrapure water unit (NANOpure Diamond, D11921)	Barnstead Int., Dubuque, IA, USA
Voltohmmeter (Millicell-ERS)	Millipore, Eschborn
Vortexer (Vortex Genie 2)	Scientific Industries, Bohemia, NY, USA
Water bath	B Braun, Melsungen
Wave shaker (Polymax 1040)	Heidolph Instruments, Schwabach

Table S 2. Chemicals

Name	Order number	Supplier
Acetone	Z.00070.9001	Zefa-Laborservice, Harthausen
Agarose	1551027	Invitrogen, Karlsruhe
Albumin from bovine serum (BSA)	A7906	Sigma-Aldrich, Steinheim
Amphotericin B	A2411	Sigma-Aldrich, Steinheim
Antibiotic-antimycotic solution (AA)	Z-18-M	CCPro, Neustadt/W.
Bovine pituitary extract (BPE)	GRB2428BK	Linaris, Wertheim
Bromphenol blue	A512.1	Roth, Karlsruhe
Calcium chloride dihydrate ($CaCl_2 \cdot 2H_2O$)	C7902	Sigma-Aldrich, Steinheim
Carbogen (5 % CO_2, 95 % O_2)	-	Linde Gas, Pullach
Chloroform	7386	Mallinckrodt Baker, Griesheim
Collagenase, type IA	C9891	Sigma-Aldrich, Steinheim
Cytosine β-D-arabinofuranoside (AraC)	C1768	Sigma-Aldrich, Steinheim
D-(+)-glucose	G7021	Sigma-Aldrich, Steinheim
Deoxyribonucelase 1	DN25	Sigma-Aldrich, Steinheim
Dextran, fluorescein (FD) (MW 70,000)	D1823	Invitrogen, Karlsruhe
Diethyl pyrocarbonate (DEPC)	32490	Sigma-Aldrich, Steinheim
Dimethyl sulfoxide (DMSO)	D2650	Sigma-Aldrich, Steinheim
Dulbecco's modified Eagle's medium (DMEM) with 4.5 g/l glucose	FG0445	Biochrom, Berlin
Dulbecco's modified Eagle's medium nutrient mixture F-12 Ham (DMEM/F12)	D8900	Sigma-Aldrich, Steinheim
Ethanol	8006	Mallinckrodt Baker, Griesheim
Ethidium bromide solution	E1510	Sigma-Aldrich, Steinheim
Ethylenediaminetetraacetic acid disodium salt dihydrate (EDTA)	8043.2	Roth, Karlsruhe
Fetal bovine serum (FBS)	10270-016	Invitrogen, Karlsruhe
Fluorescein-5-(and-6)-sulfonic acid, trisodium salt (FSA) (MW 478.32)	F1130	Invitrogen, Karlsruhe
Forskolin	F6886	Sigma-Aldrich, Steinheim
Glacial acetic acid	A6283	Sigma-Aldrich, Steinheim
Glycerol	G5516	Sigma-Aldrich, Steinheim
Glycerol	G7893	Sigma-Aldrich, Steinheim
Glycerol	4043.1	Roth, Karlsruhe
Goat serum	G6767	Sigma-Aldrich, Steinheim
Guinea pig complement	CL5000	Cedarlane, Harnby, Canada
Hank's balanced salt solution (HBSS)	H6648	Sigma-Aldrich, Steinheim
HEPES	H4034	Sigma-Aldrich, Steinheim
Hoechst 33258	861405	Sigma-Aldrich, Steinheim
Horse serum	H1270	Sigma-Aldrich, Steinheim

Table S 2. Chemicals *(Continued)*

Name	Order number	Supplier
Hydrochloride acid, 32 % (HCl)	100313	Merck, Darmstadt
Magnesium chloride hexahydrate ($MCl_2 \cdot 6H_2O$)	M2393	Sigma-Aldrich, Steinheim
Methanol	8045	Mallinckrodt Baker, Griesheim
Paraformaldehyde	P6148	Sigma-Aldrich, Steinheim
Picric acid, 1.2 %	36011	Riedel de Haen, Seelze
Poly-L-lysine solution	P8920	Sigma-Aldrich, Steinheim
Potassium chloride (KCl)	P5405	Sigma-Aldrich, Steinheim
Protease, type IX	P6141	Sigma-Aldrich, Steinheim
Interferon gamma, recombinant human (rhIFNγ)	285-IF-100	R&D Systems, Wiesbaden
Interleukin 1 beta, recombinant human (rhIL-1β)	201-LB-025	R&D Systems, Wiesbaden
Interleukin 13, recombinant human (rhIL-13)	213-IL-005	R&D Systems, Wiesbaden
Tumor necrosis factor alpha, recombinant human (rhTNFα)	210-TA-010	R&D Systems, Wiesbaden
Sodium acetate trihydrate (TRIS)	6779.1	Roth, Karlsruhe
Sodium azide (NaN_3)	S8032	Sigma-Aldrich, Steinheim
Sodium bicarbonate ($NaHCO_3$)	S5761	Sigma-Aldrich, Steinheim
Sodium chloride (NaCl)	S5886	Sigma-Aldrich, Steinheim
Sodium hydroxide (NaOH)	0402	Mallinckrodt Baker, Griesheim
Sodium phosphate dibasic heptahydrate ($Na_2HPO_4 \cdot 7H_2O$)	S9390	Sigma-Aldrich, Steinheim
Sodium phosphate monobasic (NaH_2PO_4)	S5011	Sigma-Aldrich, Steinheim
Sodium phosphate monobasic monohydrate ($NaH_2PO_4 \cdot H_2O$)	S9638	Sigma-Aldrich, Steinheim
Sucrose	107653	Merck, Darmstadt
Triton X-100	X100	Sigma-Aldrich, Steinheim
Trypsin (0.5 %)/EDTA (0.2 %) 10×	Z-26-M	CCPro, Neustadt/W.
Trypsin (2.5 %) 10×	Z-25-M	CCPro, Neustadt/W.
β-Ala-Lys-N$_\varepsilon$-7-amino-4-methyl-coumarin-3-acetic acid (Ala-Lys-AMCA)	custom-made	Biotrend, Köln

Table S 3. Consumables

Item	Order number	Supplier
Syringe filters, 0.8/0.2 µm (Acrodisc® PF)	4658	Pall, Cornwall, UK
Syringe filters, 0.2 µm (Ministart®)	16534K	Sartorius, Göttingen
Syringe filters, 0.2 µm (Nalgene)	190-2520	Nalgene, Wiesbaden
Syringe filters, 0.22 µm (Millex-GV)	SLGV013SL	Millipore, Eschborn
Glass Pasteur pipettes	747715	Brand, Wertheim
Pipette tips, 0.1-20 µl, 2-200 µl, 50-1000 µl	702504 702516 702521	Brand, Wertheim
Serological pipettes, 1 ml	4011	Coring Int., Corning, NY, USA
Serological pipettes, 5 ml	356543	BD Biosciences, Heidelberg
Serological pipettes, 10 ml	356551	BD Biosciences, Heidelberg
Serological pipettes, 25 ml	356525	BD Biosciences, Heidelberg
Syringe, 50 ml (Omnifix®)	4613554F	B Braun, Melsungen
Syringe, 10 ml (Omnifix®)	370-175	Heiland Medical, Wien, Austria
12 well Transwell® Permeable Supports (polyester membrane, 12 mm membrane diameter, 0.4 µm pore size)	3460	Coring Int., Corning, NY, USA
6 well Transwell® Permeable Supports (polyester membrane, 24 mm membrane diameter, 0.4 µm pore size)	3450	Coring Int., Corning, NY, USA
Costar®12 well microplates	3513	Coring Int., Corning, NY, USA
6 well microplates	657160	Greiner Bio-One, Frickenhausen
12 well microplates	665180	Greiner Bio-One, Frickenhausen
96 well microplates	655180	Greiner Bio-One, Frickenhausen
Cell culture flasks, 250 ml, 75 cm^2 with filter screw cap	658175	Greiner Bio-One, Frickenhausen
Cell culture flasks, 50 ml, 25 cm^2, with filter screw cap	690175	Greiner Bio-One, Frickenhausen
Cell culture flasks, 50 ml, 25 cm^2	156367	Nunc, Wiesbaden
Centrifuge tubes, 15 ml	188271	Greiner Bio-One, Frickenhausen
Centrifuge tubes, 50 ml	227270	Greiner Bio-One, Frickenhausen
Centrifuge tubes, 10 ml	347856	Nunc, Wiesbaden

Table S 3. Consumables *(Continued)*

Item	Order number	Supplier
Dissection dishes, glass, 100x20 mm and 150x25 mm	237554805 237555201	Schott, Mainz
Dissection dishes, 100x20 mm	664160	Greiner Bio-One, Frickenhausen
Tissue culture dishes, 30x10 mm and 60x15 mm	627160 628160	Greiner Bio-One, Frickenhausen
Tissue culture dishes, 100x20 mm	430167	Coring Int., Corning, NY, USA
Cryo tubes, 2 ml	122280	Greiner Bio-One, Frickenhausen
Microcentrifuge tubes, 0.5 ml, 2.0 ml	780507 780550	Brand, Wertheim
Microcentrifuge tubes, 1.5 ml, 2.0 ml	0030120.191 0030120.248	Eppendorf, Hamburg
Microcentrifuge tubes, 1.5 ml	616201	Greiner Bio-One, Frickenhausen
Exam gloves (Safeskin E330)	-	Kimberly-Clark, Zaventem, Belgium
Surgical gloves (Gammex PF)	-	Ansell, Brussels, Belgium
Surgeon-face mask (BEEM-Visma Plus)	6120652	B Braun, Melsungen
Minutien pins, Ø 0.1 mm (Insect Pins®) and Ø 0.2 mm (Insect Pins®)	2600210 2600210	Fine Science Tools, Heidelberg
Microscope slides, 76x26 mm	AA00000112E	Menzel-Gläser, Braunschweig
Cover slips, 24x24 mm, 24x32 mm, 24x40 mm, 24x60 mm	BB024024A1 BB024032A1 BB024040A1 BB024060A1	Menzel-Gläser, Braunschweig
Insect pins, Ø 0.1 mm and Ø 0.2 mm	26002-10 26002-20	Fine Science Tools, Heidelberg
Syringe, 1 ml (Dispomed®)	22006	Dispomed Witt, Gelnhausen
20-gage needle (Heiland)	370-187	Heiland Medical, Wien, Austria
1-gage needle (Heiland)	370-180	Heiland Medical, Wien, Austria

Table S 4. Antibodies used during *in vitro* experiments.

Antiserum	Oder number	Supplier
Goat anti-human GDNF	AF-212-NA	R&D Systems, Wiesbaden
Mouse anti-human CD90 (Thy-1.1)	555592	BD Biosciences, Heidelberg

Table S 5. Cell lines used in this project.

Name	Species	Type	Source	Transformed	Order number	Supplier
Caco-2	Human	Epithelial	Colon adenocarcinoma	Yes	86010202	European Collection of Cell Cultures, Salisbury, UK
IEC6	Rat	Epithelial	Small intestine	No	88071401	European Collection of Cell Cultures, Salisbury, UK
T84	Human	Epithelial	Colon carcinoma	Yes	88021101	European Collection of Cell Cultures, Salisbury, UK
HT-29	Human	Epithelial	Colon adenocarcinoma	Yes	HTB-38	American Type Culture Collection, Rockville, MD, USA
PK 29/6	Rat	Glial	Small intestine	No	self-made	(Ruhl et al 2001c)

Table S 6. Kits

Name	Order number	Supplier
FastRNA® Pro Green Kit	6045-050	Qbiogene, Heidelberg
SuperScript™ III Platinum® SYBR® Green One-Step qRT-PCR Kit	11736051	Invitrogen, Karlsruhe
Sylgard® 184 silicone elastomer kit	01673921	Dow Corning, Wiesbaden

Table S 7. DNA ladder, mRNA for positive controls

Name	Order number	Supplier
Low molecular weight DNA ladder	N3233S	New England Biolabs, Frankfurt
Rat brain total RNA	7912	Ambion, Austin, TX, USA
Rat spleen total RNA	7920	Ambion, Austin, TX, USA

Table S 8. Preparation of commonly used solutions, buffers and culture media.

Solution	Method of preparation	Comments
0.1 M Phosphate buffer (PB)	Add 3.0 g of $NaH_2PO_4 \cdot H_2O$ and 21.7 g of $Na_2HPO_4 \cdot 7H_2O$ to 800 ml of deionized water and adjust the pH to 7.44 with 1 M NaOH or 1 M HCl. Fill up to 1 l with H_2O.	
0.5 M EDTA (pH 8.0)	Add 186.1 g of ethylenediaminetetraacetic acid disodium salt dihydrate to 800 ml of H2O. Stir vigorously on a magnetic stirrer. Adjust the pH to 8.0 with 1 M NaOH. Dispense into aliquots and sterilize by autoclaving.	The disodium salt of EDTA will not go into solution until the pH of the solution is adjusted to approximately 8.0 by addition of NaOH.
1.2 M $MgCl_2$	Dissolve 244.0 g of $MgCl_2 \cdot 6H_2O$ in 800 ml H_2O. Adjust the volume to 1 l with H_2O.	
1× Tris acetate-EDTA (TAE)	Sterilize 10 ml of 50× TAE by passage through a 0.22 ml filter. Mix 10 ml of sterile 50× TAE to 490 ml of DEPC-treated water.	Working solution.
2.5 M $CaCl_2$	Dissolve 367.5 g of $CaCl_2 \cdot 2H_2O$ in 800 ml H_2O. Adjust the volume to 1 l with H_2O.	
50× Tris acetate-EDTA (TAE)	Dissolve 242 g of sodium acetate trihydrate in 800 ml of H_2O. Add 57.1 ml of glacial acetic acid and 100 ml of 0.5 M EDTA (pH 8.0). Adjust the volume to 1 l with H_2O.	Stock solution.
6× Gel-loading buffer	Mix 50 % (v/v) of glycerol and 50 % (v/v) of 10× TAE. Add 0.2 % (w/v) of bromphenol blue and dilute the solution to 6× with H_2O. Dispense into aliquots.	All chemicals were purchased from Roth, Karlsruhe.
Blocking solution	Add 2 ml of horse serum or goat serum and 250 μl of Triton X-100 to 48 ml of PBS/NaN_3. Stir vigorously on a magnetic stirrer. Dispense into aliquots and filter by passage through a 0.2 μm filter.	Store at 4-8°C.
DEPC-treated water	Treat H_2O with 0.1 % (v/v) DEPC. Use only glassware sterilized by dry heat. Dispense into aliquots and sterilize by autoclaving.	

Table S 8. Preparation of commonly used solutions, buffers and culture media. *(Continued)*

Solution	Method of preparation	Comments
Dissociation solution	Dissolve 0.1175 g of HEPES in 50 ml of Hank's balanced salt solution on a magnetic stirrer. Adjust the pH to 7.4 with 1 M NaOH. Add 125 mg of collagenase (type IA), 100 mg of protease (type IX), 15 mg of albumin from bovine serum and 1.25 mg deoxyribonucelase 1. Stir until all particles are dissolved. Sterilize by passage through a 0.2 µm filter and dispense into 10 ml aliquots. Store at -20 °C.	(Yau et al 1989)
Dulbecco's modified Eagle's medium nutrient mixture F-12 Ham (DMEM/F12)	Dissolve 15.6 g of DMEM/F12 and 2.1 g of $NaHCO_3$ in 980 ml of H2O. Adjust the pH to 7.4 with 1 M NaOH. Add water to 1 l. Sterilize by filtration and dispense into aliquots.	Store not longer than 2 weeks. If FBS is added, store not longer than 1 week.
Fixative	Add 50 ml of 0.1 M PB to 2 g of paraformaldehyde and stir on a magnetic stirrer while heating to 60 °C until the solution gets clear. Add 100 µl of 1.2 % picric acid.	Store not longer than 5 days at 2-8 °C.
Freezing medium	Add 20 % (v/v) of sterile heat inactivated FBS and 10 % (v/v) of DMSO to DMEM/F12. Dispense into aliquots and freeze at -20 °C.	
Guinea pig complement	Add 5 ml of ice-cold, sterile H_2O to the vial with guinea pig complement using a sterile 10 ml syringe with an adapted 1-gage needle and dissolve the powder. Sterilize the solution by passage through a 0.22 µm filter (PVDF membrane). Dispense into aliquots and freeze at -80 °C.	Aliquots should not be frozen once they were thawed, because the complement is very heat sensitive.
Krebs buffer	Dissolve 6.84 g of NaCl, 2.10 g of $NaHCO_3$, 1.98 g of Glucose, 0.35 g of KCl and 0.144 g of NaH_2PO_4 in 980 ml of H_2O bubbled with carbogen (5 % CO_2, 95 % O_2) using a gas-dispersion tube with a fritted disc. Add 1 ml of 1.2 M $MgCl_2$. After 15 min of gassing, add 1 ml of 2.5 M $CaCl_2$. Adjust the volume to 1 l with H_2O. pH is 7.4.	Sterilized by passage through a 0.2 µm filter. Sterile Krebs buffer was oxygenated with carbogen using a 1 ml serological pipette attached to the gassing tube.
Mounting solution	Mix 80 % (v/v) of glycerol and 20 % (v/v) PBS/NaN_3. Adjust the pH to 7.0 with 1 M of HCl.	Store at 4-8°C.

Table S 8. Preparation of commonly used solutions, buffers and culture media. *(Continued)*

Solution	Method of preparation	Comments
PBS sodium azide (0.1 %) (PBS/NaN$_3$)	Dissolve 1 g of NaN$_3$ in 1 l of PBS buffer.	
Phosphate-buffered saline (PBS)	Dissolve 8.8 g of NaCl in 800 ml of deionized water. Add 116 ml of 0.1 M PB and fill up to 1 l with H$_2$O.	
Phosphate-buffered saline (PBS) for cell culture	Dissolve 8.5 g of NaCl, 4.03 g of Na$_2$HPO$_4$ and 0.449 g of NaH$_2$PO$_4$ in 980 ml of H$_2$O. Adjust the pH to 7.4 with 1 M NaOH or 1 M HCl. Fill up to 1 l with H$_2$O.	Sterilize by autoclaving and dispense into aliquots.
Poly-L-Lysine solution	Add 0.1 % (w/v) to H$_2$O. Dilute solution before use 1:10.	Diluted solution is stable for at least month at 2-8 °C. Filter diluted solution after use.
Sucrose solution	Dissolve 3 g of sucrose to 7 ml of PBS/NaN$_3$.	
Water, Sterile	Sterilize H$_2$O by autoclaving.	

Note: All solutions were made with deionized water from an ultrapure water unit (NANOpure Diamond, D11921) (Barnstead Int., Dubuque, IA, USA). Reference: (Sambrook et al 1989).

Table S 9. Standard operating procedures (SOPs)

Poly-L-Lysine coating of microscopy slides

Poly-L-lysine solution (see Table S 8) was diluted 1:10 (v/v) with deionized water at room temperature. Microscope slides (Menzel-Gläser, Braunschweig) were cleaned with acidic alcohol (e.g. 1 % of HCl in 70 % of ethanol) if necessary and placed in diluted poly-L-lysine solution for 5 min. Drained slides were dried at 60 °C for 1 h or at room temperature over night. Per liter solution up to 900 slides could be coated.

Heat inactivation of fetal bovine serum (FBS)

FBS (Invitrogen, Karlsruhe) was slowly thawed to room temperature and the contents of the bottle were mixed thoroughly. The thawed bottle of serum was placed into a 56 °C shaking water bath (1083; GFL - Gesellschaft für Labortechnik, Burgwedel) containing enough water to immerse the bottle to just above the level of the serum. It was incubated for 30 min under constant agitation. After the heat inactivation, the serum was filtered by passage through a 0.8/0.2 syringe filter (Acrodisc® PF; Pall, Cornwall, UK) using 50 ml syringes (Omnifix®; B Braun, Melsungen) and immediately frozen at -20 °C.

Sylgard-coating of dissection dishes

Glass dissection dishes (Schott, Mainz) and plastic dissection dishes (Greiner Bio-One, Frickenhausen) were cleaned with 70 % ethanol and the inner rim of the plastic dishes was roughened with an acetone moistened Q-tip. Sylgard (Dow Corning, Wiesbaden) and the catalyst were mixed in a 10:1 (w/w) ratio under constant stirring with a glass rod for 5-10 min. The gel was poured into the dissection dishes to form a 2-3 mm bottom layer under avoidance of bubbles. The crosslinking took about 4 hours at 65 °C or 2 days at room temperature.

Table S 10. Patient data – Resectates used for the isolation of human enteric glia.

Patient No.	Date of surgery	Patient sex	Patient age (yrs)	Resected region	Plexus used for isolation of enteric glial cells	Diagnosis
1	05.07.04	f	45	Sigmoid colon	MP	Diverticulitis
2	12.07.04	m	40	Sigmoid colon	MP	Diverticulitis
3	16.07.04	m	54	Transverse colon	MP	Colorectal carcinoma
4	19.07.04	m	82	Ileum	MP	Colorectal carcinoma
5	30.07.04	f	83	Sigmoid colon	MP	Colorectal carcinoma
6	01.09.04	f	82	Sigmoid colon	MP	Colorectal carcinoma
7	09.09.04	m	89	Ileum	MP	Colorectal carcinoma
8	15.09.04	f	44	Ileum	MP	Diverticulitis
9	16.09.04	m	68	Transverse colon	MP	Multiple colonic polyps
10	21.10.04	f	58	Descending colon	MP	Colorectal carcinoma
11	29.10.04	f	72	Ileum	MP	Colorectal carcinoma
12	10.11.04	m	63	Descending colon	MP	Colorectal carcinoma
13	17.11.04	m	65	Ileum	MP	Colorectal carcinoma
14	22.11.04	f	65	Transverse colon	MP	Colorectal carcinoma
15	20.12.04	m	71	Ileum	MP	Gastric carcinoma
16	27.12.04	f	81	Jejunum	MP	Benign stenosis of the sigmoid colon
17	29.12.04	f	53	Descending colon	MP	Colorectal carcinoma
18	10.01.05	m	72	Sigmoid colon	SMP	Multiple colonic polyps
19	17.01.05	m	64	Transverse colon	SMP	Colorectal carcinoma
20	25.04.05	f	62	Sigmoid colon	SMP	Colorectal carcinoma
21	04.05.05	f	55	Descending colon	SMP	Diverticulitis
	Mean age		65	(range: 40-89 yrs)		

Table S 11. Patient data – Quantification of the human ENS.

Patient No.	Date of surgery	Patient sex	Patient age (yrs)	Resected region	Plexus used for quantification	Diagnosis
1	28.02.06	m	75	Ascending colon	Inner, intermediate and outer SMP	Colorectal carcinoma
2	20.12.05	f	68	Ascending colon	MP	Colorectal carcinoma
3	29.01.04	m	64	Ascending colon	MP	Colorectal carcinoma
4	19.01.04	m	60	Ascending colon	MP	Colorectal carcinoma
5	22.01.03	m	63	Ascending colon	Inner, intermediate and outer SMP; MP	Multiple colonic polyps
6	10.02.03	f	65	Ascending colon	MP	Colorectal carcinoma
7	20.09.04	m	61	Ascending colon	Inner, intermediate and outer SMP	Colorectal carcinoma
8	20.08.03	m	80	Ileum	Intermediate SMP	Colorectal carcinoma
				Ascending colon	Inner, intermediate and outer SMP	
9	28.11.02	m	65	Ileum	outer SMP; MP	Colorectal carcinoma
10	14.01.03	m	77	Ileum	Inner, intermediate and outer SMP; MP	Pancreatic carcinoma
11	23.01.03	f	78	Ileum	Inner, intermediate and outer SMP	Colorectal carcinoma
12	17.02.03	m	72	Ileum	Inner, intermediate and outer SMP	Colorectal carcinoma
13	27.11.03	f	52	Ileum	Intermediate and outer SMP; MP	Colorectal carcinoma
14	11.12.03	f	66	Ileum	Intermediate SMP and MP	Colorectal carcinoma
15	28.07.03	f	77	Ileum	Inner and outer SMP	Colorectal carcinoma
16	03.02.04	m	71	Ileum	Inner SMP and MP	Colorectal carcinoma
				Ascending colon	Inner, intermediate and outer SMP	
17	24.03.03	f	76	Ileum	Inner SMP and MP	Colorectal carcinoma
				Ascending colon	Inner, intermediate and outer SMP; MP	

Table S 11. Patient data – Quantification of the human ENS. *(Continued)*

18	28.10.05	m	53	Sigmoid colon	Inner, intermediate and outer SMP; MP	Colorectal carcinoma
19	09.12.02	f	59	Sigmoid colon	Inner, intermediate and outer SMP	Colorectal carcinoma
20	03.02.03	m	61	Sigmoid colon	Inner and outer SMP	Colorectal carcinoma
21	23.11.06	m	54	Sigmoid colon	Inner and outer SMP	Colorectal carcinoma
22	19.09.06	f	65	Sigmoid colon	Intermediate SMP	Colorectal carcinoma
23	13.08.03	f	82	Sigmoid colon	Inner, intermediate and outer SMP	Colorectal carcinoma
24	18.08.06	f	75	Sigmoid colon	Inner and intermediate SMP	Colorectal carcinoma
25	11.11.04	f	55	Sigmoid colon	MP	Colorectal carcinoma
26	27.01.05	m	43	Sigmoid colon	MP	Colorectal carcinoma
27	16.04.04	f	54	Sigmoid colon	MP	Colorectal carcinoma
28	22.02.05	m	68	Sigmoid colon	MP	Colorectal carcinoma
29	28.04.03	f	67	Sigmoid colon	Intermediate and outer SMP; MP	Colorectal carcinoma
	Mean age	65	(range: 43-82 yrs)			

Table S 12. Animal data – Quantification of the guinea Pig ENS.

Date	Sex	Weight	Resected regions	Plexus used for quantification
07.06.05	m	402 g	Ileum, proximal and distal colon	SMP and MP
09.06.05	m	380 g	Ileum, proximal and distal colon	SMP and MP
13.06.05	m	391 g	Ileum, proximal and distal colon	SMP and MP
14.06.05	m	388 g	Ileum, proximal and distal colon	SMP and MP
15.06.05	m	416 g	Ileum, proximal and distal colon	SMP and MP
16.06.05	m	451 g	Ileum, proximal and distal colon	SMP and MP

Publication list

Papers

S Hoff, F Zeller, CW Hann von Weyhern, M Wegner, M Schemann, K Michel, A Rühl: Quantitative assessment of glial cells in the human and guinea pig enteric nervous system with an anti-Sox8/9/10 antibody. J Comp Neurol 2008 (Accepted).

Abstracts

S Hoff, M Wegner, M Schemann, A Rühl: Immunohistochemical characterization of glial cells in the human enteric nervous system (ENS). Gastroenterology 2005; 128(Suppl 2):A42. (Oral presentation)

S Hoff, M Wegner, M Schemann, A Rühl: Immunohistochemical characterization of glial cells in the human enteric nervous system (ENS). Annual meeting of Deutsche Gesellschaft für Neurogastroenterologie und Motilität, Hohenkammer, 2005. (Oral presentation)

A Rühl, S Hoff: Enteric glia in intestinal inflammation. Annual meeting of Broad Medical Research Program, Los Angeles, USA, 2005. (Oral presentation, poster presentation)

S Hoff, M Schemann, A Rühl: Human enteric glia – specific markers and quantitative assessment. Neurogastroenterol Motil 2005; 17(Suppl 2):67. (Poster presentation)

S Hoff, M Wegner, F Zeller, M Schemann, A Rühl: Humane enterische Glia – Markerprofil und Quantifizierung. Z Gastroenterol 2005; 43:900. (Poster presentation)

S Hoff, C Pehl, F Zeller, C Hann von Weyhern, M Wegner, M Schemann, A Rühl: Enteric glia – quantitative comparison between human and guinea pig (gp) enteric nervous system (ENS). Gastroenterology 2006; 130(Suppl 2):A378. (Poster presentation)

C Hank, S Hoff, M Pfaffl, M Schemann, A Rühl: Enteric glia (EGC) support barrier functions of intestinal epithelial cells (IEC) under physiological and inflammatory conditions. Gastroenterology 2006; 130(Suppl 2):A19. (Oral presentation)

S Hoff, C Pehl, F Zeller, C Hann von Weyhern, M Wegner, M Schemann, A Rühl: Enteric glia – quantitative comparison between human and guinea pig (gp) enteric nervous system (ENS). Annual meeting of Deutsche Gesellschaft für Neurogastroenterologie und Motilität, Hohenkammer, 2006. (Oral presentation)

C Hank, S Hoff, M Pfaffl, M Schemann, A Rühl: Enteric glia (EGC) support barrier functions of intestinal epithelial cells (IEC) under physiological and inflammatory conditions. Annual meeting of Deutsche Gesellschaft für Neurogastroenterologie und Motilität, Hohenkammer, 2006. (Oral presentation)

S Hoff, C Hank, A Rühl, K Michel: Enteric glia in intestinal inflammation. Annual meeting of Broad Medical Research Program, Los Angeles, USA, 2006. (Poster presentation)

S Hoff, C Hank, M Schemann, A Rühl: Enterische Gliazellen modulieren die Barrierefunktion intestinaler Epithelzellen in einem *in vitro* Entzündungsmodell. Annual meeting of Deutsche Arbeitsgemeinschaft für chronisch entzündliche Darmerkrankung, Mainz, 2006. (Oral presentation)

S Hoff, C Hank, M Schemann, A Rühl: Enteric glial cells (EGC) support the intestinal epithelial barrier. Neurogastroenterol Motil 2006; 18(8):672. (Oral presentation)

Sebastian Hoff
Diplom-Ökotrophologe

Lebenslauf

Persönliche Information

Geburtsdatum	21 Dezember 1977
Geburtsort	München

Berufserfahrung

Seit 2007	**Clinical Research Associate** bei Kendle GmbH, München
2004 - 2008	**Promotion** am Lehrstuhl für Humanbiologie von Prof. Dr. Michael Schemann, Technische Universität München, Freising Titel: "Plasticity of glial cells in the enteric nervous system during intestinal inflammation", betreut durch PD Dr. med. Anne Rühl
2003 – 2004	Studentische und wissenschaftliche Hilfskraft an der Hochschuldozentur Humanernährung & Krebsprävention, Technische Universität München, Freising
2001	Praktikum bei der Firma Nutrisearch, Sarreguemines, Frankreich
2001 - 2003	Studentische Hilfskraft an der InformationsTechnologie Weihenstephan, Technische Universität München, Freising

Stipendien und Auszeichnungen

2006	„Young Investigator Travel Award" (Reisestipendium) für das Neurogastroenterology and Motility 2006 Joint International Meeting, Boston, USA
2006 - 2007	Stipendium nach dem Bayerischen Eliteföderungsgesetz
2004 - 2006	Stipendium des Broad Medical Research Program, Los Angeles, USA

Schule und Studium

2003	Abschluss des Studiums zum **Diplom-Ökotrophologen Univ.** (Dipl.oec.troph. Univ.) (Prädikat: sehr gut bestanden)
1998 - 2003	Studium der Ökotrophologie (Diplom) Technische Universität München, Freising
1997	**Allgemeine Hochschulreife**
1988 - 1997	Werner-von-Siemens Gymnasium, Regensburg

Zivildienst

1997 - 1998	Institut für Röntgendiagnostik, Klinikum der Universität Regensburg, Regensburg

<u>Erklärung</u>

Ich erkläre an Eides statt, dass ich die der Fakultät für

Ernährung, Landnutzung und Umwelt

der Technischen Universität München zur Promotionsprüfung

vorgelegte Arbeit mit dem Titel:

…..Plasticity of glial cells in the enteric nervous system during intestinal inflammation….

-

…………Plastizität der enterischen Glia bei intestinalen Entzündungsprozessen……….

In.....................….Freising-Weihenstephan am Lehrstuhl für Humanbiologie……………

……….……………..der Technischen Universität München...................................

(Institut, Klinik, Krankenhaus, Abteilung)

unter der Anleitung und Betreuung durch

..Herrn Prof. Dr. rer.nat. Michael Schemann und Frau PD Dr. med Anne Rühl................

....

ohne sonstige Hilfe erstellt und bei der Abfassung nur die gemäß § 6 Abs. 5

angegebenen Hilfsmittel benutzt habe.

(**X**) Ich habe die Dissertation in keinem anderen

Prüfungsverfahren als Prüfungsleistung vorgelegt.

( ) Die vollständige Dissertation wurde in ..../.....................................

................................./.. veröffentlicht. Die Fakultät für

..../.. hat der

Vorveröffentlichung zugestimmt.

(**X**) Ich habe den angestrebten Doktorgrad noch nicht erworben

und bin nicht in einem früheren Promotionsverfahren für

den angestrebten Doktorgrad endgültig gescheitert.

( ) Ich habe bereits am ..../..................................... bei der

Fakultät für ..../...

der Hochschule ..../...

unter Vorlage einer Dissertation mit dem Thema ..../.........................

..../...

die Zulassung zur Promotion beantragt mit dem Ergebnis:

..../...

Die Promotionsordnung der Technischen Universität München ist mir bekannt.

München, den ....   ……...................................

Unterschrift